Manipulating Guard Cell Anatomy and Physiology Using Biotechnological Approaches to Understanding Impact on Crop Performance

Ifeanyi Oyemike

A thesis submitted for the degree of Doctor of Philosophy

School of Biological Sciences

University of Essex

October 2018

Table of Contents

List of Figures

List of Tables

Abstract

Stomata are pores on the leaf surrounded by specialized epidermal cells called guard cells (GCs). GCs increase or decrease in volume in response to internal and external stimuli thereby regulating stomata aperture. In most plants, the changes exhibited by GCs alter stomatal aperture and affect the flux of gases between the internal leaf environment and the atmosphere and therefore have great control on photosynthetic processes and water loss from the plant. The number and patterning of stomata on a leaf are determined by a developmental pathway involving the epidermal patterning factor (EPF) protein family. Several EPF members affect epidermal cell density, stomata density as well as cell spacing, through their role in regulating cell division and differentiation. Understanding and manipulating EPFs has the potential to increase plant productivity and increase food supply.

The co-ordination of stomata activities and photosynthesis may involve GC chloroplasts, during photosynthetic electron transport chain (ETC) and Calvin cycle activities. Ferredoxin (Fd) protein plays an important role in regulating the production of ATP and photosynthetic reductants as well as activation of the Calvin cycle enzymes. Anatomical features such as stomata density, number and patterning all influence stomatal gas exchange and water use efficiency (WUE) of the plant. This study utilized transgenic plants expressing the cyanobacteria inorganic carbon transporter (ictB), which have already been shown to have high photosynthetic rates and plant growth for multiple genes cloning of EPF1, EPF2, EPFL9 and Fd.

Preliminary work on gene expression, chlorophyll fluorescence, stomata density and gas-exchange analysis were carried out to assess different photosynthetic parameters.

The operating efficiency of PSII was similar for all T0 and T1 generations of all EPFs and Fd plants. Stomata density analysis confirmed that EPF1 and EPF2 genes are negative regulators of stomata while EPF9 increase stomata density. EPF1 and EPF2 plants showed lower conductance and compare to EPF9. Fd was found to enhance plant's electron transport and Calvin cycle activities.

Dedication

This thesis is dedicated to God Almighty, Chiamaka, Chukwunonswe, Ebelechukwu and my parents who have profoundly supported me throughout my studies.

List of Abbreviations

A	Assimilation
ADP	Adenosine diphosphate
AGPase	ADP-glucose pyrophosphorylase
APX	Ascorbate peroxidase
ATP	Adenosine-5'-triphosphate
At	*Arabidopsis thaliana*
Bar	Basta or phosphinothricin
BPG	1,3-biphosphoglycerate
CaMV	Cauliflower mosaic virus
CDS:	Coding sequence of a gene
Chl	Chlorophyll
COA	Chlorophyll a oxygenase
CO_2	Carbon dioxide
Cyt	b6f Cythocrome b6f
DNA	Deoxyribonucleic Acid
EPF1	Epidermal Paterning Factor 1
EPF2	Epidermal Paterning Factor 2
EPFL9	Epidermal Paterning Factor-Like 9

ERf	ERECTA family
ETC	Electron transport chain
Fd/FD	Ferredoxin
F6P	Fructose 6-phosphate
FNR	Ferredoxin NADP Reductase
g_s	conductance
G1P	Glucose 1-phosphate
G3P	Glyceraldehydes 3-phosphate
G6P	Glucose 6-phosphate
GDC	Glycine decarboxylase
GPT	Glucose-6-phosphate/phosphate translocator
GST	Glutathione-S-transferase
H_2O_2	Hydrogen peroxide
HSP	Heat shock protein
ictB	Inorganic carbon transporter B
IPCC	Intergovernmental Panel on Climate Change
L1	Level 1
L2	Level 2
LRR	Leucine rich repeat

MDA	Monodehydroascorbate
mRNA	Messenger Ribonucleic Acid
NADP+	Nicotinamide adenine dinucleotide phosphate
NADPH	Reduced form of nicotinamide adenine dinucleotide phosphate
NoS	Nopaline synthase
NPQ	Nonphotochemical quenching
O_2	Oxygen
O_2^-	Superoxide
PaO	Phophorbide a oxygenase
P680	Photosystem II primary donor
P700	Photosystem I primary donor
PCR	Polymerase chain reaction
PEPc	Phosphoenul-pyruvate carboxylase
PGA	3-phosphoglycerate
PQH_2	Plastoquionol
PsbS	A protein associated with PSII
PSI	Photosystem I
PSII	Photosystem II
Qb	Plastoquinone

qE	High-energy-state quenching
qPCR	Quantitative polymerase chain reaction.
RNA	Ribonucleic Acid
ROS	Reactive oxygen species
RT-PCR	Reverse transcription PCR
Ru5P	Ribulose 5-phosphate
RuBP	Ribulose 1,5-biphosphate
RubisCO	Ribulose-1,5-bisphosphate carboxylase/oxygenase
SBPase	sedoheptulose-1,7-bisphosphatase
SOD	Superoxide dismutase
Taq	*Thermus aquaticus*
TB	Tobacco
T0	Parent plant
T1	1st generation plant
T2	2nd generation plant
T3	3rd generation plant
UDP	Uridine diphosphate
UTP	Uridine-5'-triphosphate
WT	Wild Type

WUE	Water-use efficiency
YFP	Yellow fluorescence protein

Acknowledgements

I would like to use this opportunity to thank Professor Tracy Lawson for her guidance, patience and support for me during the challenging times of my graduate career. In particular, I thank her for the invaluable time spent in ensuring that I will be successful during my studies in her Laboratory. I would also like to thank my second supervisor, Dr Matthew Jones who together with Tracy was very keen and supportive of my work.

I would like to thank Dr Phillip Davey who was always available to help in the physiology laboratory. Dr Silvere Vialet-Chabrand, Dr. Patricia Lopez Calcagno, Dr Andrew J Simkin and Dr Marino Exposito have all been very kind and supportive with their time and guidance whenever needed. My sincere appreciation goes to the entire plant group and members of Professor Tracy Lawson's laboratory for the precious time spent together. I will not forget to mention Professor Christine Raines and Professor Philip Mullineaux, for their constructive feedbacks and allowing the use of their laboratory.

There were so many difficult times that my uncle, Mr Festus C. Amede rose to the challenge, together with Barrister Onyemaechi Oyemike, Daniel, Dolica, Arinze, Klark and Faith. I thank my lovely sisters Chika and Vivian who has also been there for me. My Parents, wife, children and immediate family have played major parts in my stability here in England and I am grateful to you all. Most importantly, I would like to thank GOD Almighty, to whom I owe everything.

1. 0 Chapter 1

1. 1 Introduction

Sustaining efficient food production from crop plants has been and will continue to be a major challenge due to the rising world population (IPCC, 2007; Parry *et al.*, 2012) and decrease in arable land as a result of unsustainable farming practices (Parry *et al.*, 2012). Other major issues of increasing adverse weather conditions such as increasing drought episodes, rising temperatures and increasing stratospheric ozone have all contributed to the threat on crop productivity (IPCC, 2007; Parry *et al.*, 2012). The ever-increasing atmospheric carbon dioxide (CO_2) concentration from environmental pollution has not always resulted in a concomitant increase in C3 crop yield (Long *et al.*, 2006; Ainsworth, 2007; Ainsworth *et al.*, 2008) as changes in temperature contribute to lowering crop yield (Asseng *et al.*, 2011).

Plants belonging to the C3 group form the majority of the higher plants and they lack the CO_2 concentration mechanisms found in the C4 and crassulacean acid metabolism (CAM) plant groups (Ainsworth and Rogers, 2007; Fukuzawa *et al.*, 2012). Under most environmental conditions, photosynthesis in C3 plants is rate-limiting by the concentration of CO_2 at the carboxylation site and/or by the activity of ribulose 1,5-bisphospahate carboxylase/oxygenase (RubisCO) (Ainsworth and Rogers, 2007). One attempt made to raise the concentration of CO_2 at the active site of RubisCO using biotechnological approaches is the introduction of the foreign cyanobacterial gene ictB, a putative inorganic carbon transporter (Lieman-Hurwitz *et al.*, 2003, Simkin *et al.*, 2016).

Cyanobacteria offers good source of genes for plant genetic engineering and have been used extensively for studying fundamental biochemical processes such as photosynthesis and carbon assimilation (Park *et al*., 2009; Yingjun *et al*., 2015). The benefits of introducing the cyanobacteria genes into plants is enormous and cyanobacteria have existed on earth for over 3.5 billion years (Buick, 1992), during which time they have endured changing climate environment with declined CO_2 and increased O_2. These changes in the gaseous environment over time have imposed evolutionary pressure on the cyanobacteria to develop effective strategies for photosynthetic CO_2 concentration mechanism (CCM) (Figure 1.1) to improve carboxylation of its RubisCO enzyme (Price *et al*., 1998; Kaplan and Reinhold, 1999). The cyanobacteria *IctB* gene is described as a putative inorganic carbon transporter that is thought to be involved in HCO_3^- accumulation in *Arabidopsis* and tobacco and its expression has been showed to increase photosynthetic rate (Lieman-Hurwitz *et al*., 2003, 2005), although the detailed mechanisms are still unclear (Price *et al*., 1998; Simkin *et al*., 2015).

The introduction of the ictB gene has been proposed to enhance photosynthesis and plant growth by increasing the CO_2 concentration around ribulose-1, 5-bisphospate carboxylase/oxygenase (RubisCO), lowering photorespiration and increasing photosynthetic carbon assimilation. Using the ictB tobacco plants that was developed by Simkin *et al* (2016), it was possible to show synergistic effect of manipulating stomata density through altered expression of epidermal patterning factors (EPFs) and stomata behavior through altered expression of ferredoxin (Fd) specific to guard cells. During guard cell photosynthesis, Fds present at photosystem I (PS1) are actively involved in linear electron transfer (LET) to generate NADPH required for

the reduction of CO_2 in the Calvin cycle (Raines and Lloyd, 2001; Xuan et al., 2017). Fd is also important for the activation of key Calvin cycle enzymes during light induction (Hedrich *et al.*, 1985; Daloso *et al.*, 2015).

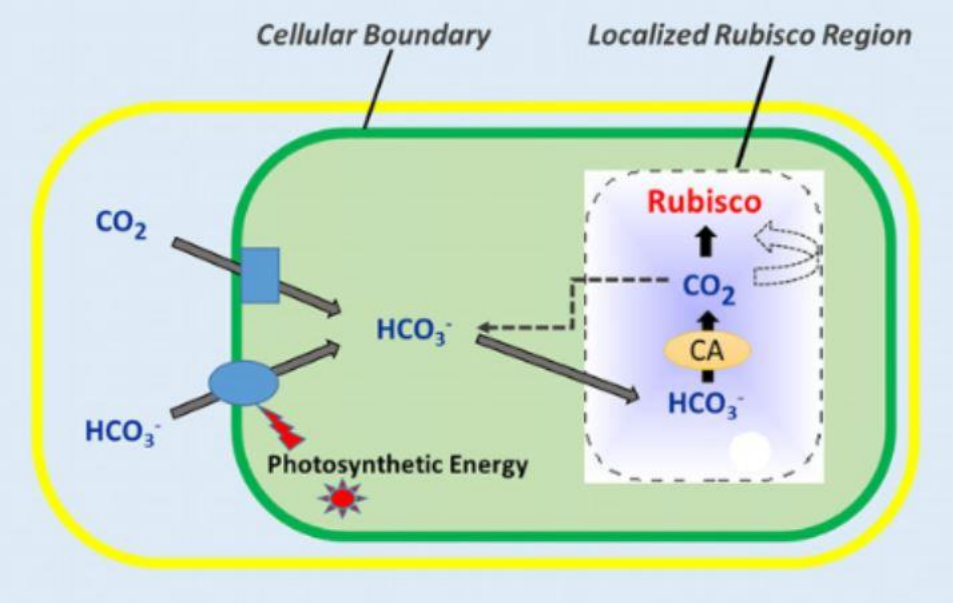

Figure 1. 1: A simplified model of the cyanobacterial CO_2 concentrating mechanism (CCM) in a single-cell-based CO_2 enrichment mechanism relying on multiple energized inorganic carbon (C_i) uptake systems. RubisCO can only use CO_2 as a substrate for carboxylation therefore, a carbonic anhydrase (CA) converts the accumulated HCO_3^- to CO_2 at or near the site of RubisCO (Yingjun *et al.*, 2015).

The pathway for CO_2 entry into the photosynthetic plants is through stomatal pores on the surface of the leaf that are surrounded by specialized epidermal cells called guard cells (GCs), (Figure 1.2). GCs increase or decrease in volume in response to internal and external stimuli thereby regulating stomata aperture (Vialet-Chabrand *et al.*, 2016; Lawson and Vialet-Chabrand, 2018). The changes exhibited by GCs alter

stomatal aperture and affect the flux of gases between the atmosphere and the internal leaf environment and therefore have ultimate control on photosynthetic processes and water loss from the plant (Vialet-Chabrand *et al.*, 2016). The co-ordination of stomatal activities and photosynthesis may involve GC chloroplasts, which have been shown to carry out photosynthetic electron transport and Calvin cycle activities (Lawson et al., 2006; Cotelle and Leonhardt, 2016; Daloso *et al.*, 2017). Manipulating the GC Fd contents in the ictB precursor plants is expected to enhance ETC for efficient stomata operation.

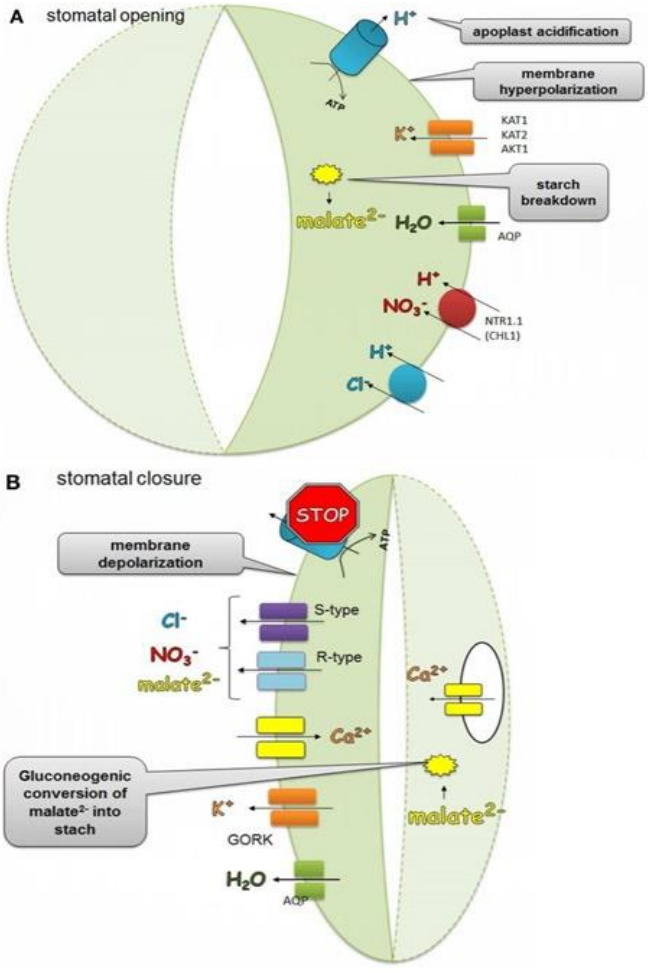

Figure 1. 2: Light signals and metabolism in guard cells trigger stomatal opening (A), the light signals are transmitted from photosystem I and photosystem II through the plastoquinone pool and to Fd, leading to the activation of H^+ -ATPase. Abscisic acid

(ABA) synthesis is inhibited, H^+ is pumped from the guard cells and the membrane hyperpolarizes which leads to the activation of K^+ inward rectifying channels (KAT1, KAT2, AKT1). Starch degradation takes place to form malate^{2-} anion while NO_3^- and Cl^- ions influx contribute to the intracellular solute assembly that can initiate sugar import or can be used for the synthesis of sugars. Ions supplied into the guard cells and water transported via aquaporins produce the turgor pressure that keep stomata opened. During stomata closure (B) H^+ -ATPase is inhibited by ABA synthesis and S-type and R-type anion channels are activated. The plasma membrane is depolarized, S-type and R-type channels facilitate the efflux of malate^{2-}, Cl^-, and NO_3^-. At the same time, K^+ outwardly rectifying channels such as GORK are activated through the depolarization of the membrane, which leads to the efflux of K^+. The decreased level of malate^{2-} is also caused by the gluconeogenic conversion of malate into starch. The elevation of the Ca^{2+} concentration as a result of the release of Ca^{2+} through channels situated in both the plasma membrane and in the tonoplast is another event that accompanies stomatal closure (Adapted from Daszkowska-Golec and Szarejko, 2013).

Fds also function in cyclic electron transfer (CET) of photosynthetic electrons for increased ATP synthesis without concomitant accumulation of NADPH. GC photosynthetic ETC provides ATP through direct electron transfer from Fds for the light activation of four Calvin cycle enzymes (Raines and Lloyd, 2001). GC photosynthesis could therefore provide the ATP and/or sucrose and other carbon equivalent from the Calvin cycle, all of which have been reported to play a role in stomatal opening. Therefore, GC specific Fd expression could play a pivotal role in coordinating stomatal response with mesophyll photosynthesis (Lawson *et al.*, 2002;

2003; 2008). The nature of stomata and the behavioral aspects of GCs are only one of the components that determines stomatal conductance and the fluxes of gas exchange between the internal leaf and external environment. Anatomical features such as stomata density, number and patterning all influence stomatal gas exchange and water use efficiency (WUE) of the plant (Doheny-Adams *et al*., 2012). The number and patterning of stomata on a leaf are determined by the epidermal patterning factor (EPF) protein family (Doheny-Adams *et al*., 2012; Casson and Hetherington, 2014).

The EPFs families have been shown to affect epidermal cell density, stomata density as well as cell spacing, through its role in cell division and differentiation (Doheny-Adams *et al.*, 2012; Casson and Hetherington, 2014). Understanding and manipulating EPFs has the potential to increase plant productivity and increase food supplies and energy sources, thereby, serving the need to develop improved plants for use by the ever-increasing world population. This study will utilize transgenic plants expressing the cyanobacteria inorganic carbon transporter (ictB), which have already been shown to have improved rates of photosynthesis and plant growth (Simkin *et al*., 2016). The construct of the ictB overexpression is shown in (Figure 1.3). In these tobacco plants, ictB was proposed to increase CO_2 concentration in the chloroplast for efficient carboxylation.

Figure 1. 3: Schematic representation of the *synechocystis* PCC 6803 inorganic transporter (ictB) expression vector. RB, T-DNA right border; Pnos, nopaline synthase promoter; NTPII, neomycin phosphotransferase gene; Tnos, nopaline

synthase terminator; P35S, cauliflower mosaic virus 35S promoter; HPT, hygromycin phosphotransferase; LB, T-DNA left board. Construct was used to transform wild type tobacco (cv samson) (adapted from Simkin *et al*., 2016)

Success in the genetic manipulation of stomata to improve plant WUE will to a large extent depend on the understanding of how genetic manipulations affect stomatal behaviour as well as stomatal size and patterning. The aim of this research is to take a molecular approach to alter anatomical and biochemical features of the guard cells by manipulating the EPF and Fd genes to alter stomata density and GC photosynthesis as possible mechanisms to improve water use efficiency (WUE) and overall plant productivity. Plants expressing the EPF1 and EPF2 are expected to have lesser stomata density that are bigger in sizes as opposed to plants expressing the EPFL9 genes that confers more stomata density. Whereas the GC specific Fd transgenic plants have enhanced ETC that would aid the stomata speed of response to light and also help to save water.

Overall, this thesis aims to address the question of how multiple expressions of the cyanobacteria *ict*B, EPF1, EPF2, EPFL9 and Fd would affect plant photosynthesis, productivity and development in *Nicotiana tabacum*?

1. 2 Crop yield improvement

The RubisCO enzyme that fixes CO_2, can also catalyse uptake of O_2 in a process called photorespiration (Figure 1.4), which is regarded as a wasteful process due to its high energy demands that are associated with recycling the 2-phosphoglycolate produced (Eckardt, 2005).

.

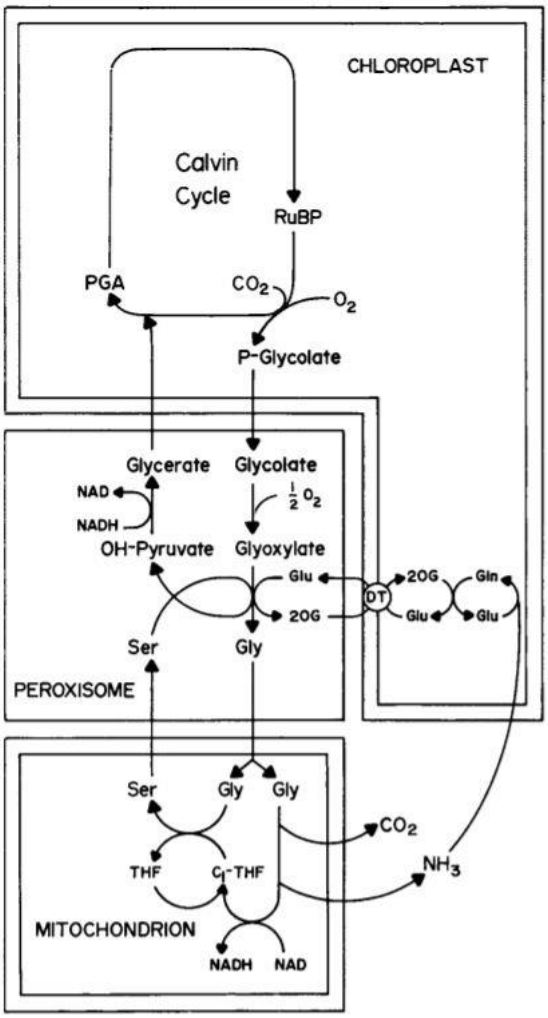

Figure 1. 4: Schematic representation of photophosphorylation; the phosphoglycolate produced by RubisCO oxygenase activity is converted to Glycolate by phosphoglycolate phosphatase in the chloroplast. The fate of the Glycolate is in the peroxisomes where it is catalysed to Glyoxylate by glycolate oxidase. Glyoxylate

undergoes transaminated to Gly by either Ser:glyoxylate aminotransferase or Glu:glyoxylate aminotransferase. The Gly enters the mitochondria where it is converted to CO_2, ammonia, and the methylene group of methylene tetrahydrofolate (C1-THF). Gly and C1-THF undergo condensation to produce Ser, which enters the peroxisome and is deaminated to hydroxypyruvate, then reduced to Glycerate by hydroxypyruvate reductase. Glycerate moves to the chloroplast and is phosphorylated to 3PGA intermediate for the Calvin cycle (adapted from Eckardt, 2005).

Recently, there have been considerable research efforts focusing on attempts to increase photosynthetic efficiency to reduce most of the side effects of photorespiration and increase Calvin cycle activity in C_3 plants (Bonfil *et al*., 1998; Lieman-Hurwitz *et al*., 2005; Raines, 2011). One such attempt was the introduction of a cyanobacterial gene that encodes for a putative inorganic carbon transporter (*ict*B) and is believed to increase the levels of CO_2 at the active site of RubsiCO (Lieman-Hurwitz *et al*., 2005; Simkin *et al.*, 2015). Analysis of ictB has shown that it is a hydrophobic protein with 10 transmembrane domains that is well conserved among cyanobacteria (Lieman-Hurwitz et al., 2005). The exact role of ictB is not yet known because it has not been possible to inactivate it or it's homologue from Synechocystis (Lieman-Hurwitz *et al.,* 2005) but *ict*B expression in transgenic tobacco has been shown to promote photosynthesis and improve yield (Price *et al.*, 1998, 2011; Simkin *et al*., 2015).

Other studies of ictB transgenic plants also indicated that the presence of the ictB resulted to a positive impact on crop photosynthetic efficiency and overall crop yield (Lieman-Hurwitz *et al*., 2012; Simkin *et al*., 2015; Hay *et al*., 2017). Therefore,

manipulating stomata density by overexpressing the EPFs or stomatal behavior via manipulation of GC electron transport in *ict*B plants would be expected to further improve the efficiency of CO_2 assimilation, better water-use efficiency (WUE), reduced leaf heat stress due to speedy stomata and possibly the increase in overall plant productivity.

1. 3 Co-ordination of guard cell and mesophyll activities during photosynthesis

In most plants, there is a co-ordination of stomatal activities with respect to photosynthetic demands. In both C3 and C4 plants, stomata open during the day to allow exchange of gases and close at night, whereas in CAM stomata open at night for CO_2 uptake which is fixed into a four-carbon oxaloacetate (OAA) and stored as malate in the vacuole overnight. During the day CAM close stomata, malate is decarboxylated and CO_2 is released for fixation by RubisCO using the end products of photosynthetic electron transport chain (Raines, 2011; Ming and Wai, 2016). The C4 and CAM plants differ from C3 in that both fix CO_2 into a four- carbon intermediate using phosphoenolpyruvate carboxylase (PEPC) (Daloso *et al*., 2017)

Photosynthetic CO_2 reduction as a light driven reaction takes place mostly during the day (Raines, 2011; Ming and Wai, 2016; Xuan *et al*., 2017). Although, there is a disparity in the mode of stomata activity in the different plant types, the close correlation between A and g_s shows that there is a co-ordination between stomata and the mesophyll cells to meet the photosynthetic needs of the plant. The ability of a plant to reduce water loss, increase CO_2 fixation and survive in dry environment is

an adaptation to operate more efficiently by separating two major events over time.

This co-ordination of stomatal GC and mesophyll activities helps to improve productivity of food crops by allocating sufficient CO_2 for energy production, and synthesis of starch and sucrose (David and Michael, 2005; Sage and Stata, 2015; Boxall *et al.*, 2016; Xuan *et al*., 2017). Four key Calvin cycle enzymes are also regulated at different times in the epidermal and mesophyll cells respectively (Michelet *et al*., 2013). Plants also adapt to certain biotic and abiotic stress by altering stomatal density and patterning on new developing leaves for efficient gas exchange. Several photoreceptors and ligands such as epidermal patterning factors (EPFs) family form series of cascade signaling events that lead to the light mediated systemic control of stomatal development (Casson and Hetherington, 2014).

1. 4 The Epidermal Patterning Factor (EPF) family and signal peptides

Members of the EPF family play a predominant role in stomatal development (Katsir *et al*., 2011; Doheny-Adams *et al.*, 2012; Casson and Hetherington, 2014; Franks *et al*., 2015). The initiation of the stomatal lineage starts with an asymmetrical division of a multipotent epidermal (protodermal) cell to give rise to a meristemoid and a larger daughter cell. Further division and differentiation leads to the generation of a specialized stomatal guard cell (GC), with the ultimate function of regulating plant gas- exchange with the atmosphere.

Generally, stomata require positional signal to coordinate the asymmetric divisions that create GC and also enforce patterning rules that dictate that two stomata are not in direct physical contact (Hara *et al*., 2007). Four EPF members have been characterized to play major roles in stomatal development: EPF1, EPF2, EPFL9 (STOMAGEN) and EPF6 (CHALLAH or CHAL) (Kondo *et al.*, 2010; Sugano *et al*., 2010; Doheny-Adams et al., 2013; Casson and Hetherington, 2014). Collectively, these ligands affect both the frequency and nature of asymmetric divisions but there exist a functional diversification among EPF family members and the receptors (TMM, ER, ERL1 and ERL2) through which they signal (Katsir *et al*., 2011; Lee *et al.*, 2015).

1. 4. 1 Distinct roles of EPF in stomata development

EPF1 and EPF2 inhibit stomatal development through a common receptor but act at relative different developmental stages (Fig. 1.5) (Hara *et al*., 2007; Doheny-Adams et al., 2012; Katsir *et al*.,2011). Hunt and Gray (2009), illustrated that EPF2 is expressed in protodermal cell that are yet to undergo division and responsible for regulating early decisions that impact both stomatal development. EPF2 overexpression was shown to inhibit asymmetric divisions into the stomatal lineage, whereas loss of EPF2 increased asymmetric divisions leading to the increased generation of both stomata and neighboring stomatal lineage ground cells (Kondo *et al*., 2010; Doheny-Adams *et al.,* 2012; Casson and Hetherington, 2014).

EPF1 has been shown to be expressed at a later stage during division and was first noticed in the meristemoids as demonstrated in EPF1 overexpression lines, where protodermal cells divide asymmetrically but the resulting meristemoids do not differentiate further (Hara *et al*., 2007). The most noticeable defect associated with

EPF1 is the abnormal orientation of asymmetric divisions leading to the development of pairs of physically adjacent stomata (Hara *et al*., 2007). The epf1 and epf2 double mutants lacking the EPF1 and EPF2 gene generated an additive phenotype that exhibit greatly increased stomatal densities, and also have stomatal pairing and additional arrested cells (Hunt and Gray, 2009; Doheny-Adams *et al*., 2012; Casson and Hetherington, 2014).

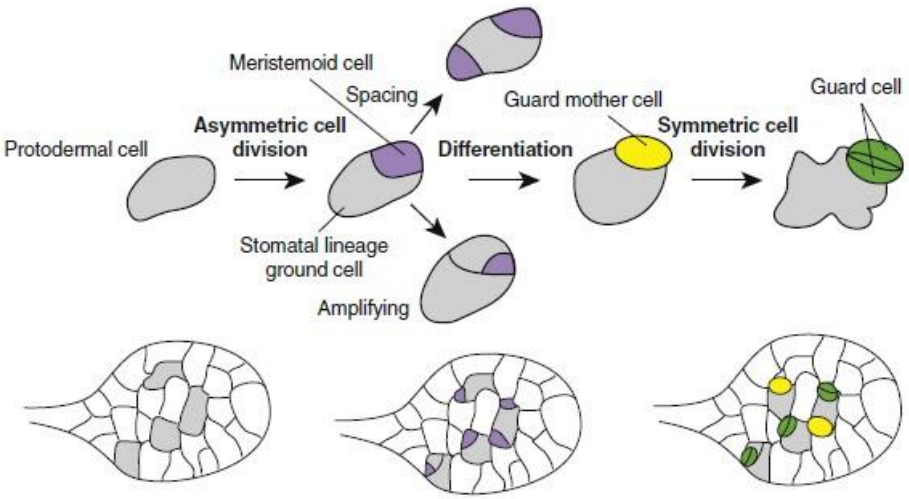

Figure 1. 5: An illustration of stomatal development process; protodermal cells undergo assymetric cell divisions to yield the stomatal lineage ground cell and a meristemoid cell (purple), which undergo further differentiation to guard mother cells (yellow). The guard mother cells undergo symmetric cell division to produce the guard cells (green) (adapted from Katsir *et al.*, 2011).

1. 4. 2 Structure of EPF Family

In Arabidopsis, the EPF family is comprised of eleven members (Hara *et al*., 2009). All EPF family members possess a C-terminal region with six to eight cysteine that are spatially conserved (Katsir *et al*., 2011; Takata *et al*., 2013). The largest degree of sequence variation among family members is seen in STOMAGEN, which has

disulphide bridges forming between cysteine residues 13 and 20, between 8 and 41, and between 16 and 43 to give rise to a predicted ‘knot’ structure with surface loop (Figure 1.6) (Katsir *et al*., 2011). This uneven loop has been suggested to lie in a position that would encourage engagement with other proteins such as cell-surface receptors and changes in this region could explain the biochemical diversity among EPF1, EPF2, CHAL and STOMAGEN (Kondo *et al*., 2010).

Biochemical analysis of STOMAGEN has indicated the structure that encodes a 102-amino acid protein, with a leading 31 amino acid signal peptide at the amino terminus (Hunt *et al*., 2010). The mature processed STOMAGEN peptide consists of 45 amino acids of the propeptide carboxy-terminal (Figure 1.7) (Katsir *et al*., 2011). The sequence flanking the cleavage site is highly conserved among EPF1, EPF2, STOMAGEN and CHAL, suggesting that all these proteins may be subjected to similar post-translational processing to yield an active ligand of 45-60 amino acid peptide (Katsir *et al*., 2011).

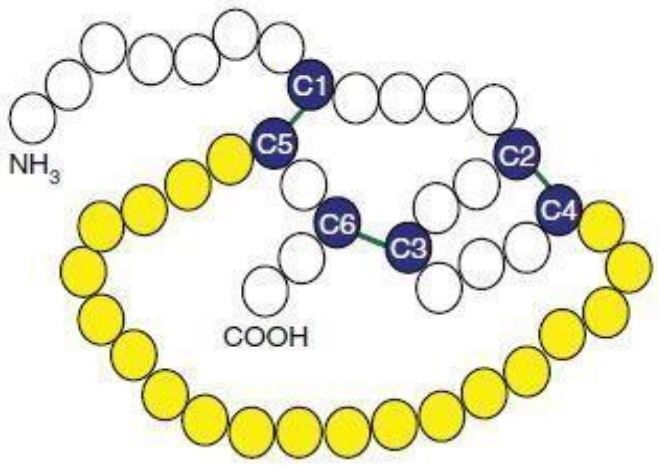

Figure 1. 6: Experimentally determined structure of STOMAGEN with conserved cysteine (blue), intramolecular disulfide bonds (green) linking the conserved cysteine

dormains and the active leading signaling peptides (yellow) (Image modeled from Katsir *et al.*, 2011).

Figure 1. 7: Processed STOMAGEN showing the active leading signaling peptide (N-terminal secretory signal sequence) and C-terminal end containing six cysteines (blue) that likely act in forming intramolecular disulfide bonds (Katsir *et al.*, 2011).

1. 4. 3 Receptors for EPF family

Genetic studies in Arabidopsis suggest that leucine rich repeat (LRR) containing receptors are responsible for EPF signaling during stomata development (Abrash and Bergmann, 2010; Katsir *et al*., 2011). The EPF receptor known as ERECTA family (ERf) was first discovered to be involved in inflorescence growth by binding to EPF4 and EPF6 (Masle *et al*., 2005; Uchida *et al*., 2012), but subsequently was also found to be involved in series of other biological roles which included heat-stress response, disease resistance and stomatal patterning (Redei, 1965; Qi *et al*., 2004; Shpak *et al*., 2004; 2005). The ERECTA family receptors (ERf) which belong to class XIIIb of the LRR receptor-like kinase family was shown to coordinate the activities of EPF1, EPF2 and CHAL (EPF6 subfamily of EPF family) (Abrash and Bergmann, 2010). Erf was also reported to mediate STOMAGEN activity during normal cell growth and oxidative stress (Cui *et al*., 2014).

Although, harmful to the plant, the antioxidant system plays a key role in redox signaling and ROS have been reported to act as signal molecules during plant

development (Potters *et al*., 2009). ERf receptors have been shown to be required for redox-mediated cortex proliferation (Cui *et al*., 2014). It has been suggested that during oxidative stress, STOMAGEN is activated and the oxidized form binds to ERf to initiate the signaling pathway (Cui *et al*., 2014). In an excellent study Yang and Sack (1995) reported another receptor-like protein called the TOO MANY MOUTHS (TMM) that is expressed in the developing epidermis and mediates the activities of EPF1, EPF2 and STOMAGEN but decreases the activity of CHAL. Unlike TMM, ERf has a broader pattern of expression and has been shown to be involved in additional developmental functions such a playing a general role in regulating cell proliferation (Shpak *et al*., 2004; 2005).

1. 4. 4 STOMAGEN opposition of EPF1 and EPF2

EPFL9 (STOMAGEN) has been shown to act as a positive regulator of stomatal development by antagonizing EPF1 and EPF2 (Sugano *et al*., 2010). STOMAGEN is usually expressed in the leaf mesophyll and overexpression was shown to increase stomatal density (D), reduced size (S) and induce the occurrence of physically adjacent stomata (Sugano *et al*., 2010). These results conform with Doheny-Adams *et al.* (2012), which showed that there is an inverse relationship between stomatal size and stomatal density which holds true across the Arabidopsis genotypes that was characterized. Altering EPF family expression levels to increase or decrease D caused an opposite effect in S (Doheny-Adams *et al*., 2012). Thus, the suggestion that the pathways controlling stomatal D and S appear to be linked but the impact of EPF signalling pathway on S is yet to be explored (Doheny-Adams *et al*., 2012).

RNA interference (RNAi) knockdown of STOMAGEN was reported to result in the production of fewer ground cells and stomata with increased S (Hunt *et al*., 2010;

Sugano *et al*., 2010). The interaction of STOMAGEN ligand with EPF1 and/or EPF2 negative regulators has elucidated and just like EPF1 and EPF2, STOMAGEN engage with the receptor TOO MANY MOUTHS (TMM) in order to function as a promoter for cell proliferation; suggesting a shared receptor (Lee *et al*., 2015).

Contrary to this, RNAi knockdown of STOMAGEN reduced stomatal density in epf1 and epf2 single and double mutants respectively; which also suggest independent ligand activity (Sugano *et al*., 2010), although STOMAGEN overexpression was shown to enhance stomatal phenotypes of *epf1* and *epf2* single mutants (Hunt *et al*., 2010). In other similar studies, synthetic STOMAGEN could not promote the stomatal density of *epf1* and *epf2* double mutants and this result supported the common receptor competition theory (Kondo *et al*., 2010).

Another EPF, CHAL (EPF6) reacts similarly to EPF1 and EPF2 as it can inhibit the development of stomata; but it does so in the absence of TMM receptor (Figure 1. 8) (Abrash and Bergmann, 2010; Kondo *et al*., 2010). CHAL act in an organ specific way and was identified to be stem-specific suppressor of *tmm* mutants. Although, *tmm* does not produce stomata on stems, they conversely display excess stomata on their leaves (Abrash and Bergmann, 2010).

A knockdown of CHAL restored stomata on the stems of *tmm* but did not affect the leaf stomata development, thereby providing a clue to the divergent phenotypes of *tmm* in the leaves and stem (Abrash and Bergmann, 2010). Although, CHAL was shown to be expressed in the inner layers of stem tissues and hypocotyl but not in leaves or epidermis, expression studies revealed that CHAL interacts with ERf to prevent stomatal development (Abrash and Bergmann, 2010).

Contrary to the EPFs, whose functions are controlled by ERf and TMM, the effects of overexpressing CHAL are amplified in the absence of TMM. Thus, the abnormal exhibited relationships lead to the assumption that TMM may act as a buffer for the ERf pathway by absorbing excess CHAL and preventing its interference with epidermal patterning (Abrash and Bergmann, 2010).

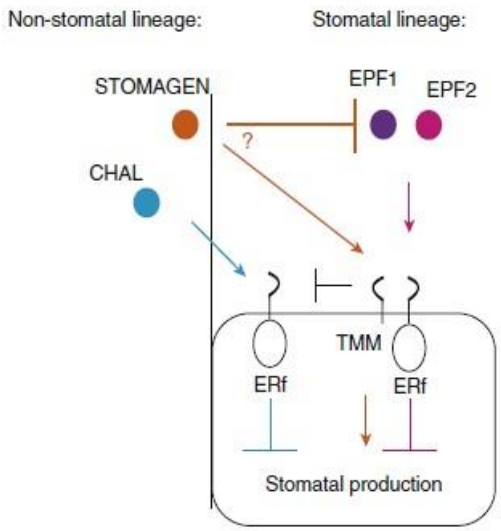

Figure 1. 8: EPF ligand–receptor interactions; EPF1 and EPF2 bind to ERf receptor to inhibit stomata development, CHAL (EPF6) also binds to ERf receptor to inhibit stomata development but STOMAGEN (EPFL9) binds to the receptor TMM to promote stomata production. In the presence of the TMM receptor, the ERf is inhibited from binding to the negative EPF ligands (Adapted from Katsir *et al.*, 2011).

The basic helix-loop-helix (bHLH) transcription factor SPEECHLESS (SPCH) was also reported as regulatory promoter of stomatal lineage initiation by being expressed in so many protodermal cells and it is required for these precursor cells to carry out stomatal generating divisions (MacAlister *et al*., 2007). EPF2 and SPCH exhibit

overlapping expression but *spch* mutants do not express EPF2 (Hara *et al*., 2009). This form of expression, coupled with the characteristics of mutants, gave an insight on a potential negative looping feedback regulation of epidermal cell development; where protodermal cells that can divide under SPCH activity turn on EPF2, which subsequently inhibit divisions (Hara *et al*., 2009).

While four of the EPF family have been characterized, the function of an additional seven members are yet to be ascertained (Katsir *et al*., 2011). Lehti-Shiu *et al*. (2009) in their study reported the existence of different homologues of TMM and ERf in various plant species. Given the array of phenotypes attributed to ERf mutants, it could be inferred that the remaining EPF ligands function in other ERf activities. The presence of these homologues of ligands and receptors in diverse plants is an indication that cell-cell signaling could be an ancient mechanism in stomatal development among species (Peterson *et al*., 2010).

1. 5 The Calvin Cycle activities in stomatal guard cells (GCc)

The photosynthetic carbon reduction cycle or the Calvin cycle is the fundamental photosynthetic process that results in the synthesis of carbohydrate from carbon dioxides (CO_2) and water (H_2O) in plants. The Calvin cycle has been shown to take place in the mesophyll cells and in the chloroplasts of the stomata guard cells (GCs) (Ainsworth and Rogers, 2007; Raines, 2011; Lawson and Blatt, 2014; Daloso *et al*., 2017). The light driven reaction of photosynthesis is powered by the NADPH and ATP that are generated during exposure of the leaves to light sources. Carbon reduction in plants is called a cycle because CO_2 is assimilated in a cyclic way that constantly regenerates key intermediate metabolites (Raines, 2011; Xuan *et al*.,

2017). The simple product of this cycle is 3- phosphoglycerate and serves as the precursor of more complex biomolecules such as sugars, polysaccharides and associated metabolites (Figure 1.9).

Generally, plants are classified based on the pathway of CO_2 fixation during photosynthesis. The plants that fix CO_2 with ribulose 1,5-bisphosphate to form 3-phosphoglycerate are called C3 (Raines, 2011). In addition to fixing CO_2, the enzyme RubisCO can also catalyze uptake of O_2 in a process called photorespiration which is regarded as a wasteful process due to its high energy demands that are associated with recycling the 2-phosphoglycolate produced (David and Michael, 2005).

The rate of CO_2 fixation in C3 plants is often rate limited by the low level of CO_2 at the carboxylation site of RubisCO where O_2 abound leading to photorespiration and inhibiting the CO_2 fixation process. Also, at high temperature, the affinity of RubisCO for CO_2 decreases leading to the promotion of the wasteful oxygenase reaction. It is worth noting that the stomata play a very crucial role in maintaining leaf temperature for efficient photosynthesis through evaporative cooling (Urban *et al.*, 2017). Therefore, adequate stomata density and density as well as speed of stomatal response to varying leaf temperatures is critical to efficient photosynthesis. However, some plants that grow in the tropics, arid and few temperate-zones crops such as maize, sugarcane, sorghum, pineapple and cactus, have evolved solutions to bypass the problem of photorespiration (Raines, 2011).

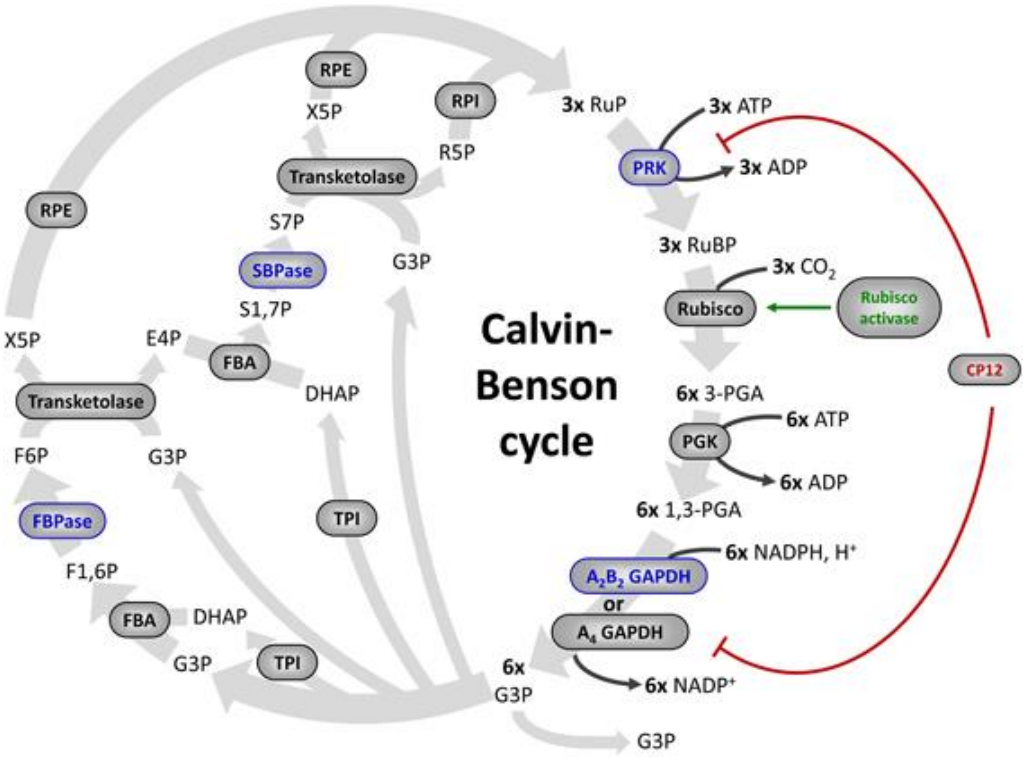

Figure 1. 9: The Calvin cycle pathway in guard cell (GC) chloroplast showing the four enzymes (blue) that are activated directly by the ferredoxin/thioredoxin (Fd/TRX) system. Some proteins CP12 (red) and RubisCO activase (green) are also regulated by TRX. CP12 binds to glyceraldehyde-3-phosphate dehydrogenase (GAPDH) and phosphoribulokinase (PRK) thereby inhibiting both enzymes in the dark. Fructose-1,6-bisphosphate aldolase (FBA) and sedoheptulose-1,7-bisphosphatase (SBPase) are two other enzymes that are light induced by electrons from Fd (Adapted from Michelet *et al*., 2013).

1. 5. 1 Ferredoxin (Fd) in guard cell (GC) metabolism

Ferredoxin is directly or indirectly involved in the deactivation and activation of a number of enzymes in carbon fixation, translation, malate shuttling, lipids and starch metabolism as well as in the detoxification of reactive oxygen species (ROS) (Schurmann and Buchanan, 2001; 2008). Thioredoxins (TRXs) are enzymes that

accept electrons from Fd, interact with specific disulphide sites on targets protein thereby reducing them to their sulfhydril forms, thereby changing their structures and catalytic activity (Figure 1.10).

Investigation of the molecular mechanism of this light-dependent regulation led to the identification of the ferredoxin/thioredoxin (Fd/TRX) system that plays a crucial role in numerous redox- and light-dependent reactions in chloroplasts. Four enzymes of the Calvin cycle namely; glyceraldehyde-3-phosphate dehydrogenase (GAPDH), phosphoribulokinase (PRK), Fructose-1,6-bisphosphate aldolase (FBA) and sedoheptulose-1,7-bisphosphatase (SBPase) that are regulated by light were shown to contain a regulatory disulfide oxidized in the dark and reduced in the light by TRX. This reduction allows transition from a low active form to a fully active enzyme.

Other enzymes that accept electrons directly from Fd such as FNR, glutamine:2-oxoglutarate aminotransferase (GOGAT) and nitrite reductase (NiR) as well as Fd isoforms have been shown to target or interact with TRX (Hall *et al*., 2010; Lichter and Haberlein, 1998; Marchand *et al*., 2004). Chloroplast ferredoxin thioredoxin reductase (FTR) catalyzes the reduction of thioredoxins for the activation of four Calvin cycle enzymes (Figure 1.10) (Michelet *et al*., 2013; Daloso *et al*., 2017).

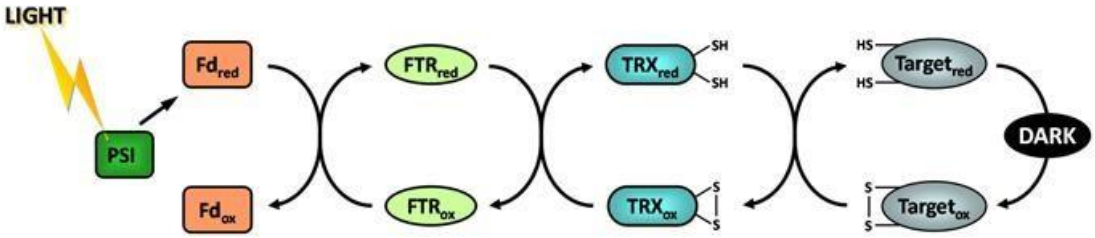

Figure 1. 10**:** The Fd/TRX system showing Fd-enzyme light activation pathway. Light energy from sunlight releases electrons from PSI, the electrons reduces the oxidized Fd_{ox}, the Fd_{red} then reduces the FTR_{ox}, the FTR_{red} then reduces the TRX_{ox}, the TRX_{red} then acts on the oxidized regulatory region of its target by reducing it to make the target molecule active (Adapted from Michelet *et al*., 2013).

1. 5. 2 History and Backgrounds

The term ferredoxin (Fd or Fdx) is still widely used to describe a variety of small soluble [Fe- S] cluster-containing proteins including a protein that was isolated from *Spinacia oleracea* and found to be the stromal electron acceptor from PS1 (Tagawa and Arnon, 1962). This Fd molecule have been found to contain a [2Fe-2S] active centre, coordinated by the S-side chains of four highly conserved cysteine (Cys) residues (Figure 1.11) (Fukuyana *et al*., 1980). The iron-sulphur cluster was also found to confer a redox potential of around -300 to -460mV (Williams-Smith and Cammack, 1977).

Plant type Fds are small in size (around 10kDa) with highly conserved amino acids sequences from cyanobacteria to higher plants (Bertini *et al*., 2002). Fds are composed of three to five β-strands and one to three α-helices, with the [2Fe-2S] cluster located at one end. A short distance separates the active Fe in the cluster and the soluble environment and the [2Fe-2S] is usually surrounded by a hydrophobic patch. The protein surface outside the hydrophobic patch is rich in charged amino

acid residues particularly glutamic and aspartic acids with side chains conferring the negative charges that are fundamental to the alignment of Fd in the active site of its partner enzymes (Kurisu *et al*., 2001).

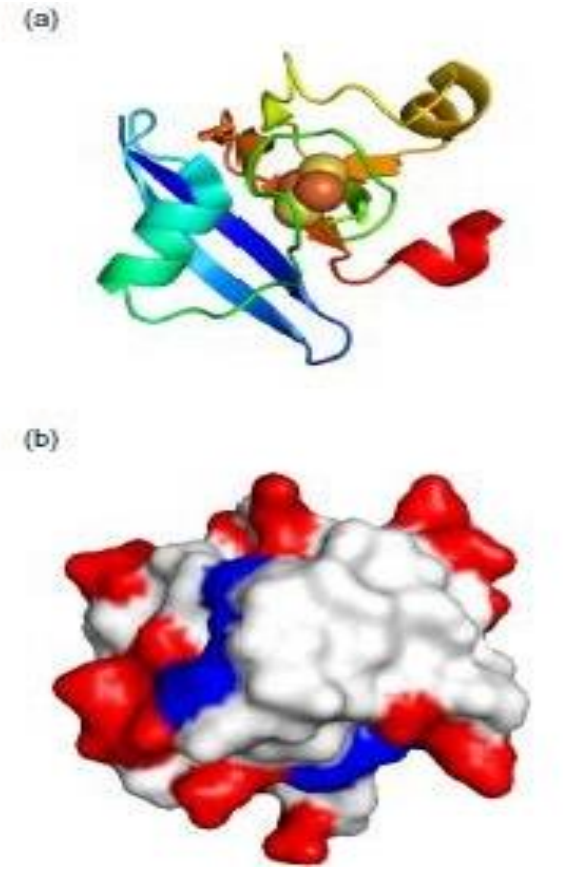

Figure 1. 11: The structure of maize ferredoxin (Fd), (a) secondary structure in cartoon form, protein in N-terminal (blue)to C-terminal (red), Fe in brown and S in yellow, and (b) showing charge distribution in a ring around a hydrophobic patch that immediately surrounds the [2Fe-2S] cluster (Adapted from Hanke and Mulo, 2013).

The hydrophobic interaction between the surface of Fd and its partner enzymes cannot be too complementary, and if the affinity between the two proteins is increased by mutation, the activity of the enzyme can be diminished due to the

competitive binding inhibition of reduced Fd (Fd_{Red}) binding to the enzyme active site, which is blocked by oxidized Fd (Fd_{Ox}) (Thomsen-Zieger *et al*., 2004).

1. 5. 3 Photosynthetic Fds

Leaf-type Fds play a key role in LET by transferring electron from Fd_{Red} to Fd-$NADP^+$ oxidoreductase (FNR) which then reduces nicotinamide adenine dinucleotide phosphate ($NADP^+$) (Yamamoto and Shikanai, 2017). The final reduction of one molecule of $NADP^+$ requires two electrons while Fd can only donate one electron and therefore two molecules of Fd_{Red} must bind accordingly for full reduction to NADPH (Figure 1.12A). This NADPH provides the reducing power in a number of reactions including CO_2 fixation in the Calvin Cycle (Karplus and Bruns, 1994; Karplus *et al.,* 1991; Yamamoto and Shikanai, 2017).

In addition to the LET, electrons derived from PSI may be channeled to CET, which cycles the electrons to the Cytochrome *b6f* complex through Fd (Johnson, 2011). During CET (Figure 1.12B) the proton gradient that drives ATP synthesis is formed without concomitant production of NADPH and results in the reduction of non-photochemical quenching (NPQ) (Heber and Walker, 1992). Consequently, it has been assumed that CET is needed to satisfy the chloroplast ATP requirements at low to moderate light or to function as a safety valve for excess electrons under adverse environmental conditions such as extremely high light, low ambient CO_2 concentration or drought (Makino *et al.*, 2002; Lehtimaki *et al.*, 2010; Yamamoto and Shikanai, 2017).

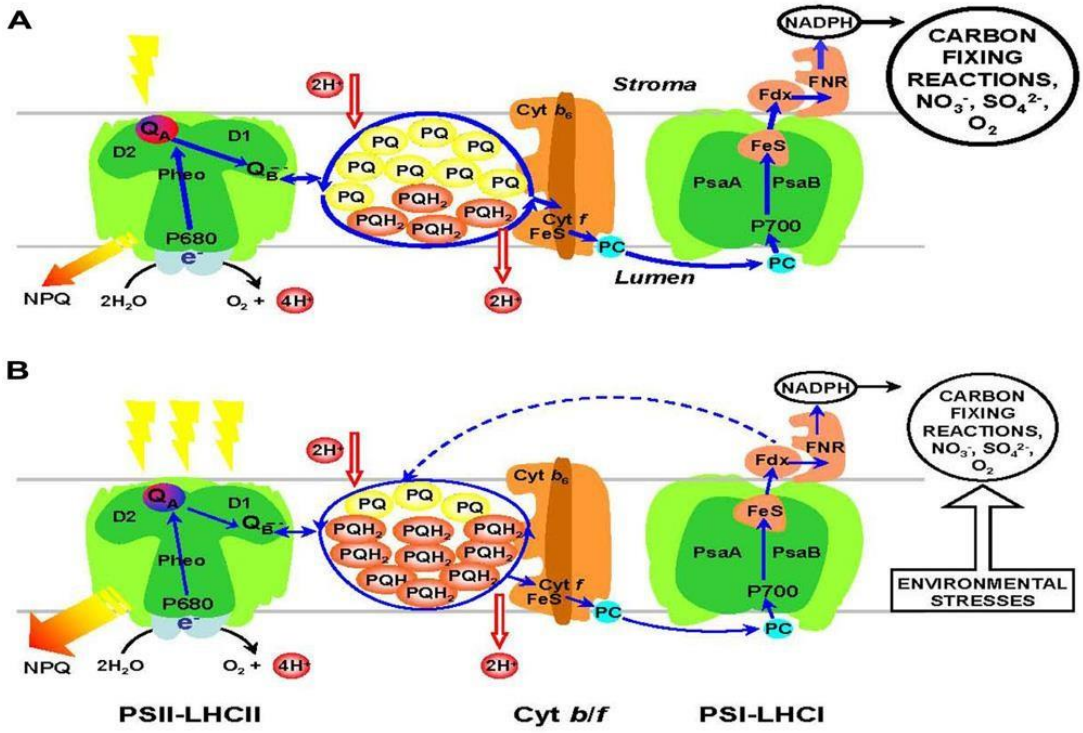

Figure 1. 12: The Linear (**A**) and cyclic (**B**) photosynthetic electron chain. The ferredoxin (Fdx) plays crucial role channeling electrons for generating high energy molecules and for regulating the plastoquinone pool under adverse weather conditions (Figure adapted from Huner *et al*., 2012).

1. 5. 4 Role of Fd in chlorophyll biosynthesis and catabolism

The process of chlorophyll biosynthesis in the chloroplast requires chemical energy in form of ATP and the reducing potential from NADPH (Tanaka *et al*., 1998; Yamamoto and Shikanai, 2017). In the above reaction, the first precursor for chlorophyll *a* synthesis is 5-aminolevulinic acid which leads to the subsequent accumulation of chlorophyll *a* and chlorophyll *b*. However, the conversion of chlorophyll *a* to chlorophyll *b* is catalysed by an Fd dependent enzyme called chlorophyll *a* oxygenase (CAO) which is also implicated in the importation of chloroplast proteins and stabilization of the light harvesting proteins Lhcb1 and

Lhcb4 (Reinbothe *et al*., 2006). Under certain conditions such as bright sunlight, chlorophyll *b* may be converted to chlorophyll *a* by a 7-hydroxymethyl chlorophyll *a* reductase enzyme that is Fd-dependent (Meguro *et al*., 2011).

Fd also plays a key role in the biosynthesis of phytochromes by serving as the reducing power for haem oxygenase and phytochromobilin in higher plants (Tanaka and Tanaka, 2006, 2007; Dammeyer and Frankenberg-Dinkel, 2008). It also functions in the formation of glycerolipids that make up the lipid bilayers of cellular membranes in the plastids, Fd serves as an electron donor for the lipid desaturase enzymes that catalyses fatty acids desaturation (McKeon and Stumpf, 1982; Wada *et al*., 1993).

The light excitation of free chlorophyll (photo-oxidation) and associated catabolites results to the production of ROS which are degraded through the chlorophyll degradative pathway. Fd activates two key enzymes in this pathway; pheophorbide a oxygenase (PaO) and red chlorophyll catabolite which are involved in leaf senescence (Rodoni, 1997). Senescence is the final stage of leaf development, that leads to the death of the entire leaf. The process is highly regulated and involves degradation of chloroplast components, such as thylakoid membranes, along with the remobilization of amino acids from chl *a*/*b*-binding proteins, and the subsequent release of potentially phototoxic chl. It is commonly believed that chl degradation in plants helps to avoid this toxicity (Rodoni, 1997; Matile *et al*., 1999).

Another sink for the chloroplast ETC sink is the monodehydroascorbate (MDA). In an excellent study, Asada (1999) showed how excess electrons from PS1 under

limiting conditions, may photoreduce O_2 to superoxide radical (O^-) which is subsequently disproportionated to hydrogen peroxide (H_2O_2). The H_2O_2 generated can be eventually reduced to water by Fd-dependent ascorbate. This detoxification is catalysed by ascorbate peroxidase (APX) enzyme with the spontaneous release of MDA which can be reduced to ascorbate by Fd (Miyake and Asada, 1992). This process is very important in non-photochemical quenching (NPQ). The process of NPQ is one of the short-term responses of plants to excessive lighting due to the build-up of low pH within the thylakoid by switching the light antenna into heat dissipation mode rather than trying to utilize the excess light (Kulheim *et al.,* 2002).

1. 5. 5 Fd Family diversity

Significant data is available to show the multiple gene copies of Fd isoproteins within a single cultivar; *Arabidopsis*, maize and *Oryza sativa* respectively contain six, eight and five coding sequences listed as Fd in genomic and cDNA databases (Hanke and Mulo, 2013). Due to the important roles of Fd in photosynthetic electron transport and a broad range of enzymes, it can be inferred that some of these variant Fds are redundant or simply constituted in mechanisms that favour channeling into different metabolic processes. Voss *et al*. (2011) suggested that the high conservation of these Fd genes across the evolutionary tree is an indication that they might have specific conserved functions from cyanobacteria to chloroplast metabolism and the differences in gene expression as well a protein activity are well documented in relation to nitrate assimilation in *Chlamydomonas* and maize (Terauchi *et al*., 2009; Matsumura *et al*., 1997).

Amongst higher plants, the most understood diversity in Fd sequences is between photosynthetic and heterotrophic roots. Root Fds have a more positive redox potential compared to leaf type as a result of their highly differentially conserved sequences (Onda *et al*., 2000). The redox potential of root type Fd measured around -340mV, which is close to that of NADPH at -320mV making electron transfer from NADPH more favorable to root Fd_{ox} than to photosynthetic Fds, with a more negative redox potential of around -420mV (-80mV difference) (Gou *et al*., 2006). Although root type Fds have been detected at low levels in photosynthetic tissues, it is not clear if they are present in non-photosynthetic cells in leaves or co-expressed in the same cell as photosynthetic Fds (Hanke *et al*., 2004).

Higher plants also possess at least two more genes for different and highly conserved proteins that appears on sequence alignment to be chloroplast [2Fe-2S] Fds but are divided into two different groups, both of which possess significantly extended C-terminus in comparison to already studied Fds and therefore have been named FdC1(AT4G14890) and FdC2 (AT1G32550) (Voss *et al*., 2011). Information for the expression of FdC2 is lacking but FdC1 appears to be up-regulated under limiting conditions of electron acceptance at PS1 and an analysis of the purified protein showed a more positive redox potential than other plant type Fds (-200mV) which is an indication of being able to be photoreduced by PS1 but unable to transfer these electrons to NADPH (Voss *et al*., 2011).

Fds are important signaling peptides in plant metabolic processes. Similarly, several other peptides have been reported to play a crucial role in stomatal development. The photosynthetic operation of the stomata such as opening of its aperture requires a lot

of co- ordinated signal between different cells. Most of these signaling peptides have been reported as key regulators during stomatal development in plants and are classified into families of peptides that partake in epidermal-mesophyll cell to cell communication (Katsir *et al*., 2011). The co-ordination of signals within stomatal development context demands regulated expression and regulated activity of these peptides and corresponding signal receptors. In some cases, the cells involved in these processes act as both the recipients and producers of these signals; thus, generating cell-cell cross-talk or feedback loops that are central to the development of the stomata density and number that determines the rate of gas exchange.

1. 6 Conclusion

In order to gain more information on the *ict*B transgenic tobacco plants that were used for this work, phenotypical and physiological studies were done to gain further insight into the functions of EPFs and Ferredoxins. These multiple transformed plants with EPFs and Fd are predicted to show increase in leaf CO_2 uptake compared to the WT and single *ict*B lines. This research work addresses the question of whether multiple gene expression of *ict*B, EPF and Fd is a viable means of improving plant photosynthesis? It provides the opportunity for more research work around the long-term conservation of these genes by these transgenic plants given that the atmospheric CO_2 continues to increase everyday as a result of global warming.

In order to study the functional expression of Fd in guard cells (GCs) and gain insight into their role in stomatal opening during photosynthesis;

- The coding region of Ferredoxin “leaf-type was isolated and prepared for molecular and physiological analysis using a YFP reporter gene in *ict*B Tobacco and *Arabidopsis.*
- Parallel physiological and molecular studies were carried out to assess the impact of EPFs on stomatal development and leaf photosynthetic functions.

2.0 Chapter 2

2. 1 Materials and Methods

2. 1. 1 Plant material and growth conditions for physiology study

Seed stocks of wild type Samson tobacco (WT) and ictB independent lines (TB4-7 and TB6) were obtained from Prof. C. A. Raines laboratory, University of Essex. All seeds were grown on soil (Levington F2, Fisons, Ipswich, UK) for two weeks in a controlled environment at an irradiance of 150 (μmol photons m^{-2} s^{-1}), temperature of 25°C, relative humidity of 60%, under 16-h photoperiod (long days). After which 12 plants from the two independent transgenic ictB tobacco lines and WT controls were re-potted into (3-inch) individual pots and grown under the same conditions for further two weeks. Then plants were transferred to 7-inch pots and grown in a controlled green house for further three weeks at 21/20°C day/night, in a 16-h photoperiod and natural light supplemented with high-pressure sodium light bulbs, giving between 200-350 μmol m^{-2} s^{-1} and 600-1,400 μmol m^{-2} s^{-1} from the pot level to the top of the plant, respectively. Positions of the plants were changed weekly and watered with a nutrient medium (Hoagland and Arnon, 1950).

2. 1. 2 Selecting ictB transformants using selective media

Plant material and growth analysis was carried out using the same *Nicotiana tobacum* L.cv. Samson seeds stocks for WT and the two transgenic lines (TB4-7 and TB6). Seeds were sterilized for 10 minutes by washing in a 20% v/v commercial bleach plus one drop of Tween 20 in separate Eppendorf tubes for 10 minutes. Bleach solution was removed with a pipette and the seeds washed five times for 5 minutes with

distilled water. Following this, seeds were placed on filter papers and allowed to dry in the flow-hood cabinet.

Seeds were germinated on 0.8% (w/v) agar containing 0.44% Murashinge and Skoog medium (MS) with 1% Sucrose, 1% Kanamycin antibiotic, pH 5.9 stabilized by KOH. The plates were placed in a growth cabinet at 25^{o}C, 16h light/8h dark, light level of 200µmol $m^{-2}s^{-1}$ and allowed to geminate for 3 to 4 weeks. Non-transformed plants turned yellow and were not selected for next phase. Six- eight plants were selected and grown for seed from each of the independent lines and transferred into pots (7-inch) with soil and grown in the green house controlled environment for further 4 weeks in 300 (µmol photons m^{-2} s^{-1}), 25°C–30°C day/20°C night, relative humidity of 60%, in a 16-h photoperiod and natural light supplemented with high-pressure sodium light bulbs, giving between 200-350 µmol m^{-2} s^{-1} (lowlight), 600-1,400 µmol m^{-2} s^{-1} (highlight) from the pot level to the top of the plant. Plants were watered with ¼ strength Hoaglands solution and grown for seed (T2) collection.

The T2 seeds were used for another tissue culture selection in a Kanamycin resistant plate and from these plates, a segregating population was identified. In this case it is expected that the ratio of plants that would be alive to dead would be 3:1. From these plates with this growth pattern, 1/2 of the germinated plants would be heterozygous, 1/4 would be homozygous and the other 1/4 would be WT (azygous). Transporting these plants in soil for T3 seeds was done to limit error in selecting homozygous lines for transformation. The seeds from T3 plants were further cultivated in a kanamycin plate and the plates with 100% growth would be homozygous and can be confirmed

with PCR. Similarly, azygous control would yield 100% dead plants when grown on a kanamycin media.

2. 1. 3 DNA Extraction

DNA extractions from leaf discs were carried out for PCR verification of the presence of ictB inserts on the transgenic lines while using the WT as control. The leaf extraction was done by placing approximately 10 mg of plant material in a 1.5ml microfuge tube with a metal bead, followed by addition of 200µl of suspension solution (DNA extraction buffer) and tissue ground using a mechanical grinder/homogenizer for 3 minutes. The mixture was centrifuged for 5 minutes using a micro centrifuge at 13,000g, after which 150µl of aqueous (upper) phase was transferred by pipetting to a fresh 1.5ml tube containing 100µl of isopropanol and vortexed gently for 30 seconds. Centrifugation was repeated at 13,000g for 10 minutes and the supernatant was removed by pipetting while the micro-centrifuge tube was allowed to dry for 30 minutes on the bench.

2. 1. 4 Polymerase Chain Reaction (PCR)

PCR was run to determine the presence of ictB DNA cloned into the transgenic tobacco lines using DNA extracts from individual plants from WT, TB4 and TB6. The PCR reaction contained 3.5µL of each primer (ictB forward: 5´-ACTGTCTGGCAAACTCTGACTTTTGC and NOS terminator reverse: 5´-TGCCAAATGTTTGAACGATC developed from ictB expression vector) (Simkin, *et al.*, 2015), 490µL of dH_2O, 52.5µL of Buffer, 11µL of dNTPs and 8.5µL of Taq

Polymerase Enzyme in a total volume of 569 µL reaction mixture. 14 µL of the reaction mix was added to 2µL of the DNA extracts from the different plant respectively to make a total of 16 µL in each tube of the PCR tray. PCR was according to the following thermal profile: initial 96°C at 2 minutes, then followed by 35 cycles each of 15 seconds denaturation at 96ºC, 15 seconds annealing at 60ºC and 45 seconds of synthesis at 72°C respectively.

2. 1. 5 IDna Genetics

All seeds from a more diverse ictB lines (TB1, TB4, TB6) and WT were grown on soil (Levington F2, Fisons, Ipswich, UK) for two weeks in a controlled environment at an irradiance of 150 (µmol photons m^{-2} s^{-1}), temperature of 25°C, relative humidity of 60%, under 16-h photoperiod (long days). After which 12 plants from the three ictB line and WT controls were re-potted into (3-inch) individual pots and grown under the same conditions for further two weeks. Plant leaf was collected from the WT and transgenic ictB lines (Table 3.1) in a 2.0 ml microfuge and sent for IDna molecular genetic screening (approximately 10 mg of plant material). This is a professional service used to screen plants in order to identify the copy numbers of ictB gene present in the plants' chromosomes. The technology is novel, but the exact principle is the intellectual property of IDna Genetics Ltd, The Norwich BioIncubator, Norwich Research Park, Norfolk, Norwich, UK, NR4 7UH. This allowed elimination of unwanted plants, saving time and costs of progeny testing.

2. 1. 6 Chlorophyll *a* Fluorescence Imaging

Chlorophyll fluorescence (CF) imaging was carried out using a Fluoroimager imaging system (Technologica Ltd., Colchester, Essex, UK). CF was performed on 3-week-old tobacco seedlings that had been initially grown in a controlled growth cabinet at 200µmol mol^{-2} s^{-1} and 400µmol mol^{-2} s^{-1} CO_2. After which all plants were transferred to the greenhouse to grow in natural irradiance with supplemental light (400-600 µmol mol^{-2} s^{-1} PPFD) at bench level. On the day of measurement, plants were dark adapted for 30 minutes to 1 hour before imaging. The operating efficiency of photosystem II (PSII) photochemistry, (*F*q′/*F*m′), was calculated from measurements of steady-state fluorescence in the light (*F ′*) and maximum fluorescence in the light (*F*m′) that was obtained after a saturating 800 ms pulse of 6231 µmol m^{-2} s^{-1} PPFD using the following equation *F*q′/*F*m′ = (*F*m′-*F*′)/*F*m′. Images of *F*q′/*F*m′ were taken under stable PPFD of 150, 50, 150, 300, 450, 600, 800, 1100 and 1400µmol m–2 s–1 PPFD respectively (Baker *et al.*, 2001; Murchie and Lawson, 2013).

2. 1. 7 Infra-red Gas exchange analysis to assess photosynthetic capacity

Gas exchange analysis was carried out using Li-cor (*LI*-6400XT, Lincoln, Nebraska, USA) portable infra- red gas analysis (IRGA) with a combined fluorescence head. The response of assimilation (*A*) was measured as a function of internal CO_2 concentration (C_i). Measurement were performed on the youngest attached fully expanded leaf, which was placed in the leaf chamber and left to be stabilized at saturating photosynthetic photon flux density (PPFD) of ca. 2000 µmol m^{-2} s^{-1} and ambient CO_2 concentration (*Ca*) of 400 µmol mol^{-1}. Each measurement was taken at

ambient CO_2 concentration before *Ca* was altered in a stepwise manner to 50 µmol mol^{-1} before returning to the initial value and increased in a stepwise manner to ca. 1700 µmol mol^{-1}. Readings were captured at each *Ca* concentration when measurements have stabilized (ca 1-2 min). Cuvette conditions were maintained at a leaf temperature of 25°C and a relative humidity 50-60%. The maximum carboxylation rates of RubisCO- (Vc_{max}); and the maximum rate of electron transport for RuBP regeneration (J_{max}) was determined and standardized to a leaf temperature of 25°C based on equations from Bernacchi *et al*. (2001), and using a spreadsheet provided by Sharkey *et al.* (2007).

2. 1. 8 Diurnal Photosynthesis

Diurnal measurements of leaf photosynthesis(*A*) and stomatal conductance (g_s) of a fully expanded leaf of about 19cm-21cm in length was determined with application of a sinusoidal light pattern with a maximum intensity of 2000 µmol m^{-2} s^{-1} in the middle of the photoperiod. Measurements were recorded every 30 minutes between 09.00h and 17.00h. All other cuvette conditions were kept constant; leaf temperature was maintained at 25°C and relative humidity 50-60%. The measurements were carried out using Li-cor (*LI*-6400XT, *LI-COR* 4, Lincoln, Nebraska, USA) portable infra- red gas analysis (IRGA). From this measurement of *A* and g_s, the intrinsic water-use efficiency (WUE_i) can be estimated (Simkin *et al.*, 2015).

2. 1. 9 Leaf impressions and measurements of stomatal density

Separate mature leaves were harvested, three each from wild type (WT) and ictB transgenic lines (TB4 and TB6) grown under identical controlled environment

conditions for 12 weeks. Nail polish was applied to the abaxial side of the leaf and allowed to dry completely to provide a negative impression. The negative impression was carefully peeled off the leaf using a transparent cellotape, transferred to a microscopic slide and mounted on a calibrated light microscope for investigation and imaging. Detailed stomata counts were carried out using the program Image J (http://imagej.nih.gov/ij/index.html) to adjust the colours, contrast and other effects on the leaf image so that the stomata can be more visible before counting automatically or manually.

2. 2 Searching for DNA Sequence of Interest

Eukaryotic genes have nucleotides that are made of introns and exons. Introns do not code for proteins and are therefore removed from the nucleotide sequence before further processing to protein. Exons on the other hand are the translated nucleotides that yield the amino acids that serve as the building blocks of proteins. Exons are separated from intron by splicing sites (Berg *et al.*, 2002; David and Michael, 2005). The final coding template used for protein synthesis is the intron-free messenger RNA (Figure 2.1)

The complete coding sequences of the genes of interest and primers was searched using basic local alignment search tool (BLAST) on the National Center for Biotechnology Information (https://www.ncbi.nlm.nih.gov/ , NCBI, Bethesda MD, 20894, USA) data base. The following sequences were retrieved; AT5G10310 complete EPF1 coding sequence (cds), AT4G37810 complete cds (EPF2), AT4G12970 complete cds (EPFL9) and AT1G10960 complete cds (Fd). All four cds were digitally proof checked for the restriction sites of BsaI and DraIII enzymes that

would be used for restriction cloning and if there was any, the nucleotide sequence is substituted using the genetic code so as not to alter the desired protein. After this, the 5'-CACTCTGTGGTCTCAA and 3'- GCTTTGAGACCACGAAGTG goldengate cloning overhangs which contain the restriction sites for BsaI and DraIII were attached to the 5' and 3' ends of all cds to be synthesized digitally using geneious bioinformatic software and all cds sent for chemical synthesis using Thermofisher Scientific services, Leicestershire, UK.

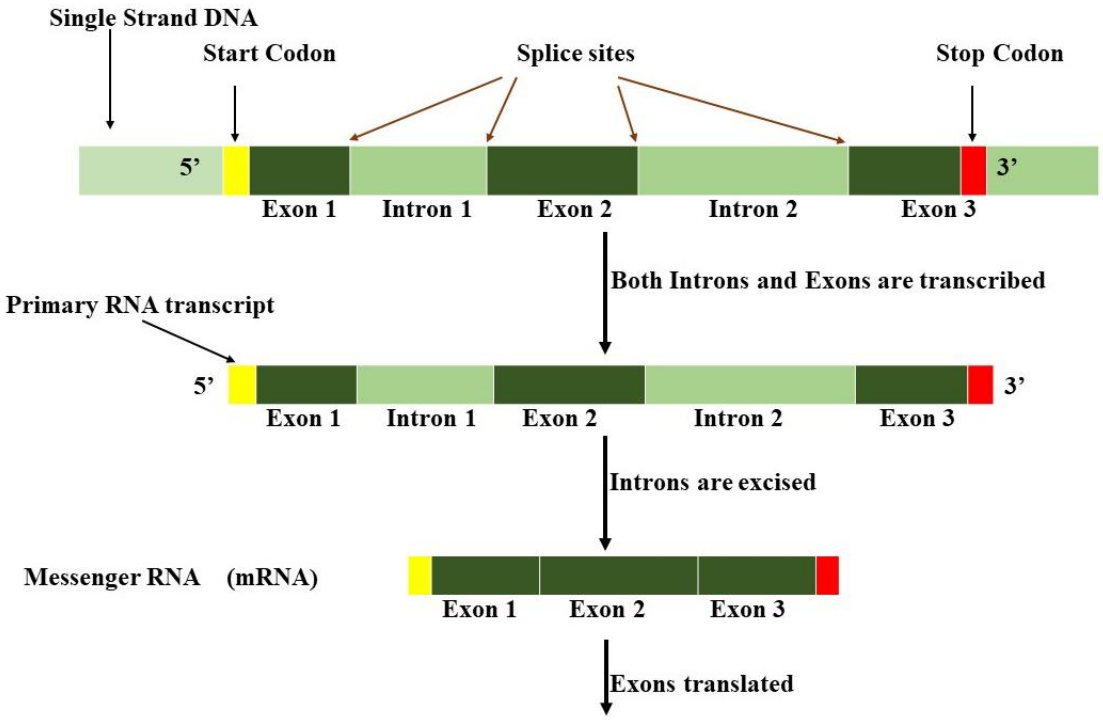

Figure 2. 1: A single stranded DNA model depicting the exons and introns along a DNA nucleotide sequence. Constitutive exons are filled in dark green while introns are filled in light green. The enzyme called RNA polymerase is responsible for the transcription and processing the primary RNA transcript to produce the mRNA. The start codon (yellow) serves as the binding site of the RNA polymerase while the stop codon (red) signal the enzyme to terminate the transcription process.

2. 2. 1 Golden gate Cloning of EPFs and Fd gene constructs

This technique is an alternative to gateway cloning and it does not involve site-specific recombination but rather relies on the use of Type IIs restriction enzymes. The Type IIs restriction enzymes cleave DNA outside their recognition site resulting in a 5' to 3' DNA overhangs consisting of any nucleotides (Berger et al., 1993; Engler *et al.*, 2008). This property of Type IIs has been used to develop protocols for the efficient assembly of multiple DNA fragments in a single restriction-ligation reaction. The inserts and cloning vectors are designed to place the Type IIs recognition site distal to the cleavage site, such that the Type IIs enzyme can remove the recognition sequence from the assembly. The net result is the ordered and seamless assembly of DNA fragments in one reaction (Figure 2.2). The accuracy of the assembly is dependent on the length of the overhang sequences.

Therefore, Type IIs restriction enzyme that create 4-base overhangs (such as BsaI/BsaI-HF®v2, BbsI/BbsI-HF, BsmBI and Esp3I) are preferred. Insert assembly must be designed carefully for the overhangs to direct the assembly. Proper checks must also be done to verification that the Type IIs restriction sites used are not present in the fragments for the assembly of the expected product (https://international.neb.com/applications/cloning-and-synthetic-biology/dna-assembly-and-cloning/golden-gate-assembly).

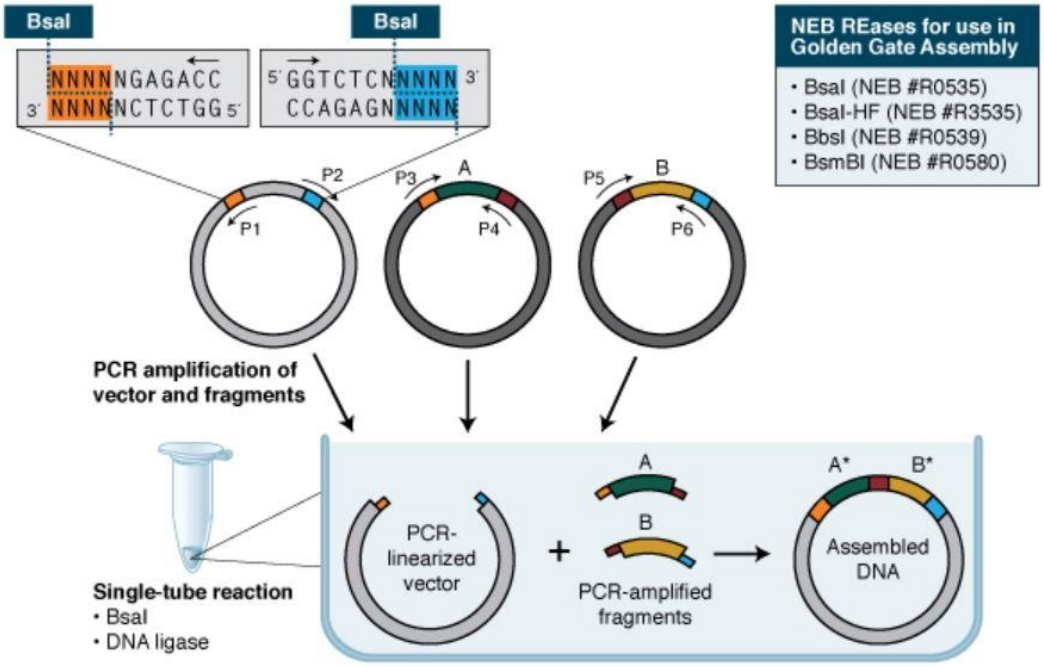

Figure 2. 2: The golden gate assembly showing the circularised destination vector (P1), entry clones P4 and P6 with respective genes of interests (A and B). The A and B inserts are involved in a 4-base overlap that are insert-derived to generate a seamless assembled DNA entry plasmid with the genes of interest (https://www.neb.com/applications/cloning-and-synthetic-biology/dna-assembly-and-cloning/golden-gate-assembly).

Using the protocols for New England Biolabs golden gate assembly kit, I developed the different levels of EPFs and Fds construct for level 0 (L0) which consist of cds and overhangs; level 1 (L1) which is an assembly of one cds with its promoter and terminator (Table 2.1); while level 2 (L2) are multiple assemblies of L1 which would contain selective markers, genes of interest by series of chemical reactions following the golden gate construct assembly. It is very important before the chemical reactions was carried out, for all reaction to be probed digitally using the bioinformatic applications such as geneious bioinformatics software (developed by Biomatters,

Auckland, New Zealand) to ensure accuracy and perfection of the one pot multiple digestions.

2. 2. 2 EPF Constructs

In order to alter the expression of the Arabidopsis thaliana EPFs in transgenic ictB tobacco plants with high photosynthetic rates, single and double constructs were made using golden gate technology. Individual constructs were developed with EPF1, EPF2 and EPFL9 synthesized cds, cloned into a goldengate level 1 vector under the expression of a 35S promotor and NOS terminator (Figures 2.3 to 2.5). The promoters used in L1s are the nopaline synthase promoter (pNOS), the Cauliflower mosaic virus 35S promoter (CaMV2x35S) and the potato (*KST1)* promoter (Simkim *et al.,* 2015). These promoters drive the expression of the associated L0 gene. The role of the terminator is to trigger end of gene transcription. On these constructs, the nopaline synthase (tNOS) terminator and *Arabidopsis thaliana* putative heat shock protein terminator (HSP) was used.

Positive selection of bacteria containing the L1 construct was initially performed using growth medium with ampicillin as the selection media. To verify the construct PCR was performed and most of the tested colonies showed positive bands of the expected sizes on the electrophoresis gel images (see figure legend for details). The results of DNA sequencing on the selected positive colonies also showed to have the correct nucleotide sequences of the promoters, coding sequences and terminators as designed with geneious (Appendix). These L1 constructs were the building blocks for all the L2 constructs (Figures 2.6 to 2.8).

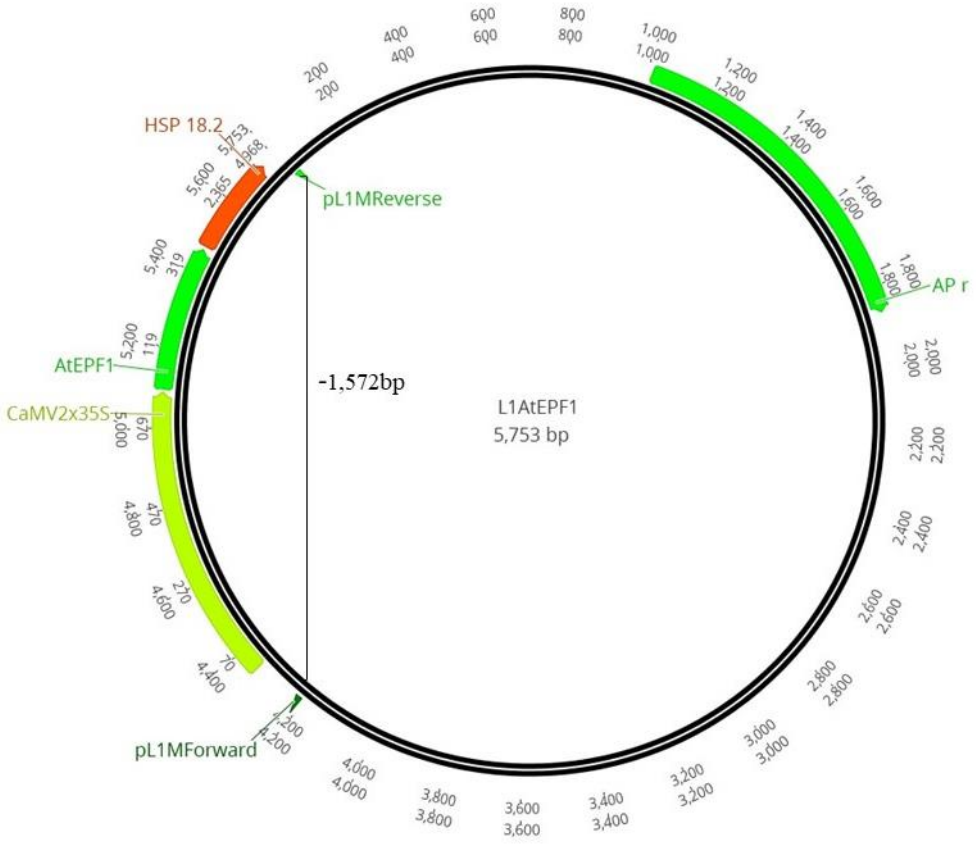

Figure 2. 3: The level 1 fusion construct showing the Arabidopsis thaliana EPF1 (L1AtEPF1) construct showing coding sequence flanked by a constitutive promoter from Cauliflower mosaic virus (CaMV2x35S) promoter and the Arabidopsis heat shock protein terminator (HSP). The vector backbone also contains ampicillin resistance gene (APr). Virtual primer tests using geneious bioinformatics software with (pL1MForward and pL1MReverse) indicated the expected band size on agarose gel image (1,572bp).

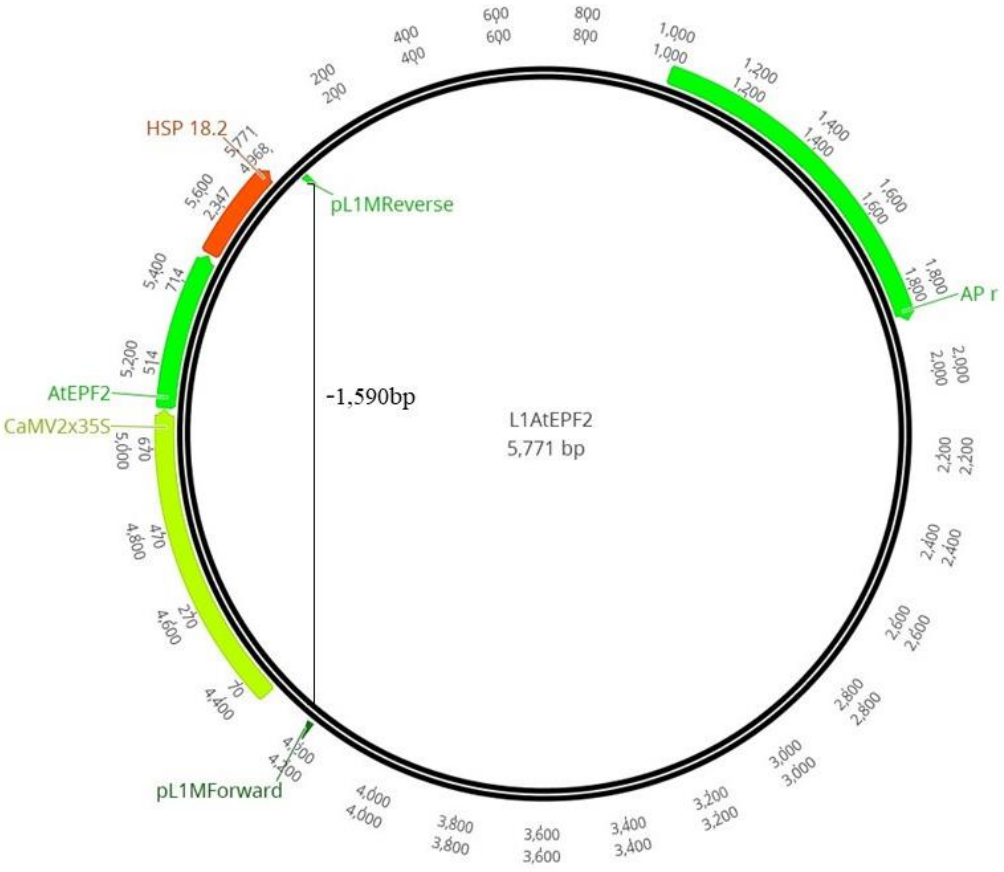

Figure 2. 4**:** The level 1 fusion construct showing the Arabidopsis thaliana EPF2 (L1AtEPF2) construct showing the coding sequence flanked by Cauliflower mosaic virus (CaMV2x35S) promoter and the Arabidopsis heat shock protein terminator (HSP). The vector backbone also contains ampicillin resistance gene (APr). Virtual primer tests using geneious bioinformatics software with (pL1MForward and pL1MReverse) indicated the expected band size on agarose gel image (1,590 bp).

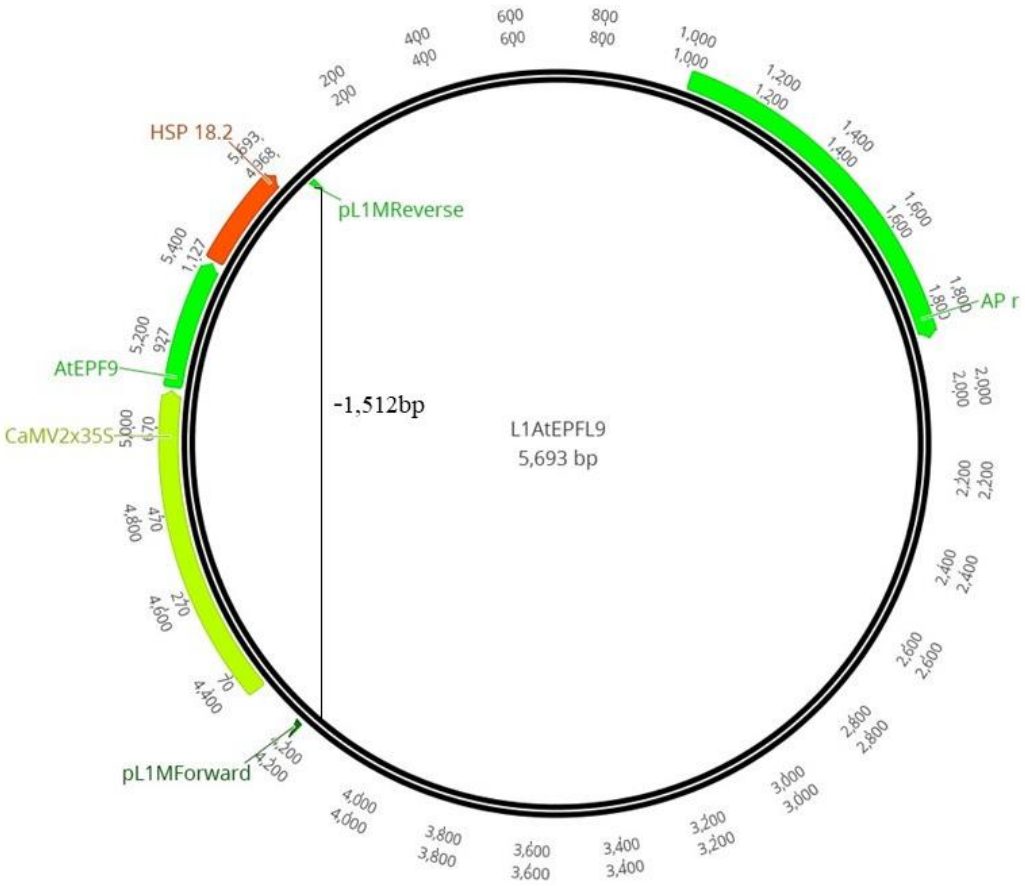

Figure 2. 5**:** The level 1 fusion construct showing the Arabidopsis thaliana EPFL9 (L1AtEPFL9) coding sequence flanked by Cauliflower mosaic virus (CaMV2x35S) promoter and the Arabidopsis heat shock protein terminator (HSP). The vector backbone also contains ampicillin resistance gene (Apr). Virtual primers test using geneious bioinformatics software with (pL1MForward and pL1MReverse) indicated the expected band size on agarose gel image (1,512 bp).

Unlike the L1s, the vector for L2s has a neomycin phosphotransferase II (NPTII) gene that confers kanamycin resistance to the positive bacteria colonies with the L2 constructs. The result of the L2 reactions (Table 2.2) was also analysed using gel electrophoresis fragmentation resulting from colony PCRs. The selected colonies for

screening as can be seen from the gel image yielded the expected band sizes of 552bp. Given that the primers used here are designed to amplify the full length of the basta gene, a positive PCR indicates that these colonies have the basta gene. The highlighted lanes in red from the gel images are the bands for the colonies that were selected for DNA sequencing.

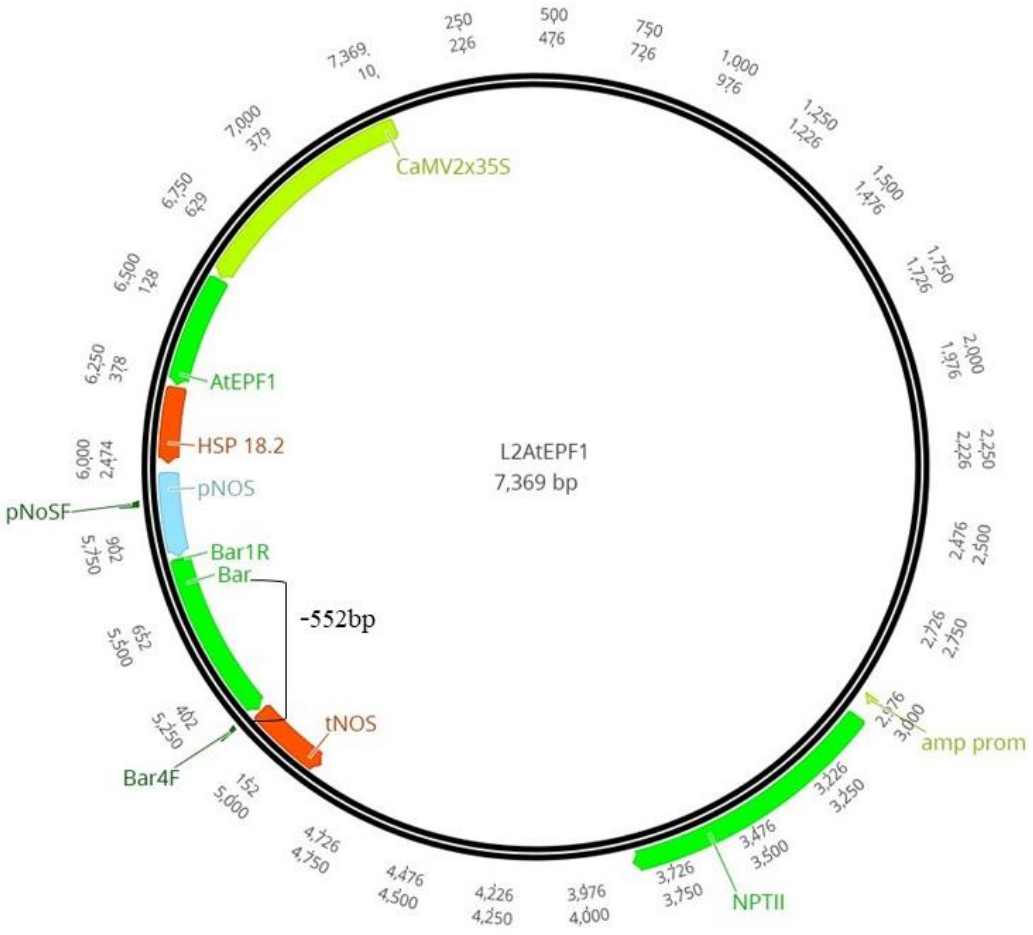

Figure 2. 6**:** Analysis of level 2 Arabidopsis thaliana EPF1 (L2AtEPF1) construct shows the L1AtEPF1 in position two (R2), flanked by the Cauliflower mosaic virus (CaMV2x35S) promoter and the Arabidopsis heat shock protein terminator (HSP). There is a L1Bar (Basta) gene in position one (R1) flanked by nopaline synthase promoter (pNOS) and terminator (tNOS). The vector also carries a neomycin

phosphotransferase II gene (NPTII) which confers resistance to Kanamycin. Virtual primer digest on geneious bioinformatics software using (Bar4F and Bar1R) to check the presence of the bar gene was positive and expected band size on agarose gel image is (552bp).

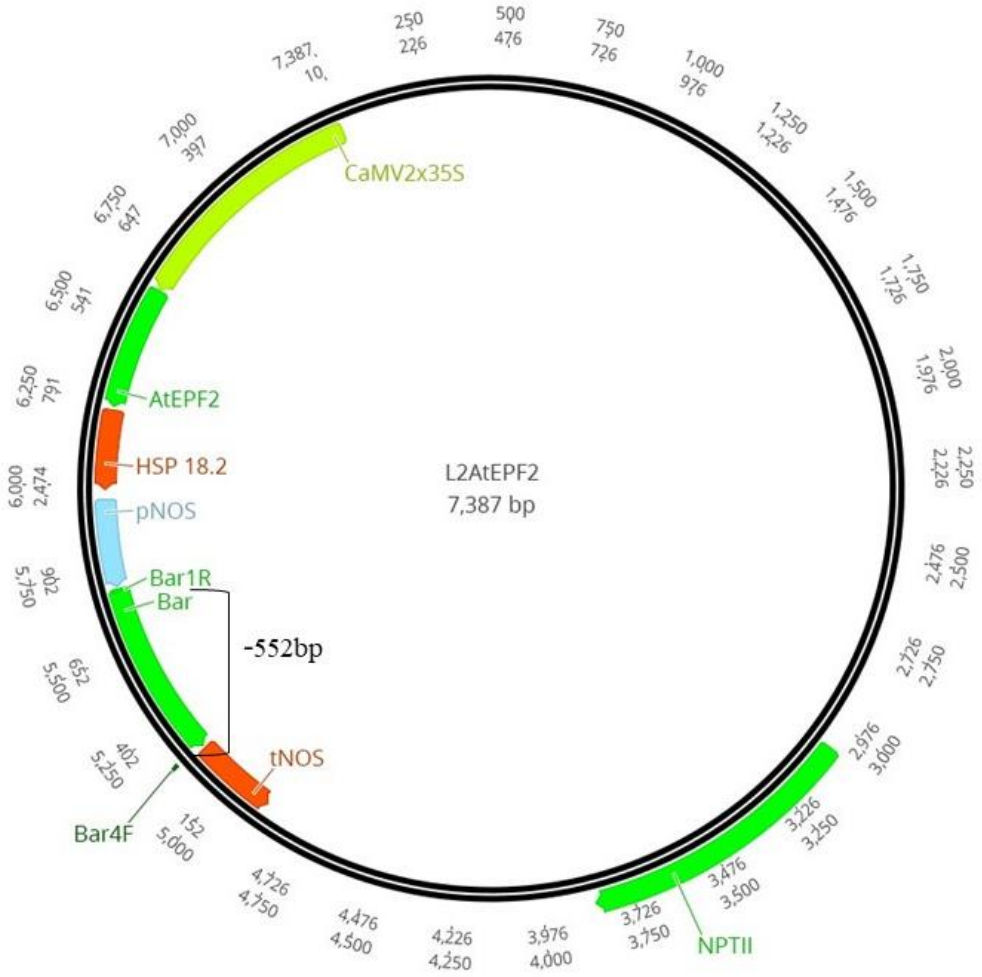

Figure 2. 7: Analysis of level 2 Arabidopsis thalian EPF2 insert (L2AtEPF2) construct showing the L1AtEPFL9 in position two (R2), flanked by the Cauliflower mosaic virus (CaMV2x35S) promoter and the Arabidopsis heat shock protein terminator (HSP). There is a L1Bar (Basta) gene in position one (R1) flanked by nopaline synthase promoter (pNOS) and terminator (tNOS). The vector also carries a neomycin phosphotransferase II gene (NPTII) which confers resistance to

Kanamycin. Virtual primers test using geneious bioinformatics software with (Bar4F and Bar1R) to check the presence of the bar gene was positive and expected band size on agarose gel image is (552bp)

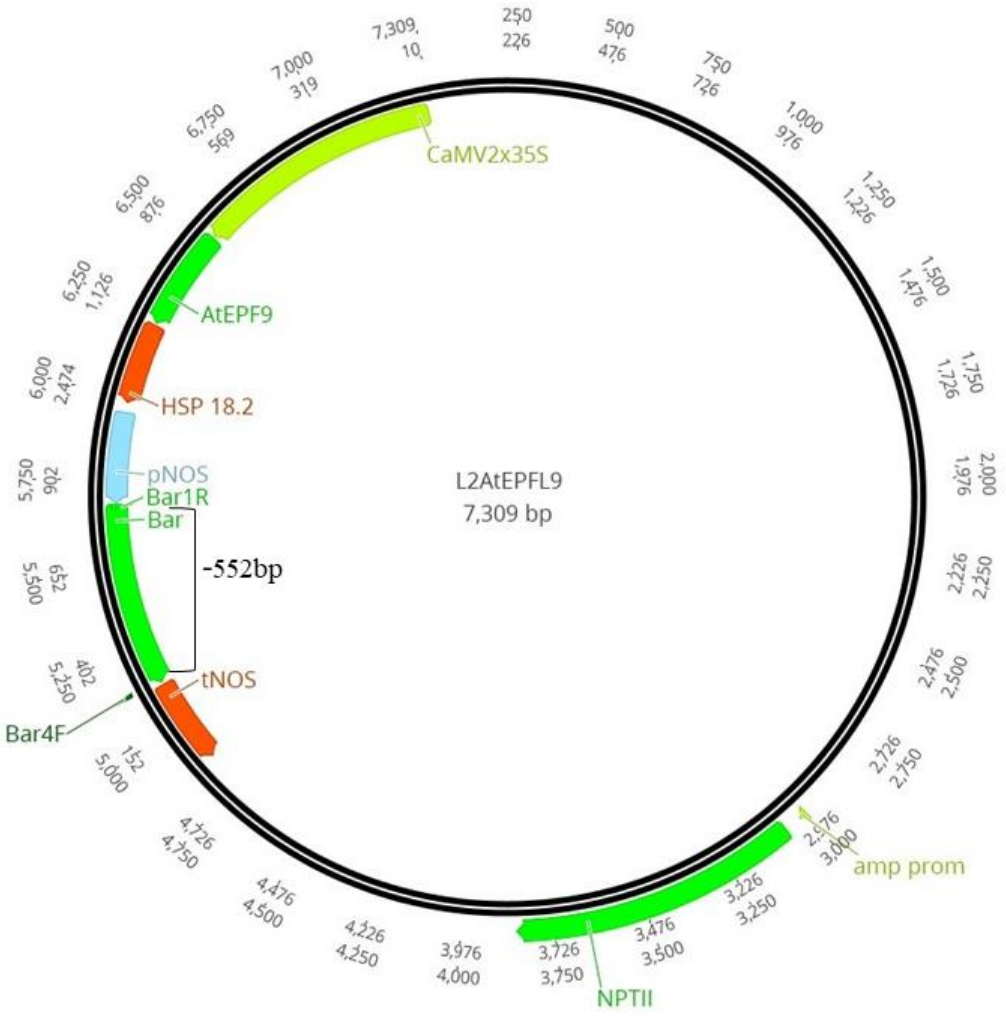

Figure 2. 8: Analysis of level 2 Arabidopsis thaliana EPFL9 (L2AtEPFL9) construct showing L1AtEPFL9 in position two (R2), flanked by the Cauliflower mosaic virus (CaMV2x35S) promoter and the Arabidopsis heat shock protein terminator (HSP). There is a L1Bar (Basta) gene in position one (R1) flanked by nopaline synthase promoter (pNOS) and terminator (tNOS). The vector also carries a neomycin phosphotransferase II gene (NPTII) which confers resistance to Kanamycin. Virtual primer test using geneious bioinformatics software with (Bar4F and Bar1R) to check

the presence of the bar gene was positive and expected band size on agarose gel image is (552bp).

The digestion of DNA from *E.coli* colonies with these L2 constructs with the restriction enzyme (EcoRI) gave the expected fragments sizes after 14 hours digestion at 37^{o}C. This is a confirmation that all the sequenced L1 components are present and transformation into agrobacterium can proceed except in some circumstances when DNA sequencing of these L2s is required. The nature of the golden gate cloning makes it unnecessary to sequence the L2 if all L1 components have been sequenced because the whole L2 reaction is a restriction-ligation process and does not involve polymerization which may introduce some error in the process. In these L2, the bar gene (L1) is designed in a way that it only fits in the first position (R1) and the EPFs fits in the R2 of the L2 vector. A successful ligation would yield colonies that are resistant to Kanamycin.

Overexpress the EPF1 and EPF2 genes together in a given plant, would require ligating the L1 of these two genes as shown in Figure (2.9). Multiple independent transgenic lines were developed but four independent lines of EPF1, EPF2 and EPFL9 have been selected from T0 and T1 generations. Seeds from these plants were screened and characterised to assess impact of the genetic manipulations on the photosynthetic efficiency of transformants. The EPF phenotypes have been observed in the T0 and T1 generations. In these plants, stomatal density revealed a difference in leaf architecture; size, number and shapes of stomata (Figures 4.9 and 4.10).

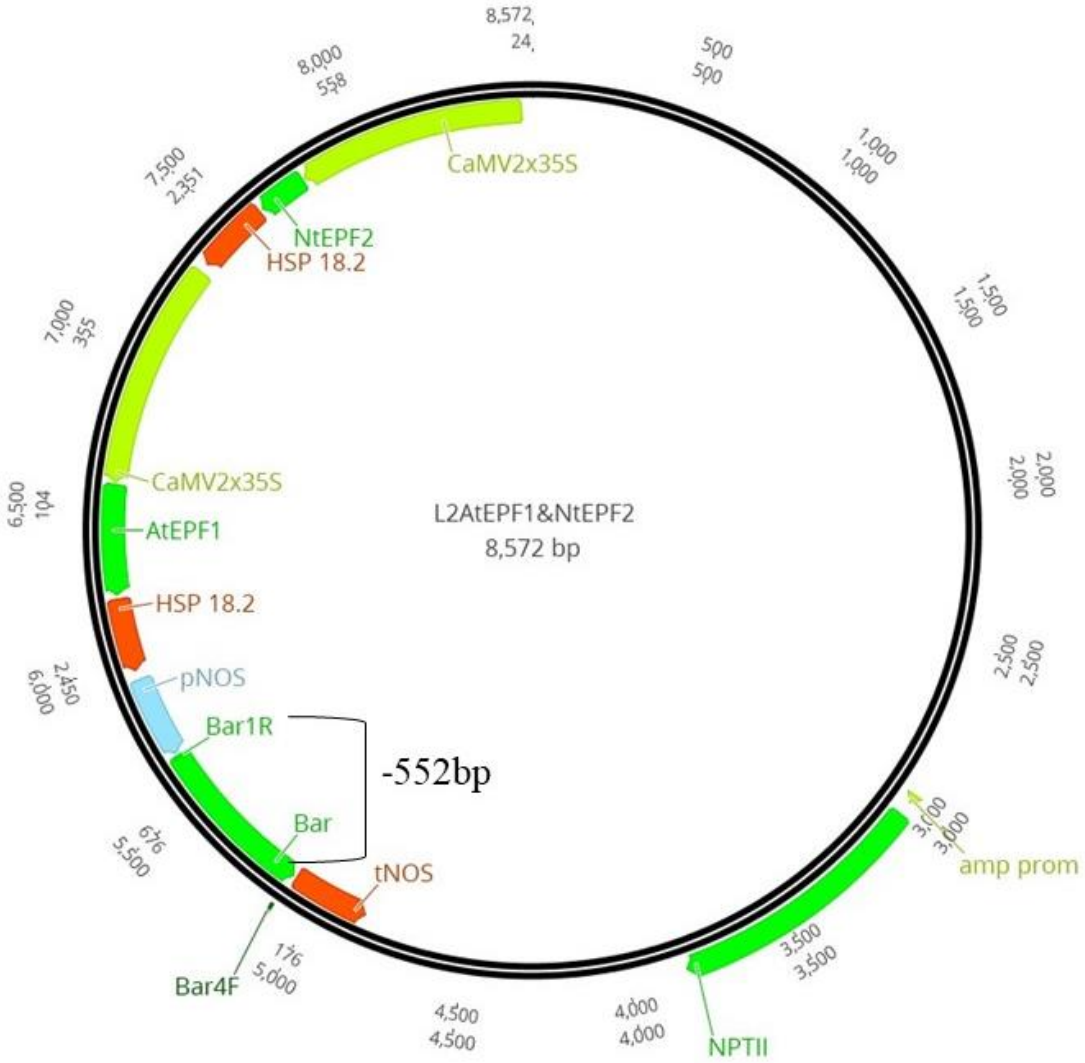

Figure 2. 9: Analysis of level 2 Arabidopsis thaliana EPF1 and Nicotiana tobacco EPF2 double construct (L2AtEPF1&NtEPF2), showing the L1 EPF1 and L1EPF2 genes in positions 2 and 3 respectively, both under the expression of a Cauliflower mosaic virus (CaMV2x35S) promoter and the Arabidopsis heat shock protein terminator (HSP). There is a L1Bar (Basta) gene in position one (R1) flanked by nopaline synthase promoter (pNOS) and terminator (tNOS). The vector also carries a neomycin phosphotransferase II gene (NPTII) which confers resistance to Kanamycin. Virtual primer test using geneious bioinformatics software with (Bar4F

and Bar1R) to check the presence of the bar gene was positive and expected band size on agarose gel image is (552bp).

2. 2. 3 Ferredoxin constructs

In order to investigate the effect of increased level of ferredoxin on guard cell function and stomatal behaviour of the *ict*B plants, the L1 and L2 ferredoxin constructs (Figures 2.10 and 2.11) were developed using the protocol from Tables (2.1 and 2.2). The Fd cDNA (L0) was cloned into a goldengate level 1 vector as in L1 EPFs but the promoter used here is the KST (the potato *KST1*) which is guard cell specific while the terminator remained as the *Arabidopsis thaliana* putative heat shock protein terminator (HSP).

The L1 vector that was used also contains a gene that confers ampicillin resistance therefore a positive selection of bacteria containing the L1 construct was initially performed using growth medium with ampicillin. Colony PCR and sequencing was used to verify the L1 construct and results can be seen (Figure 5.1). The L2 single construct was made of a L1 Fd in position (R2) of the vector, flanked by the potato KST promoter and the Arabidopsis (HSP) terminator. There is a L1Bar (Basta) gene in position one (R1) flanked by nopaline synthase promoter (pNOS) and terminator (tNOS) (Sinkim *et al.,* 2015). The L2 vector also carries a neomycin phosphotransferase II gene (NPTII) which confers resistance to Kanamycin. Therefore, it is expected that ictB plants that will be transformed to over-express this construct will have higher GC electron transport rates given that the site of Fd over-expression is in the GC chloroplast.

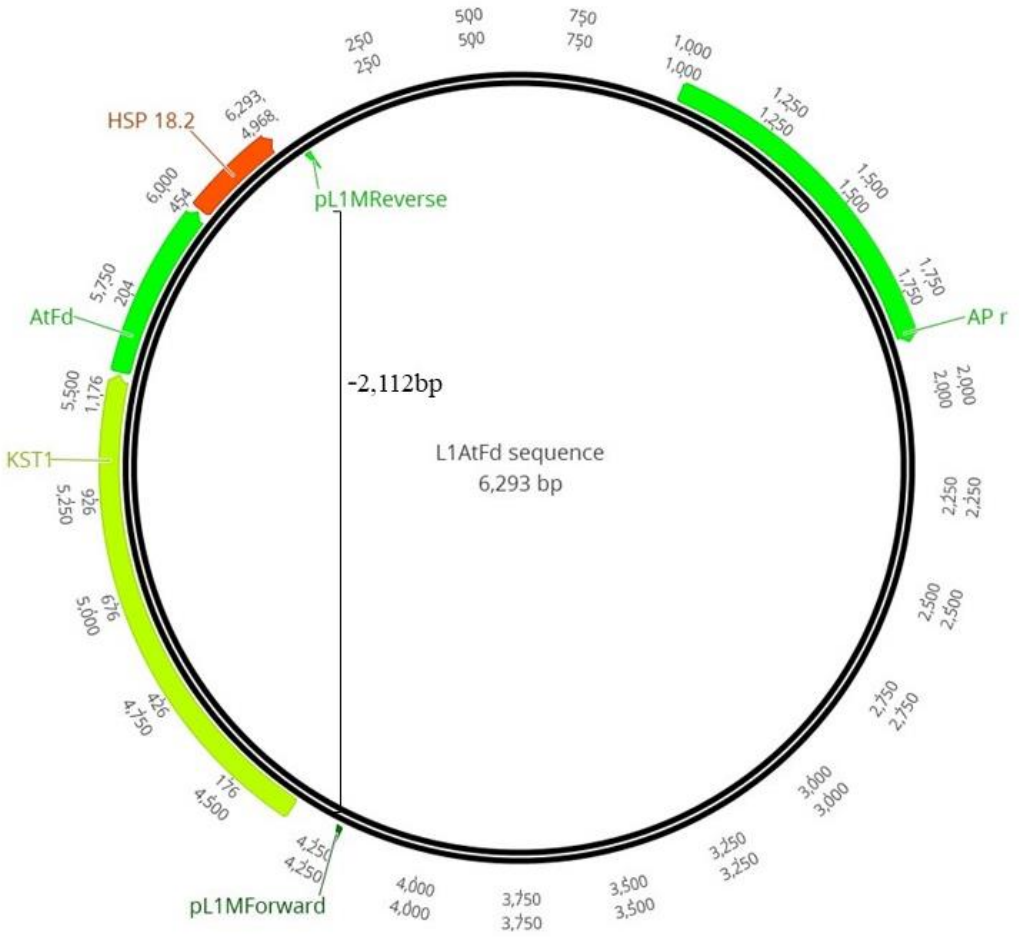

Figure 2. 10: Analysis of level 1 fusion construct of Arabidopsis thaliana Fd (L1AtFd) showing AtFd coding sequence flanked by the potato guard cell specific (KST1) promoter and the Arabidopsis heat shock terminator (HSP). The vector backbone also contains ampicillin resistance gene (APr). Virtual primer test using geneious bioinformatics software using (pL1MForward and pL1MReverse) gave the expected band size on agarose gel image (2,112bp).

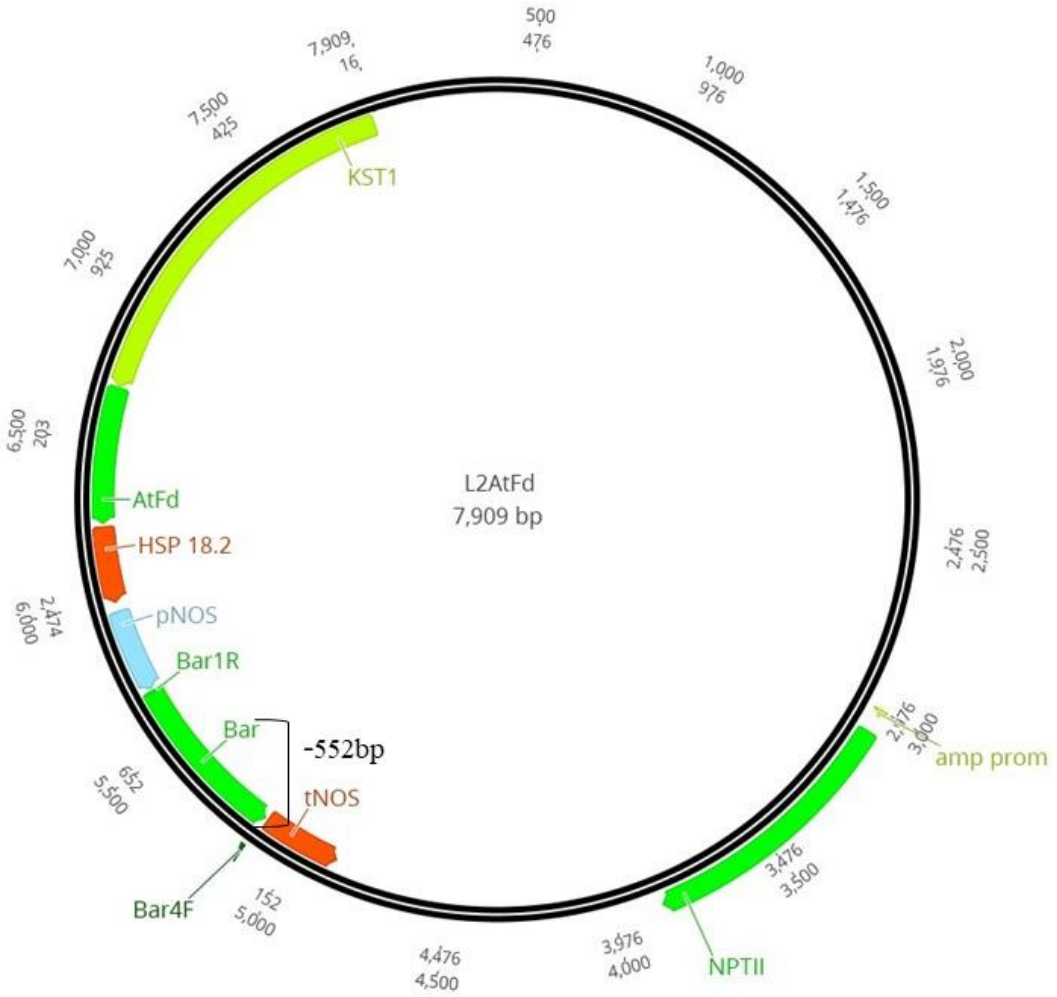

Figure 2. 11: Analysis of level 2 Arabidopsis thaliana Fd construct (L2AtFd) showing the L1AtFd in position two (R2), flanked by the potato (KST) promoter and the Arabidopsis heat shock protein terminator (HSP). There is a L1Bar (Basta) gene in position one (R1) flanked by nopaline synthase promoter (pNOS) and terminator (tNOS). The vector also carries a neomycin phosphotransferase II gene (NPTII) which confers resistance to Kanamycin. The virtual primer test using the geneious bioinformatics software with (Bar4F and Bar1R) to check the presence of the bar gene was positive and yielded the same band size on agarose gel image is (552bp).

2. 2. 4 Ferredoxin and EPF double constructs

Other L2 Fd double constructs developed are the combination of L1 Fd and L1 YFP (Figures 2.12) as well as the triple L1 Fd, EPF1 and EPF2 (Figure 2.13). In Figure 2.12, the L2AtFdYFP construct shows the L1YFP gene in position three (R3) and L1AtFd in position two (R2). Both genes are under the expression of the potato KST promoter and the Arabidopsis heat shock protein promoter (HSP). There is a L1Bar (Basta) gene in position one (R1) flanked by nopaline synthase promoter (pNOS) and terminator (tNOS).

The L2 vector also carries a neomycin phosphotransferase II gene (NPTII) which confers resistance to Kanamycin. The YFP tag when expressed would give information of the tissues specificity of the Fd protein. It is expected that the Fd protein would be expressed in the guard cells of the ictB plants therefore the fusion of the YFP protein would aid in the detection of this Fds through fluorescence microscopy.

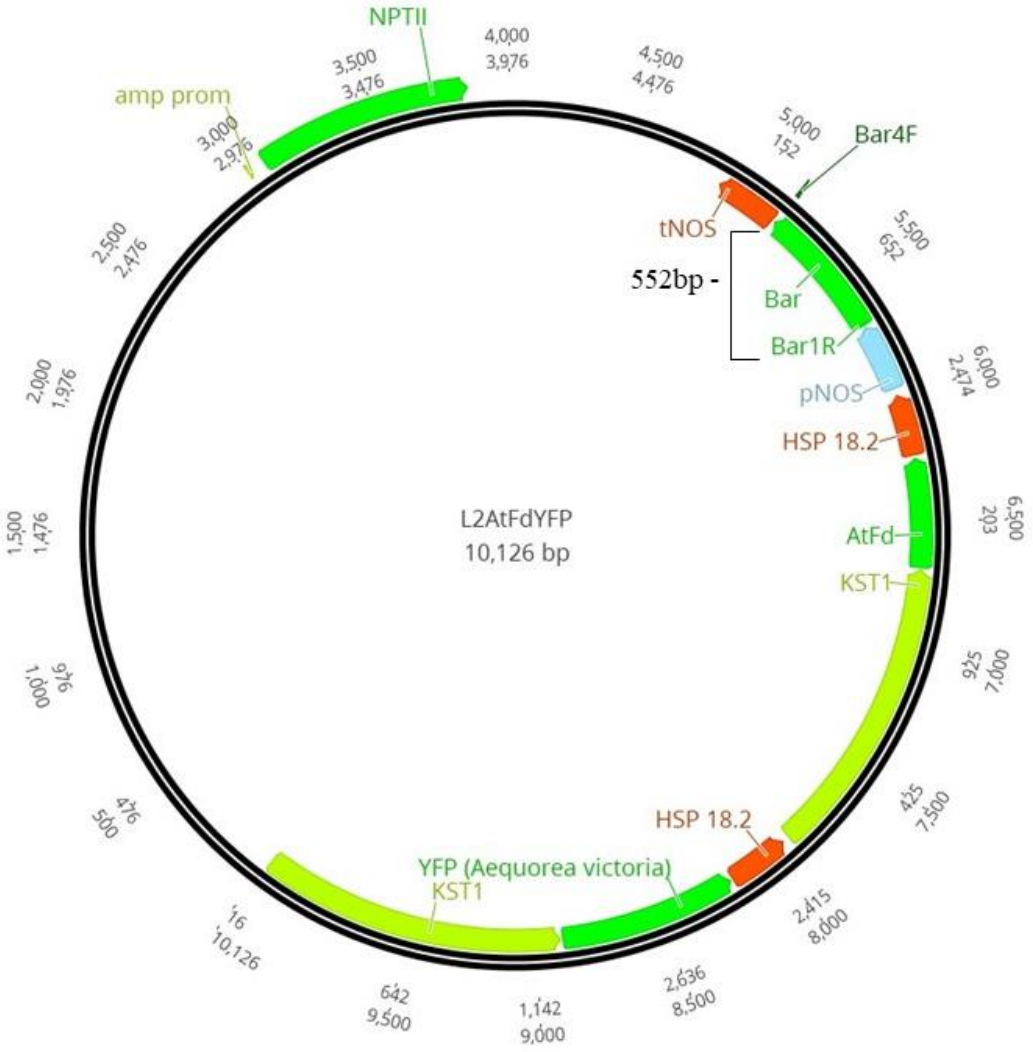

Figure 2. 12: The map of level 2 Arabidopsis thaliana Fd and the yellow fluorescence protein (YFP is a mutant of the green fluorescent protein from jellyfish Aequorea Victoria), showing the L1YFP gene in position three (R3) and L1AtFd in position two (R2). Both cds are under the expression of the potato KST promoter and the Arabidopsis heat shock protein promoter (HSP). There is a L1Bar (Basta) gene in position one (R1) flanked by nopaline synthase promoter (pNOS) and terminator (tNOS). The vector also carries a neomycin phosphotransferase II gene (NPTII) which confers resistance to Kanamycin. Virtual primer test with geneious

bioinformatics software using (Bar4F and Bar1R) to check the presence of the bar gene yielded the same size as the band size on agarose gel image is (552 bp).

The L2AtFdNtEPF1&EPF2 triple constructs (Figure 2.12) shows the L1 EPF genes in positions two and three. Both EPFs genes are under the expression of the Cauliflower mosaic virus (CaMV2x35S) promoter and the Arabidopsis heat shock protein terminator (HSP). There is an L1Bar (Basta) gene in position one (R1) flanked by nopaline synthase promoter (pNOS) and terminator (tNOS). The vector also carries a neomycin phosphotransferase II gene (NPTII) which confers resistance to Kanamycin. EcoRI digestion of the L2AtFdNtEPF1&NtEPF2 construct yielded four bands with two inseparable bands fused together due to the little difference in their molecular weights (Figure 5.4).

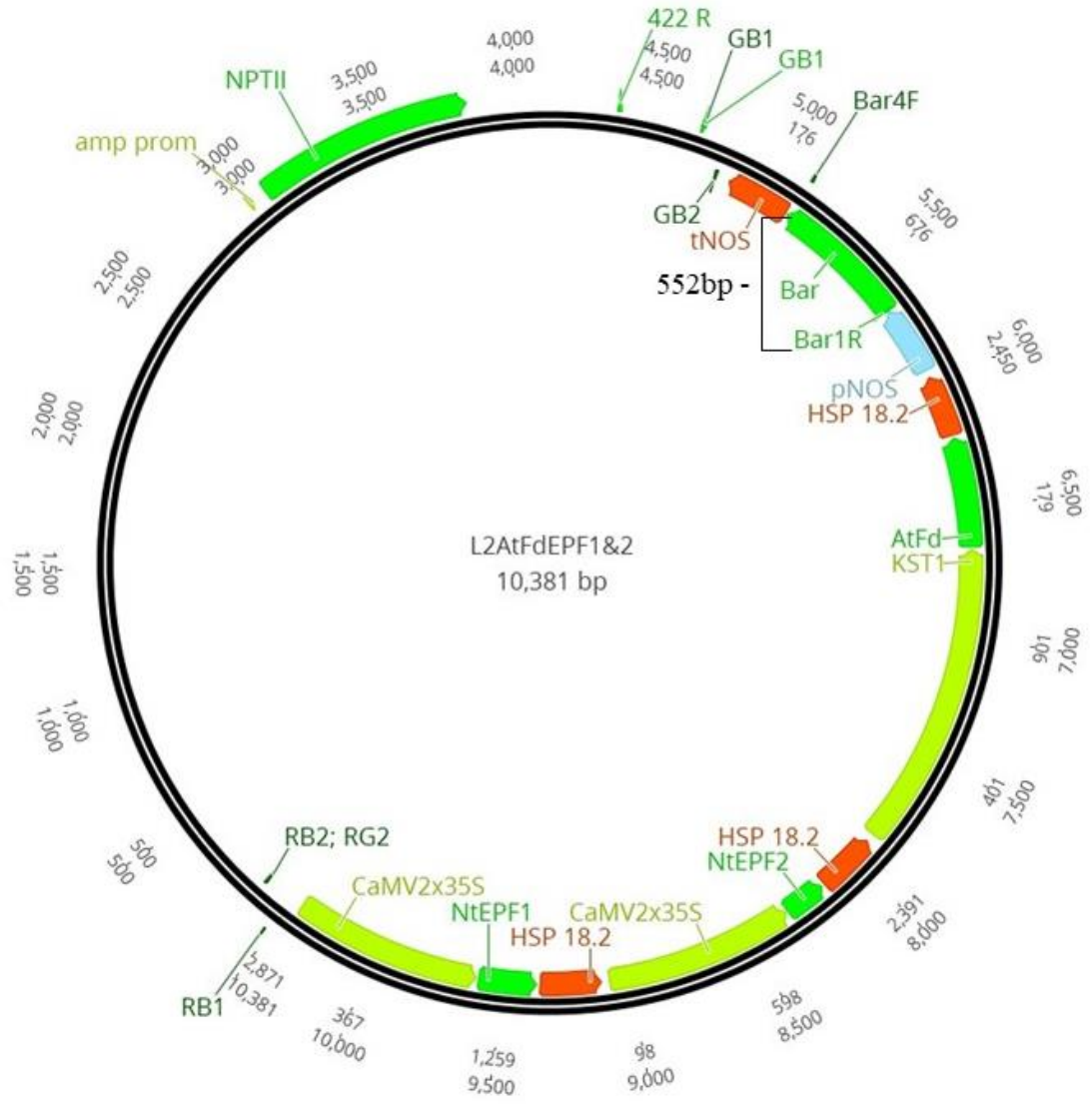

Figure 2. 13: The map of Level 2 Arabidopsis thaliana Fd, Nicotiana tobacco EPF1&2 triple constructs (L2AtFdEPF1&2) showing the L1 EPFs genes in positions two and three. Both EPF genes are under the expression of the Cauliflower mosaic virus (CaMV2x35S) promoter and the Arabidopsis heat shock protein terminator (HSP) while the Fd cds is under the expression of the potato KST promoter and the Arabidopsis heat shock protein promoter (HSP). There is a L1Bar (Basta) gene in position one (R1) flanked by nopaline synthase promoter (pNOS) and terminator (tNOS). The vector also carries a neomycin phosphotransferase II gene (NPTII) which confers resistance to Kanamycin. Virtual primer test with geneious

bioinformatics software using (Bar4F and Bar1R) to check the presence of the bar gene yielded the same size as the band size on agarose gel image is (552 bp).

The L0s single sequences of genes of interest were sent for synthesis through online at ThermoFisher Scientific website. The L1 constructs was made in a one pot restriction-ligation assembly with the following components in one tube; 2.6µl golden gate T4 buffer (10x), 1.3µl of promoter, 1.3µl of terminator, 1.3µl Bsal, 1.3µl of ligase, 1.3µl of vector backbone and 19.3µl of ddH^20. This was mixed gently and made into four 6.5µl aliquots before the addition of 1.5µl each of the purified EPFs (1, 2 and 9) and Fd per aliquot (Table 2.1). The thermocycling programme was in three steps: initial 37°C at 20 seconds, then followed by 30 cycles each of 3 minutes digestion at 37ºC, 4 minutes ligation at 16ºC. The last step is a 10 minutes denaturation of enzymes at 80°C and holding reaction at 16ºC. After the reaction 4 µl each of L1 reaction is transformed into a TOP10 competent cells.

2. 3 Heat Shock Transformation of E. coli competent cells

Chemically competent *E.coli* cells were transformed using the methodology described in Singh (2007). In separate 1.5 mL micro tubes, 4 µL of each L1 PCR product was added to 50 µL of $CaCl_2$ *E.coli* competent cells, mixed gently using pipette and incubated on ice for 30 minutes. After this, the cells were heat shocked in a water bath at 42ºC for 30 seconds and placed on ice for 20 minutes. Immediately after this, 250 µL of room temperature LB medium was added and cells incubated at 37ºC for 1 hour with gentle shaking. Finally, cells were plated on a Kanamycin selection media and placed at 37ºC overnight to incubate.

2. 4 Colony PCR of transformed E. coli to select for cell with L1 EPF fragment

The PCR reaction was done to determine the presence of L1 constructs in the resulting E. coli colonies. The reaction mixture contained 20µL of each primer (pL1M Forward 5´-CGGATAAACCTTTTCACGCCC and pL1M Reverse 5´-GTACTGGGGTGGATGCAGTG), 730µL of dH_2O, 100µL of Buffer, 20µL of dNTPs and 10µL of Taq Polymerase Enzyme in a total volume of 900 µL reaction mixture. 18 µL of the reaction mix was added to 44 individual tubes in a PCR tray and a pipette tip was used collect DNA samples from 44 different colonies from the transformants. PCR was according to the following thermal profile: initial 96°C at 2 minutes, then followed by 35 cycles each of 15 seconds denaturation at 96^{o}C, 15 seconds annealing at 60^{o}C and 45 seconds of synthesis at 72°C respectively. At the end of thermocycling, the amplified PCR reaction was fractionated on 1.5% percentage agarose gel. If there was an insert, the expected band size of PCR product would be visible. The positive colonies were inoculated and DNA extracted for sequencing.

2. 5 Sequencing of DNA from positive PCR colonies

Growth of selected positive colonies for DNA purification was done using the protocol from GeneJET Plasmid Miniprep Kit according to the manufacturer's instruction (Fisher Scientific, Leicestershire, LE11 5RG). After purification, 15µL of each DNA (100ng/µl) sample was aliquot in 1.5 µL micro tube, labelled and sent for sequencing with the sample of the primers used for PCR amplification (5µl times number of forward and reverse reaction).

2. 6 Development of L2 multiple constructs

Once the sequence of the L1 sequence is confirmed, the L2 constructs was made using the golden gate one pot restriction-ligation assembly with the following components in one tube; 7.5µl golden gate T4 buffer (10x), 5µl of L1 Basta, 5µl L2 Vector Backbone, 5µl Bpil, 0.75µl of BSA(100x), 5µl of ligase, and 31.5µl of ddH^20. This was mixed gently and made into 6.5 µl aliquots before the addition of 1µl of the corresponding purified L1 DNA and 0.5µl end linker (Table 2.2). Thermocycling programme followed the same as in L1 restriction–ligation reaction above and electrophoresis used check the PCR result.

2. 7 Preparation of *Agrobacterium* competent cells and transformation by electroporation

Preparation of Agrobacterium strain LBA 4401 and electroporation was done as illustrated by the protocol in Singh (2007). For this process, a single colony from a fresh plate was used for inoculating 10 mL of LB (containing 50µg/mL rifampicin and 30µg/mL of streptomycin) and allowed to grow for 48 h at 28^oC with vigorous shaking. After this, the stationary culture was quickly chilled on ice and then spun down for 15 min at 4^oC and 3000 g. The cells were then resuspended in 10mL of ice cold sterile ddH_2O and centrifuged again using the above parameters. This washing process was repeated 4 times, after which the cells were finally resuspended in a 200 µL of ice cold 10% glycerol solution. The competent cells were aliquoted into 40 µL aliquots and placed into 1.5 mL tubes for storage at -80^oC or used immediately.

2. 8 Colony PCR of transformed *E. coli and Agrobacterium* to select for cell with L2 constructs

The PCR reaction was done to determine the presence of L2 constructs in the resulting E. coli colonies. One reaction contained 0.4µL of each primer (BAR4-Forward 5´-TCAAATCTCGGTGACGGG and BAR1-Reverse 5´-ATGAGCCCAGAACGACG), 14.6µL of dH_2O, 2µL of Buffer, 0.4µL of dNTPs and 0.2µL of Taq Polymerase Enzyme in a total volume of 18µL reaction mixture (scaled up to the number of colonies to be screened). DNA samples from the colonies were collected with a pipette tip previously dipped in the middle of a fresh colony (labelled plates) and then dipped into the 18 µL PCR mixture for one reaction. DNA samples can be washed by pipetting gently up and down. At the end of thermocycling, the amplified PCR reaction was fractionated on 1.5% percentage agarose gel. If there was an insert, then PCR product would be visible and the corresponding colony on the labelled plate would be used to inoculate a liquid selection media for L2 plasmid mini-prep DNA extraction.

To transform competent Agrobacterium cells, 1-2 µL of purified plasmid DNA from selected L2 *E.coli* colonies were gently mixed into a tube containing 40 µL of competent Agrobacterium cells. This mixture was transferred into and ice-cold electroporation cuvette and the cells were then electroporated at 2500 V using an EasyJect Prima electroporator from EQUIBIO. The cuvette was immediately removed after the beep and 1 µL of ice-cold SOC or LB media added. The culture was then placed back into the 1.5 mL tube and incubated at 28^{o}C with gentle shaking for approximately 2h. Finally, 150 µL of cells were spread onto LB plates with

antibiotics (rifampicin, streptomycin and Kanamycin) and transformants allowed to grow at 28^{o}C for 48 hours.

2. 8. 1 Restriction Enzyme Digest

Single EcoR1 restriction enzyme digestion was used to produce different restriction fragments by following the manufacturer's protocol (NEW EGLAND BioLabs, Massachusetts, USA). The restricted fragments generated are flanked by identical enzyme sticky ends and size selected usually by gel electrophoresis.

2. 8. 2 WT and ictB Tobacco Transformation with constructs

It was essential to use a freshly transformed Agrobacterium (LBA4404) cells to start a 10 ml culture (LB + antibiotics), and grow overnight at 28°C. From the overnight culture 2-4ml was taken to start a 150ml culture (LB + antibiotics). Growth was at 28° C for approximately 24hrs and I ensured that the speed of the incubator was not excessive to avoid foaming on the culture surface. Following this, the cells were harvested and divided into cultures in three 50 ml sterile falcons then centrifuge for 15-20 min at 3000g (room temperature). The cells were resuspended in same volume of liquid MS to be used for leaf disc transformation.

2. 8. 3 Leaf Disc Transformation

This procedure involved using leaf pieces from sterile plant material and coculturing with *Agrobacterium* (McCormick *et al.,* 1986). During cocultivation, the *Agrobacterium* Vir genes are induced; the bacteria bind to plant cells around the cut edges (wounds) of the leaf explants and initiate T-DNA transfer (McCormick *et al.*,

1986). Explants from leaf tissue of 6-8 weeks old tobacco plantlets (about a hundred for each construct) are preferred for increased transformation frequency. In coculturing, leaf explants are incubated with the *Agrobacterium* (10-30 min depending on the strain used). Following this, leaf explants are placed upside down (abaxial face up) onto NBM (BAP and NAA no antibiotics) plates and kept in a growth chamber (22-14°C, 16h light) for 48 h. After this, leaf explants are transfered into fresh NBM media with basta herbicide and Cefotaxime antibiotics (400 ug ml^{-1}). The basta helps to select for transformants while Cefotaxime was used to control the Agrobacterium growth.

All explants should be maintained in the growth chamber and media should be refreshed every 7-10 days until shoots develop. After 14-20 days (or second change of media) media can be changed to EM (BAP and IAA). The concentrations of growth hormones are shown in the appendix. This combination of media composition and timing seems to strongly encourage a faster and more prolific differentiation of shoots. As soon as shoot starts to differentiate the explants can be moved into tall plates/magenta pots containing MS media plus antibiotics (rooting media) (Figure 4.9A). Transgenic plants should develop roots and will be then ready to move into soil.

All transformed plants were screened after three weeks on soil by the application of the herbicide basta alongside the wild type control. It is expected that the transformed plant treated by topical application of this herbicide on its leaves will survive but those that are not transformed will show similar susceptibility to the basta herbicide

by exhibiting progressing browning of the leaves over the course of one week and subsequently dying off (Figure 4.9C). Leaf samples were collected for qPCR analysis and these T0 plants were allowed to grow for another two weeks under the above conditions before gas exchange and stomata density analysis was done to select plants with high transformation efficiency (Figure 4.10).

Table 2. 1: Component of the level 1 (L1) golden gate reaction.

Name of Level 1	**L1 Components**	**Component conotations**
L1AtEPF1	pL1VR2+p35S+AtEPF1+tHSP	pL1VR2 (Vector Backbone)
L1AtEPF2	pL1VR2+p35S+AtEPF2+tHSP	p35S (CaMV 35S constitutive promoter)
L1AtEPFL9	pL1VR2+p35S+AtEPFL9+tHSP	tHSP (HSP promoter)
L1AtFd	pL1VR2+KST+AtFd+tHSP	KST1 (guard cell specific promoter)
		AtEPFs (purified DNA of interest)
	Golden gate Reaction mix X 4rx (µl)	**X 1rx**
H2O	19.3	4.825
T4 buffer	2.6	0.65
Bsal	1.3	0.325
Ligase	1.3	0.325

Promoter	1.3	0.325
pL1VR2	1.3	0.325
Terminator	1.3	0.325
Final Volume	28.4	
Aliquot 6.5 µl/tube then add 1.5µl of each EPFs DNA per tube to a total of 8µl/tube		

Table 2. 2: Component of the level 2 (L2) golden gate reaction.

Name of Level 2	**L2 Components**	**Component conotations**
L2AtEPF1	pAGM4723 +L1AtEPF1+L1BAR+ELE2	pAGM4723 (L2 Vector)
L2AtEPF2	pAGM4723 +L1AtEPF2+L1BAR+ELE2	L1BAR (L1 Basta gene)
L2AtEPFL9	Pagm4723+L1AtEPFL9+L1BAR+ELE2	ELE2 (End-Linker 2)
L2AtFd	pAGM4723+L1AtFd+L1BAR+ELE2	ELE3 (End-Linker 3)
L2AtFdEPF1	pAGM4723+L1AtFd+L1AtEPF1+L1BAR+ELE3	ELE4 (End-Linker 4)
L2AtFdEPF2	pAGM4723+L1AtFd+L1AtEPF2+L1BAR+ELE3	
L2AtFdEPFL9	pAGM4723+L1AtFdEPFL9+L1BAR+ELE3	
L2NtEPF1&2	pAGM4723+L1AtEPF1+L1NtEPF2+ELE3	

L2AtFdEPF1&2	pAGM4723+L1AtFd+L1NtEPF1+L1NtEPF2+ ELE4	
	Golden gate Reaction mix X 10 rx (µl)	**X 1rx**
H2O	31.5	3.15
T4 buffer	7.5	0.75
100X BSA	0.75	0.075
BpiI	5	0.5
Ligase	5	0.5
pAGM4723	5	0.5
L1BAR	5	0.5
Final Volume	59.75	
Aliquot 6.5µl/tube then add 1µl of each of complementary L1 DNA component and 0.5µl ELE		

2. 8. 4 RNA Extraction

The RNA was extracted from leaf samples using a Qiagen RNAeasy Kit (Qiagen, Crawley, UK) following the manufacturer's protocols. All leaf samples were harvested from growth conditions, in 1.5µl Eppendorf tubes and immediately frozen in liquid nitrogen. The plant samples were then ground using glass pestle and mortar in liquid nitrogen to preserve the integrity of the RNA from rapid degradation. Following the RNA extraction protocol as cited above all RNAs samples were recovered and the quality of RNA verified using the Nanodrop spectrophotometre ND-1000 UV/Vis (3411 Silverside Road, Wilmington, DE 19810 United States).

Recovered RNA samples can either be used immediately for the qPCR reaction or stored at -80 in the freezer to be used later.

2. 8. 5 Quantitative Polymerase Chain Reaction (qPCR)

Complementary DNA (cDNA from EPF1, EPF2, EPFL9 and FD plants that was transformed) was synthesized from 481.8ng of RNA extracted from leaf materials and utilised for qPCR reaction. The treatment samples were cDNA from the three EPFs and Fd while WT cDNA served as control. I performed the qPCR using actin primer as the reference gene and primers from my genes of interest (EPFs and FD). The quantitative PCR reactions were performed in 96-well plates. Each group under investigation were tested using three technical replicates, and three no-template controls were also included for each gene being investigated. In each well, the qPCR mix consisted of: 10 µL Sensifast SYBR green, 3.4 µL RNase free water, 0.8 µL forward primer, 0.8 µL reverse primer and 5µL of cDNA adding up to a 20µL. The thermocycling protocol consisted of three stages: Step 1: 2minutes at 95 °C; Step 2: 40 cycles at 95 °C for 10 seconds followed by 60 °C for 1 minute (data collection); Step 3: Melting curve. The expression levels of my genes of interest were measured relative to actin (relative quantification). Calculation of the relative gene expression from the qPCR data was done using delta-delta Ct method in Microsoft excel spreadsheet.

2. 9 Graphs, charts and statistical analysis

Graphs, charts and statistical tests within and across the different groups were done using the statistical analytical tool pack in Microsoft Excel; t-tests and one-way parametric ANOVA was used to analyse the results from the different measurements in a Microsoft Excel spreadsheet (Sokal and Rohlf, 1982).

Table 2. 3: Some independent transformed lines from T0 generation and their associated transgenes.

Some Transformed T0 Tobacco Plants	**Transgenic Components**
WTFD	WT + Transgenic *At*FD gene
WTFDYFP	WT + Transgenic *At*FD gene + YFP
4-7FD	ictB Line7 (T2 plant 4 + Transgenic *At*FD gene
WTEPFL9	WT+ Transgenic *At*EPFL9
6GEPFL9	ictB Line G (T2 Line 6) + *At*EPFL9
WTEPF1	WT+ *At*EPF1
4-7EPF1	ictB Line7 (T2 plant 4) + *At*EPF1
6GEPF1	ictB Line G (T2 plant 6) + *At*EPF1
WTEPF2	WT+ *At*EPF2

4-7EPF2	ictB Line7 (T2 plant 4) + *At*EPF2
6GEPF2	ictB Line G (T2 plant 6) + *At*EPF2
WTEPF1&2	WT + *At*EPF1 +*At*EPF2
WTFDEPF1&2	WT + Transgenic *At*FD gene +*At* EPF1 + *At*EPF2
4-7FDEPF1&2	ictB Line7 (T2 plant 4 + Transgenic *At*FD gene + *At*EPF1 +*At*EPF2

Table 2. 4: T1 transgenic tobacco plants generated

Selected Transformed T1 Tobacco Plants
WTFD8 (WT + Transgenic *At*FD gene) plant 8
WTFD7 (WT + Transgenic *At*FD gene) plant 7
4-7FD1 (ictB Line7 plant 4 + Transgenic *At*FD gene) Plant 1
4-7FD3 (ictB Line7 plant 4 + Transgenic *At*FD gene) Plant 3
WTEPFL9-1 (WT + Transgenic *At*EPFL9 gene) plant 1
6GEPFL9-1 (ictB Line G Plant 6 + *At*EPFL9) plant 1
6GEPFL9-4 (ictB Line G Plant 6 + *At*EPFL9) plant 4
6GEPFL9-7 (ictB Line G Plant 6 + *At*EPFL9) plant 7

WTEPF1-7 (WT + Transgenic *At*EPF1 gene) plant 7
4-7EPF1-7 (ictB Line 7 Plant 4 + *At*EPF1) plant 7
4-7EPF1-8 (ictB Line 7 Plant 4 + *At*EPF1) plant 8
6GEPF1-1 (ictB Line G Plant 6 + *At*EPF1) plant 1
WTEPF2-5 (WT + Transgenic *At*EPF2 gene) plant 5
6GEPF2-3 (ictB Line G Plant 6 + *At*EPF2) plant 3
6GEPF2-5 (ictB Line G Plant 6 + *At*EPF2) plant 5
6GEPF2-9 (ictB Line G Plant 6 + *At*EPF2) plant 9
WTEPF1&2-2 (WT + *At*EPF1 +*At*EPF2) Plant 2
WTFDEPF1&2-5 (WT + *At*FD + *At*EPF1 +*At*EPF2) Plant 5
4-7FDEPF1&2-2 (ictB Line7 plant 4 + *At*FD + *At*EPF1 +*At*EPF2) Plant 2

3. 0 Chapter 3

3. 1 Characterising the physiology of transgenic tobacco plants with improved photosynthesis due to the inclusion of ictB: *Selecting homozygous lines for multigene transformation.*

A great deal of current research focusses on improving photosynthesis to increase crop yield (Long *et al.*, 2006; Zhu *et al.*, 2010; Raines, 2011), with approaches including reducing photorespiration through either bypass pathways (Kebeish *et al.*, 2007) or altering RubisCO kinetics (Parry *et al.*, 2012) as well as increasing Calvin cycle activity in C_3 plant (Raines, 2011). Several models (based on ordinary differential equations (ODEs) have been developed and used to predict the limitation on carbon assimilation by the Calvin cycle as well as sucrose and starch metabolism (Zhu *et al.*, 2011).

These models have shown that increasing the Calvin cycle enzymes sedoheptulose-1,7-bisphosphatase (SBPase) and fructose-1,6-bisphosphate aldolase (FBPA) as well as the starch biosynthesis enzyme ADP-glucose pyrophosphorylase (AGPase) lead to improve photosynthesis (Lefebvre *et al.*, 2005; Raines, 2011; Simkin *et al.*, 2015; Azoulay-Shemer *et al.*, 2016). They also highlighted that altering other pathways such as photorespiration through increasing the activity of the enzyme glycine decarboxylase (GDC) also benefit photosynthetic carbon assimilation (Zhu *et al.*, 2007). The value of the predictive power of these models was demonstrated by research in the Raines laboratory, that initially demonstrated that increasing the activity of one enzymes (SBPase) involved in the regeneration of RuBP as part of the

Calvin cycle resulted in higher photosynthetic rates in tobacco plants that translated in to increased biomass in both glasshouse (Lefebvre *et al.,* 2005) and field conditions (Rosenthal *et al.,* 2011). Since these early studies additional work has illustrated that altering the expression of multiple native genes involved in the Calvin cycle, have additive effects and can result in 100% increases in photosynthesis and growth (Simkin *et al.,* 2015) in Arabidopsis.

In addition to altering the expression of native genes the introduction of a non-native gene has also been demonstrated to increase C3 photosynthesis. For example the expression of the putative-inorganic carbon transporter B (ictB), in Arabidopsis, and in tobacco plants resulted in an improved photosynthesis and increased biomass (Lieman-Hurwitz *et al.,* 2003, 2005). Bonfil *et al.* (1998), identified ictB from a knockout mutant of *Synechococcus* strain PCC 7942 that could only grow normally in a high CO_2 condition, indicative of a loss of functional CO_2 concentration mechanism and therefore suggested that it was involved in the transport of inorganic carbon. The encoded ictB protein contains 10 putative transmembrane regions, located in the inner-membrane and was putatively classified as a HCO3- transporter (Bonfil *et al.,* 1998).

IctB from cyanobacterium has already been engineered into *Arabidopsis thaliana* and *Nicotiana tabacum* L. (Simkin *et al.,* 2015; Lieman-Hurwitz *et al.,* 2003). Although, its mode of action is not clear, the expression of the *ictB* gene increases leaf CO_2 assimilation rate, plant productivity and water use efficiency (WUE) (Lieman-Hurwitz *et al.,* 2003). These and other studies have suggested that expressing of ictB

increases photosynthesis by increasing the concentration of CO_2 at Rusbisco and on the site of activation (Lieman-Hurwitz *et al.*, 2003), however to date the experimental evidence for this is not entirely convincing due to lack of reliable antibody for ictB and absence of an independent method for directly determining CO_2 concentration in close proximity to RubisCO.

During photosynthesis, the entry of CO_2 into the leaf as well as water loss from transpiration is controlled by stomata (Lawson *et al.*, 2008). The guard cells (GCs) are the stomatal structures that perform the function of regulating the sizes of the stoma aperture during this exchange of gases (Minguet-Parramona *et al.*, 2016). Therefore, the alteration of stomatal function in transgenic plants in which the photosynthetic CO_2 pathways has been manipulated could provide unexploited opportunity to improve plant water use efficiency (WUE). Increasing or decreasing the number of stomata can improve or reduce stomatal conductance (Doheny-Adams *et al.*, 2012), although manipulating stomatal behaviour can eliminate these effects (Lawson *et al.*, 2010).

The aim of this chapter is to assess physiology of ictB plants and select homozygous plants with improved photosynthetic capacity driven by the expression of ictB by characterising photosynthetic capacity and stomatal function in these transgenic plants.

3. 2 Results

3. 2. 1 Plant growth on selective media

The ictB tobacco and WT plants were collected from seed stock at Raines laboratory at Essex. The third-generation seeds (T3) of transgenic plants were carried forward for plant transformation with EPFs and Fd. During plant germination using ampicillin selective marker in growth media, TB6 and TB4-7 (independent ictB lines) showed similar and better growth rates compared to the WT after two weeks (Figure 3.1A); the WT plants and the azygous lines (Figure 3.1B) show susceptibility to the kanamycin selective media. Azygous lines were selected to be used as control alongside WT seeds. All the ictB seeds on plates (TB6G) and (TB4-7) geminated with even growth rates while the WT showed stunted growth. The stunted growth observed in the WT was as a result of the absence of the ictB gene which confers resistance to the selective marker used in the media. The same growth pattern was observed when repeated and similarly stunted growth was observed on the azygous lines indicating absence of the ictB gene.

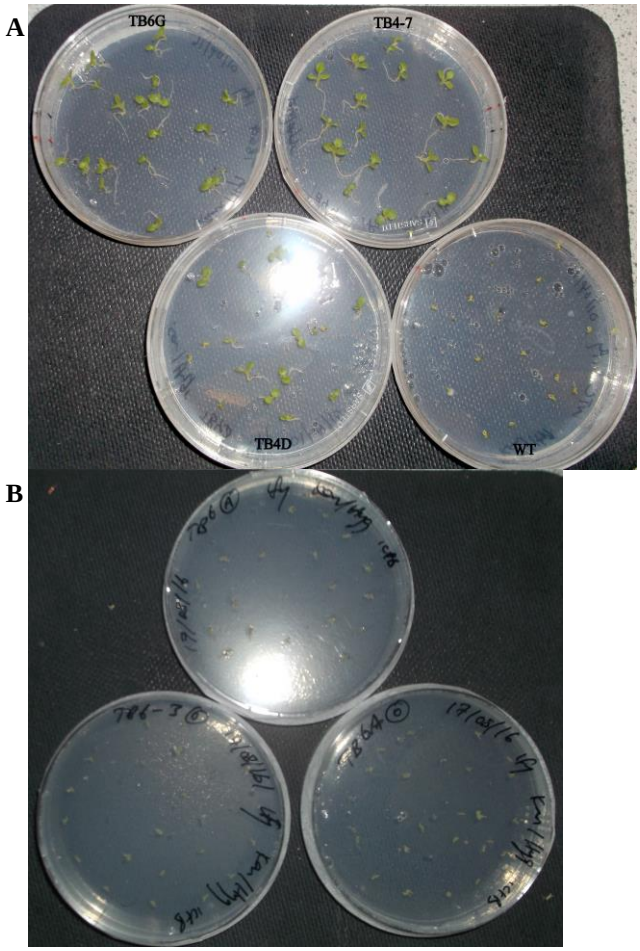

Figure 3. 1: Plant tissue culture to select independent T3 ictB homozygous lines with kanamycin resistance gene. (A): TB6G, TB4-7, TB4D and Wild-Type, (B): TB6A and TB6-3 azygous lines. The plates were placed in a controlled growth cabinet at 25oC, 16h light/8h dark, light level of 200µmol m-2s-1 and allowed to geminate for 3 to 4 weeks.

3. 2. 2 IDna genotyping and PCR screening for transgene

The IDna screening result (Table 3.1) was also used to verify the tissue culture experiment and plants with 2 copy numbers of ictB were identified and carried forward for physiology analysis. PCR screening of DNA samples from leaf extracts showed band for the selected lines of plant (Figure 3.2). The expected band size was

1570bp after amplification of the target sequence. The PCR result was used to confirm the result of the tissue culture selection and IDna analysis which indicated the presence of the ictB gene in the selected transgenic tobacco plants. The TB4-7 and TB6G plants were selected for transformation with EFPs and Fd.

The result of the IDna genetic screening revealed transgene copy numbers which is important to identify plants with multiple integration events that may either undergo silencing or unreliable gene expression. This result helped to accurately select the transgene homozygotes and eliminate hemizygotes and nulls. IDna technology enabled the number of transgene loci to be determined rapidly, allowing me to focus efforts on the optimal transgenic events. Only the two independent lines with 2 copy numbers of transgene was carried forward as homozygous lines.

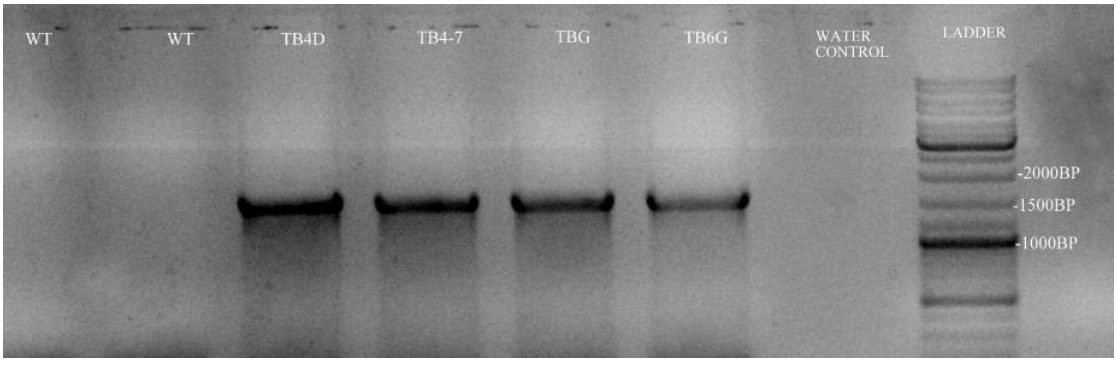

Figure 3. 2: Molecular analysis of PCR products from agarose gel image to detect ictB transcript in T3 transgenic tobacco lines (TB4, TB4-7, TB4G and TB6G respectively). The expected band size was 1570bp as seen on the TB lines. There was no band on the WT and water negative control. The ladder on the right is a molecular

weight marker from invitrogen. All the plants with positive bands on the gel was carried forward for further analysis.

Table 3. 1: Result of IDna screening showing 6 independent ictB lines and WT which was used to validate PCR and tissue culture screenings. The copy numbers represent number of ictB inserts in a chromosome i.e. All the ictB lines with copy numbers 0, 2, 3 to 4 were investigated alongside the WT using a selective media in a tissue culture.

Samples	Copies
TB4-1	3
TB4-7	2
TB6-1	0
TB1-F	1
TB1G	1
TB4D	3 to 4
TB6G	2
WT-1-1	0

3. 2. 3 Chlorophyll *a* fluorescence (CF) imaging of seedlings

The CF imaging was done in order to detect potential changes in photosynthesis between all experimental plants. Twelve T2 plants were analysed for all transgenic lines and WT. The chlorophyll a fluorescence imaging system was used to examine the quantum photosynthetic efficiency (*Fq*'/*Fm*') of PS11 reaction centre. *Fq*'/*Fm*' had a tendency to be higher at all PPFDs in the transgenic lines compared to the WT control, a finding which is in agreement with Simkin *et al.* (2015). However, there was no significant difference between values for transgenic plants and WT (Figure 3.3).

Images of chlorophyll fluorescence at 200 and 800 µmol m^{-2} s^{-1} PPFD (Figure 3.4), illustrate spatial variation between and within leaves. These images also show a tendency for higher efficiency in the leaves of transgenic plants compared with the WT. This is illustrated by the warm colours observed in the transgenic plants compared with the cooler colours in the WT.

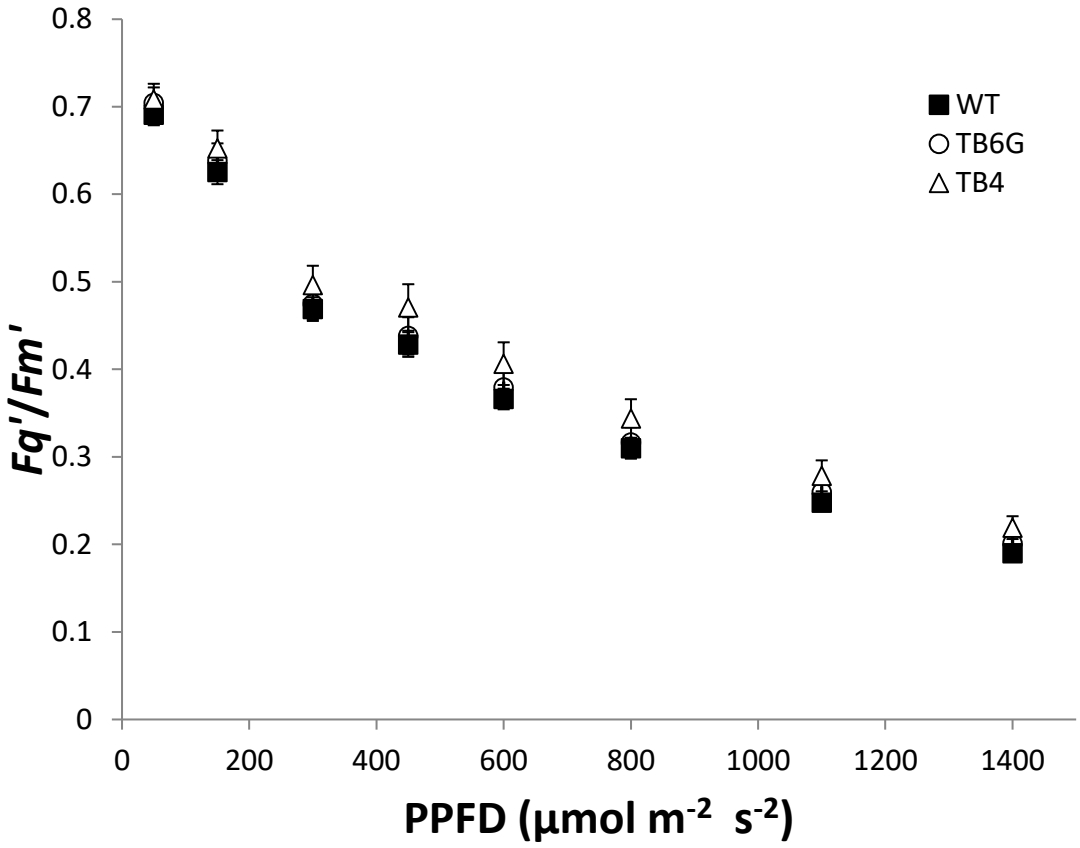

Figure 3. 3**:** PSII operating efficiency as a function of light for seedling capture using chlorophyll fluorescence imaging of WT and ictB lines (TB4-7 and TB6). WT and transgenic plants were grown in controlled environment conditions as described above. Chlorophyll fluorescence was used to determine *F*q'/*F*m' (maximum PSII operating efficiency) at nine light intensities: 150, 50, 150, 300, 450, 600, 800, 1100 and 1400 µmol m^{-2} s^{-1} respectively. The data were obtained using 12 individual plants, from 2 independent transgenic lines alongside WT. There were no significant

differences across all transgenic lines as compared to WT (P>0.05). Error bars represent standard errors of mean.

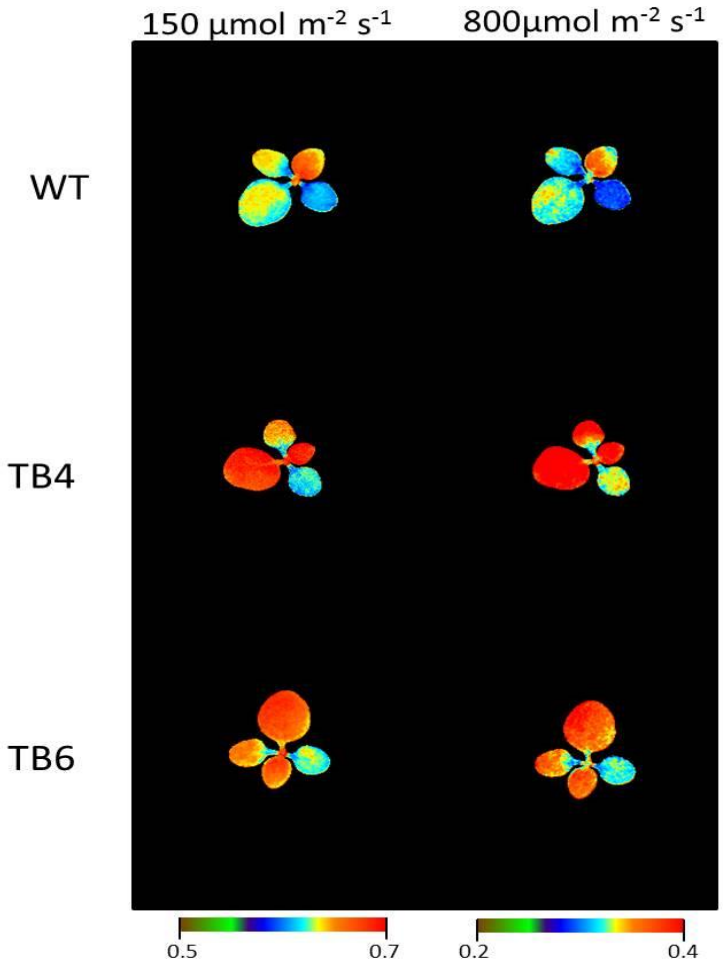

Figure 3. 4: Chlorophyll imaging highlights the differences in photosynthetic efficiencies of TB4 line as compared to WT and TB6. The hotter colours show higher *F*q'/*F*m'. The spatial variation in *F*q'/*F*m' here is represented at two light levels (150 µmol m^{-2} s^{-1} and 800 µmol m^{-2} s^{-1}). The colour bar represents a *F*q'/*F*m' of 0.5 - 07 and 0.2 - 0.4 for the two respective light levels.

3 .2. 4 Infra-red gas exchange

After the CF imaging, the 12 T3 plants from the two independent ictB lines and WT controls were re-potted into (3-inch) individual pots and grown under the same conditions for further two weeks. The gas exchange data analysis is shown in the A/C_i curve (Figure 3.5). From this it is evident that all plants from line TB6G with to copy numbers of ictB transgene have greater photosynthetic rates at all C_i levels, which was an indication of a higher photosynthetic capacity compared to WT. Plant from line TB4 also showed better rates of assimilation but only at the higher C_i concentration. The maximum rate of RubisCo carboxylation (Vc_{max}) determined from the initial part of the curves was not significantly different between transgenic and WT plants (Figure 3.6A). However, the maximum electron transport rate (J_{max}) taken from the saturating part of the curves was significantly higher in ictB plants compared with the WT controls, illustrating higher maximum rates of photosynthesis and therefore greater photosynthetic capacity (Figure 3.6B).

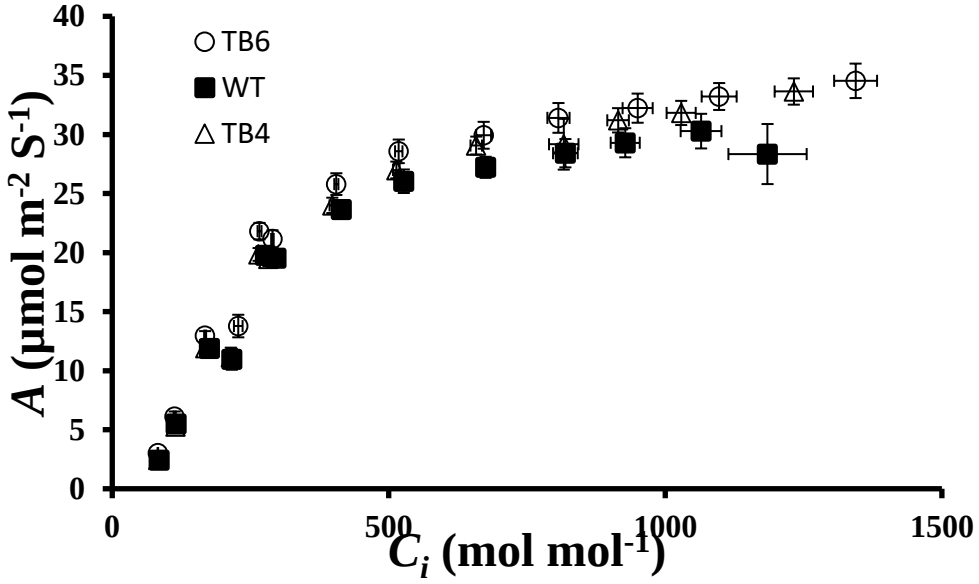

Figure 3. 5: A/C_i curves indicating photosynthetic responses of WT and ictB tobacco plants as a function of internal CO_2 concentration. Rates of photosynthetic CO_2

fixation were recorded when rates were stable at different CO_2 concentrations (A/C_i) at saturating-light levels in fully expanded leaf from both WT and ictB plants. All plants were grown in natural light conditions in the greenhouse, light levels were between 600 and 1400 μmol m^{-2} s^{-1} (supplemental light maintain a minimum of 600 μmol m^{-2} s^{-1}) (Lefebvre *et al.,* 2005).

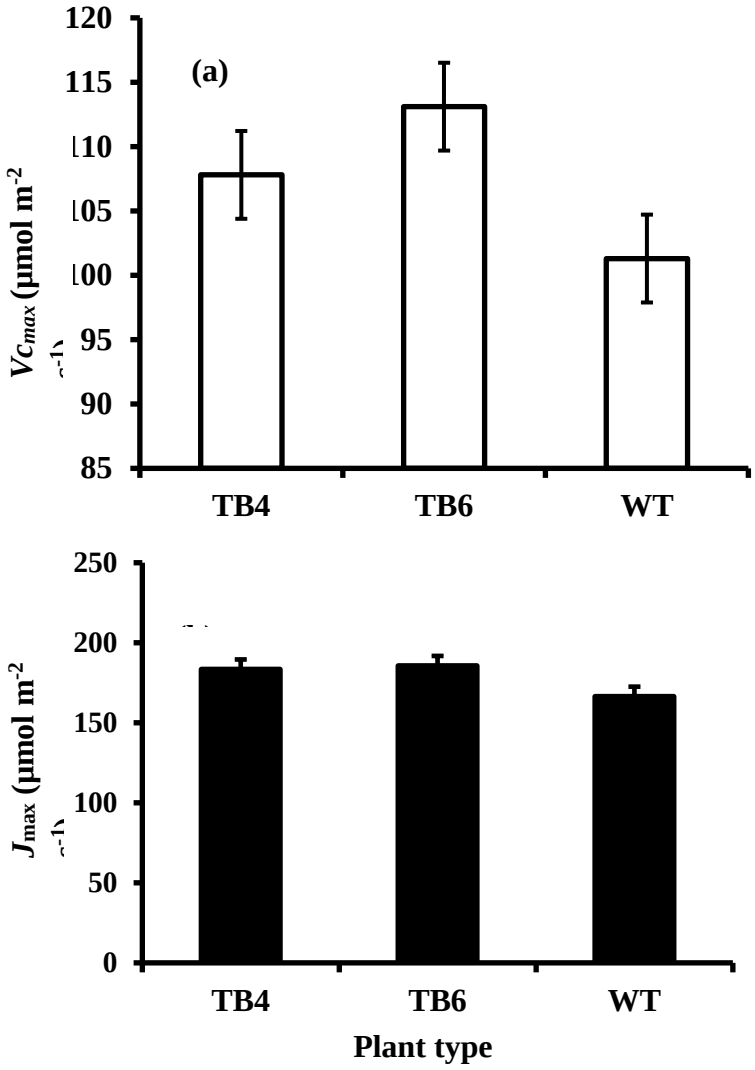

Figure 3. 6: Vc_{max} (a) and J_{max} (b) and derived from A/Ci response curves. Values represent 12 plants from 2 independent TB lines and WT. Analysis of Vc_{max}; maximum rate of RubisCO carboxylation in fully expanded leaves revealed no significant difference between transgenic and WT plants (>0.05) but there was a

significant difference in the maximum electron transport rate of all TB lines compared to WT (<0.05).

3. 2. 5 Diurnal photosynthesis

The diurnal photosynthetic curves (Figure 3.7) shows similar patterns of assimilation rate for both WT and transgenic plants over the course of the day. Although, assimilation rate peaked more in ictB plants, the WT showed increases in *A* with increasing light to a peak 4 hour into the light at 1pm, followed by a general decrease in *A* that coincided with the decreases in PPFD later in the day. Photosynthesis was higher at mid-day at the highest PPFD intensity in the transgenic plants compared with the WT ($t=3.216$; d.f. 232; $P<0.001$). Peak photosynthesis occurred earlier in the WT around 2-3 h into the light, whilst this occurred about 1h later in the transgenic plants. Photosynthetic rate was maintained in the transgenics for a further 2-3 h, whilst the WT started to show a slow decrease in rate, before rapidly decreasing towards the end of the photoperiod, when light dropped below 1000 µmol m^{-2} s^{-1}.

Stomatal conductance (g_s) showed a similar response as *A*, although not unexpectedly there was much greater variation in the values. The WT plants tend to have a higher stomatal conductance (g_s) during the middle of the day when there is peak light source and towards evening, which is an indication that the WT plant lose more water during this period and would have a reduced water use efficiency (WUE). However, there was no significant difference between g_s in WT and transgenic plants.

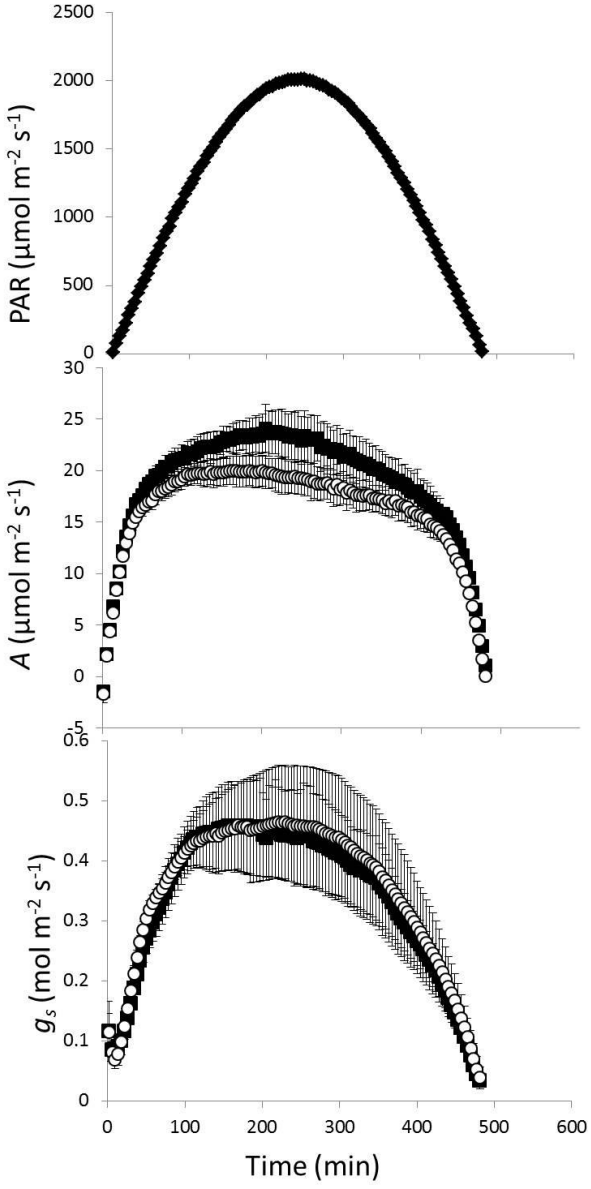

Figure 3. 7: Diurnal measurement of leaf photosynthesis (*A*) and stomatal conductance (g_s) of tobacco plants under ambient temperature. Measurement occurred between 07.00h and 15.00h. A sinusoidal photosynthetic photon flux density (PPFD) pattern was programmed into the LI-CORs and measurements of gas exchange taken every minute. Diurnal patterns of *A* and g_s was used to determine WUE_i. Open circle symbol (WT), close square symbol (ictB) and closed diamond symbol (PPFD).

Measurements are an average of three replicates and error bars are standard error. For clarity every 10^{th} data point is plotted.

3. 2. 6 Stomata Density Analysis

The evidence from stomata density analysis of three mature leaves from three separate plants of all experimental lines seem to show that TB4 had a lower stomatal density per mm^2 area of abaxial leaf surface, followed by WT and TB6 respectively (Figure 3.8 and 3.9). Although, there was no significant difference on the stomata density of these plants but the ictB plants corresponded to higher photosynthetic CO_2 efficiency as shown on the gas exchange analysis.

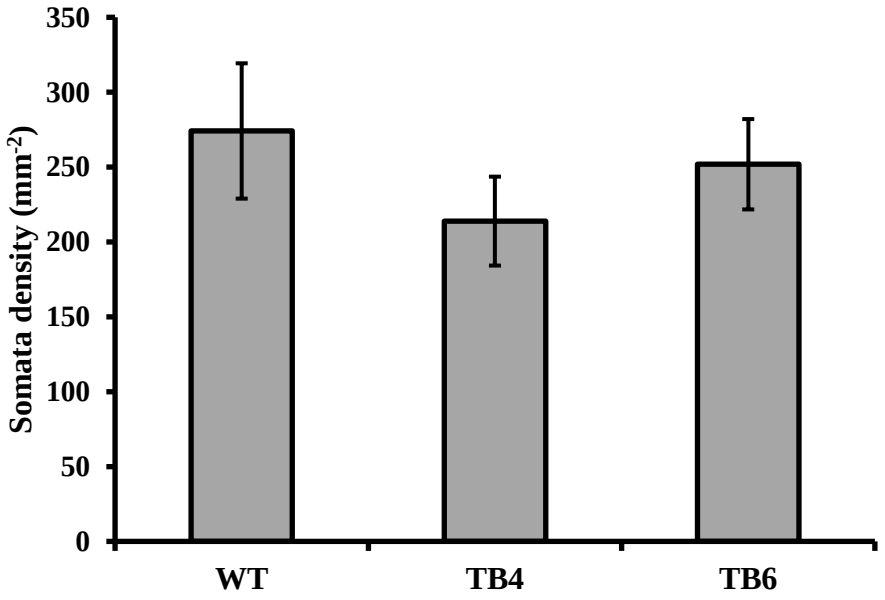

Figure 3. 8: Stomata density of the abaxial surfaces of from three different leaves from 12 WT tobacco, TB4-7 and TB6G respectively. There is no significant difference between the stomata densities of WT and the TB lines (>0.05).

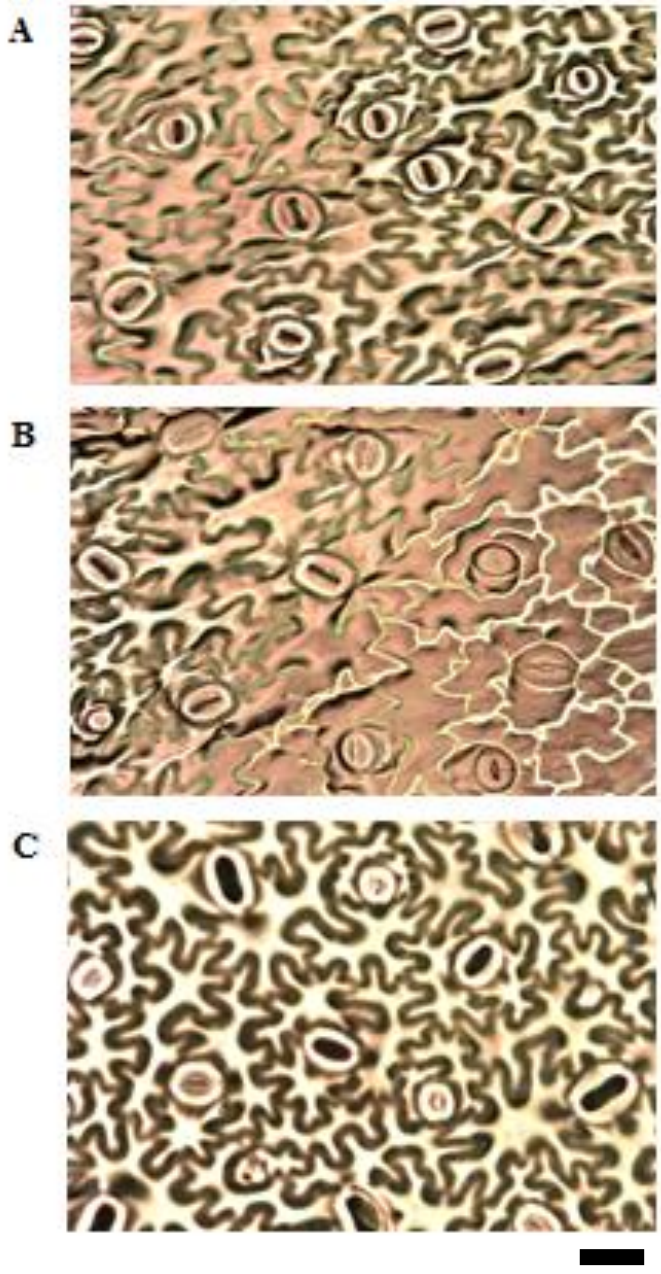

Figure 3. 9: Images of leaf negative impressions of WT tobacco plant (**A**), TB4-7(**B**) andTB6G (**C**). Stomata are clearly obvious in amongst the wavy epidermal cells. Scale bar represents 10 µm.

3. 3 Discussion

There is strong evidence that ictB expression in tobacco plants increases photosynthetic rate in the studied transgenic plants. The TB plants had higher rates of *A* determined by gas exchange and higher photosynthetic capacity. Diurnal step change measurements confirmed the high rates of photosynthesis in TB plants and the fact that *A* peaked later in the diurnal period and at a higher light level in the transgenic plants support the suggestion that the ictB plants have greater photosynthetic capacity. This work agrees with the work of Simkin *et al.* (2015) and other previous studies (Lieman-Hurwitz *et al.*, 2005) that suggest that ictB increases photosynthesis in tobacco. Both transgenic and WT plants showed similar values of photosynthetic efficiency at all light levels, which is maybe not surprising, as higher CO_2 assimilation rate would not necessarily be observed by chlorophyll fluorescence assessment of PSII photochemistry unless the measurements were taken under non-photorespiratory conditions (Lawson & Murchie, 2014). This can be explained because both O_2 and CO_2 fixation of RubisCO will act as a sink for end products of electron transport and therefore *Fq'/Fm'* is not linearly related to CO_2 fixation (see McAusland *et al.*, 2013).

The images of *Fq'/Fm'* at various light levels indicted a degree of spatial heterogeneity in photosynthetic efficiency between and within leaves. Both WT and transgenic plants appear to have similar spatial variation although the transgenic plants were often observed to have slightly high values, but this was not significant when all replicates were considered. Spatial heterogeneity in photosynthetic efficiency has been reported previously in transgenic plants (von Caemmerer *et al.*, 2004; Lawson *et al.*, 2008), however these reports suggested that greater variation

was generally found in transgenic plants compared to WT. However, it should be noted that these previous studies were performed on antisense studies.

The observed transgenic plants showed a trend of lower g_s over the diurnal period, which would have implications for WUE, these differences were not significance. This agrees with previous studies on antisense tobacco with reduced photosynthetic enzyme activity which showed no difference in stomatal conductance (g_s') between WT and transgenic lines despite large reduction in assimilation (*A*') rate resulting in a significant reduction in WUE (Quick *et al.,* 1991; Hudson *et al.,* 1992). However, the focus of these studies was not on g_s and experiments were designed to examine *A*. Lawson *et al,* (2008) examined stomatal responses in the antisense SBPase tobacco and reported higher g_s and differences in the speed of stomatal responses to a step changes in light that was colour dependant. These studies suggested that the link between *A* and g_s was altered in these plants. Earlier work on the antisense RubisCO plants (von Caemmerer *et al.,* 2004) also showed higher than necessary g_s values in transgenic plants but no significant differences in g_s between WT and transgenic (Baroli *et al.,* 2008).

Again, no difference in stomatal density were observed and this agrees with the earlier studies on transgenic plants (von Caemmerer *et al.,* 2004; Lawson *et al.,* 2008; Baroli *et al.,* 2008) which indicates that manipulating stomatal numbers is a sound hypothesis for altering gas exchange and water use efficiency in these plants. Manipulating stomatal density of these ictB plants provided a route to manipulating g_s and water loss without effecting *A* and therefore provide an important tool to either

further enhance CO_2 assimilation (*A*) and/or improve WUE. However, alterations in stomata density could be off-set by changes in stomatal function and therefore it is yet to be ascertained if the best approach to manipulate g_s would be as a result or a combination of the reduced stomata number, size of aperture, alterations to function through manipulations of GC electron transport. Conclusively, the selected homozygous ictB plants were transformed with the *Arabidopsis thaliana* EPFs and Fd to assess the synergistic effects of these foreign genes on stomata characteristics and overall photosynthetic capacity.

4. 0 Chapter 4

4. 1 The effect of co-expressing EPFs and ictB in transgenic plants.

The stomata serve as the valve for the exchange of gases in and out of the leaf. The guard cells (GC) are responsible for the opening and closing mechanism of the stomata. These GCs adjust the stomatal aperture in response to internal and external signals in order to maximize carbon dioxide (CO_2) uptake for photosynthetic carbon assimilation (*A*) and minimise the amount of water loss during transpiration. Stomatal conductance (g_s) is not only determined by the pore aperture but also the density and size of stomata on the leaf surface. During the early stages of plant development, the number and density of stomata are regulated by some genetic and environmental factors. Some of the internal signalling molecules involved in stomatal development and regulation are the epidermal patterning factors (EPF1, EPF2 and EPFL9) (Doheny-Adams *et al.,* 2012). The data provided here will focus on the analysis of transgenic ictB Tobacco plants overexpressing the *Arabidopsis thaliana* EPFs which can be used to understand the impact of changes in stomatal density and metabolism on the plants photosynthetic capacity.

Epidermal patterning factor genes have been shown to be involved in the regulation of stomatal development. Previous studies have illustrated that over expression of EPF1 and EPF2 decrease stomatal density (Doheny-Adams *et al.,* 2012), whilst over expression of EFPL9 (also known as STOMAGEN) increases the number of stomata per leaf (Doheny-Adams *et al.,* 2012). EPF1 and EPF2 genes are both inhibitors of stomata development (Hara *et al.,* 2009) and have been demonstrated to exhibit different but overlapping functions in this process. EPF1 is mainly involved in the orientation of cell division and prevention of stomata from forming in clusters and

pairs while the EPF2 inhibits the formation of meristemoids and also promotes the formation of pavement cells (Doheny-Adams *et al.,* 2012; Hunt and Gray, 2009). EPFL9/STOMAGEN on the other hand, was shown to promote stomatal development by inhibiting EPF1 and EPF2 peptides from binding to their receptors (Kondo et al., 2010).

4. 2 Results

4. 2. 1 PCR and DNA sequence

To confirm the presence of the L1 construct in the different transformed colonies before sequencing, several colony PCR reactions were carried out using the specific primers for the L1 plasmids (PL1Forward and pL1Reverse as shown on Table of primers) for the genes of interest. The PCR protocol was conducted following the description in the material and methods. The PCR screening showed bands for the selected constructs during gel electrophoresis. The expected band size for EPF1 clone was 1572bp (Figure 4.1) after amplification of the target DNA sequence and this was visible in colony 25 (lane C25). For EPF2 clone, colony 40 (lane C40) gave the required band size of 1590bp (Figure 4.2) while EPFL9 clone (lane C15) gave a band size of 1512bp (Figure 4.3). The PCR result was compared to the virtual PCR gel analysis using geneious software and all reactions yielded the same result as shown on the physical maps of L1 plasmids of EPF1, EPF2 and EPFL9 (Figures 2.2 to 2.4). DNA sequence analysis also showed correct sequence matches to confirm the result of the tissue culture selection and IDna analysis which indicated the presence of the ictB gene in the selected transgenic tobacco plants. It was expected that plants over-expressing the EPF1 and EPF2 genes will have a very few stomata. The variation in ratio of the densities and sizes of stomata that would be observed in WT and the ictB

plants bearing these EPFs construct would be an important tool in studying how these plants regulates their stomata conductance and photosynthetic assimilation.

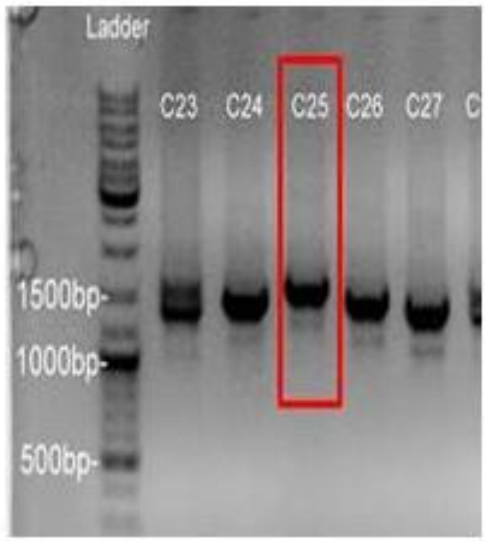

Figure 4. 1: Analysis of L1AtEPF1 insert using colony PCR with the primers (pL1MForward and pL1MReverse) gave the expected band size on agarose gel image (1,572bp). Sequencing data confirmed colony 25 (C25) on the gel image to be L1AtEPF1 and DNA from this *E.coli* colony was used for making L2 construct.

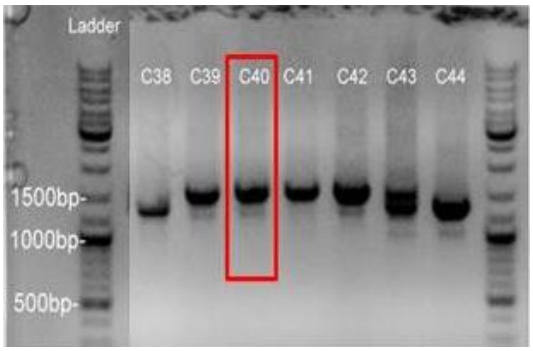

Figure 4. 2**:** Analysis of L1AtEPF2 insert using colony PCR with primers (pL1MForward and pL1MReverse) gave the expected band size on agarose gel image (1,590 bp). Sequencing data confirmed colony 40 (C40) on the gel image to be L1AtEPF2 and DNA from this *E.coli* colony was used for making L2 constructs.

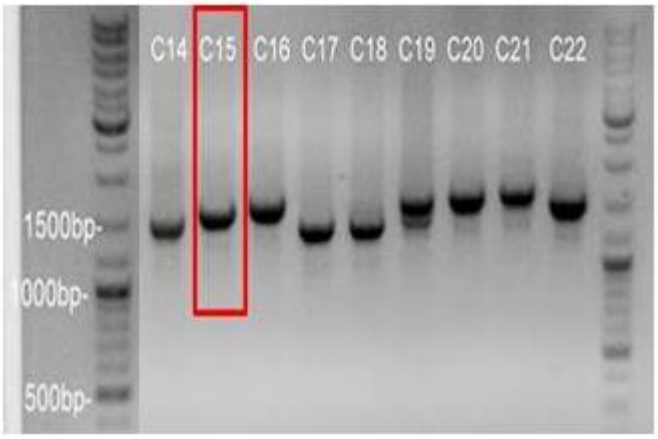

Figure 4. 3**:** Analysis of L1AtEPFL9 insert using colony PCR with primers (pL1MForward and pL1MReverse) gave the expected band size on agarose gel image (1,512 bp). Sequencing data confirmed colony 15 (C15) on the gel image to be L1AtEPFL9 and DNA from this E. coli colony was used for making L2s.

L2 Plasmid PCR Analysis was also conducted using the same protocol as in L1 above, making reductions to the elongation time due to the smaller size of the expected DNA fragment of 552bp as shown on the physical maps of all L2 plasmids (Figures 4.4 to 4.6). All PCR gel analysis yielded the same size as shown in physical maps (Figures 2.5 to 2.7). The similarity in sizes was possible with the different EPFs constructs because the same set of specific primers (Bar4F and Bar1R) for the L2 plasmids was used in the PCR reaction. These primers were designed to anneal to the complete sequence of the basta gene that serves as a selective marker for the transgenic plants that would develop after a successful transformation.

Multiple DNA sequence analysis was done to confirm the presence of the sequence of interest before Agrobacterium transformation of the EPFs L2 plasmids into the selected tobacco plants. All sequence analysis returned a positive match (see appendix) and contained the same base pairs as the physical maps of all L2 plasmids when virtually compared using geneious software. For the double L2 EPF1 and EPF2 construct, an EcoR1 restriction enzyme digest following the protocol as described in the materials and methods section yielded three different band sizes of 6051bp, 1401bp and 1120bp (Figure 4.7), that when summed up, made up to be the entire size of 8572bp plasmid as indicated by the physical map (Figure 2.8) generated using geneious molecular analysis software.

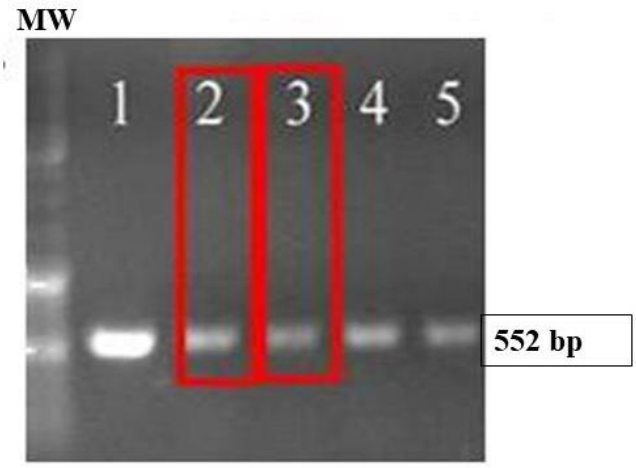

Figure 4. 4**:** PCR fragment of L2AtEPF1 using primers (Bar4F and Bar1R) to check the presence of the bar gene was positive. Expected band size on agarose gel image is (552bp). The highlighted columns (colonies 2 and 3) were sequenced but only plasmid DNA from colony 2 was used for agrobacterium transformation.

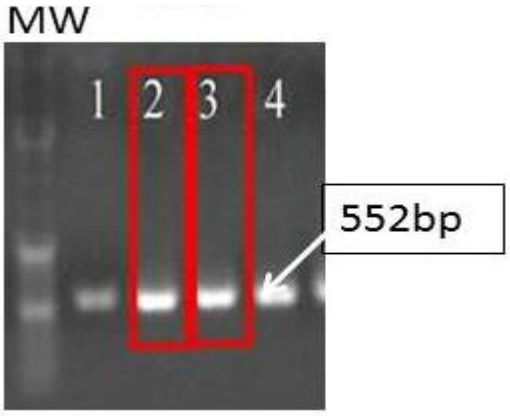

Figure 4. 5: PCR fragment of L2AtEPF2 using primers (Bar4F and Bar1R) to check the presence of the bar gene was positive. Expected band size on agarose gel image is (552 bp) and molecular weight marker (MW) used was from invitrogen. The highlighted columns (colonies 2 and 3) were sequenced but only plasmid DNA from colony 3 was used for agrobacterium transformation.

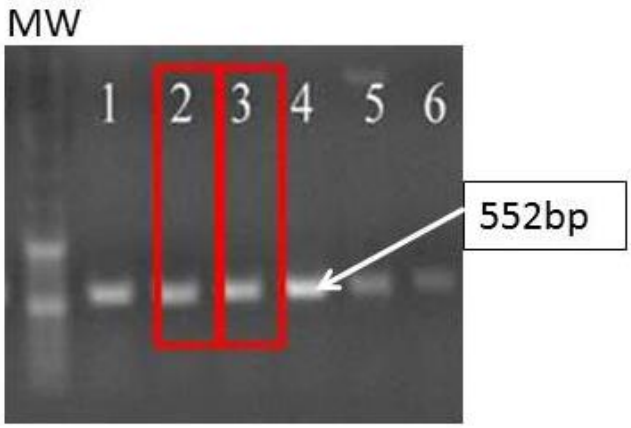

Figure 4. 6: PCR fragment of L2AtEPFL9 using primers (Bar4F and Bar1R) to check the presence of the bar gene was positive. Expected band size on agarose gel image is (552bp) and molecular weight (MW) marker used was from invitrogen. The highlighted columns (colonies 2 and 3) were sequenced but only plasmid DNA from colony 2 was used for agrobacterium transformation.

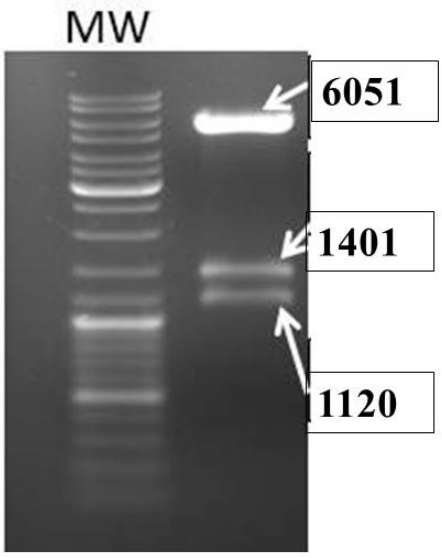

Figure 4. 7: Restriction enzyme digest of the L2AtEPF1&NtEPF2 construct using EcoRI yielded three clear bands on the gel image (1120bp, 1401bp and 6051bp). These bands were verified by a virtual EcoRI digest using the geneious bioinformatics software.

4. 2. 2 Plant transformation and screening

All tobacco plants were transformed and selected using the same protocol as described in the material and methods. Successful transformed plants were expected to germinate from the selective media. From these sets of plants, 19 independent lines was transferred to magenta pots and screened further (Figure 4.8A). The plants that germinated were the plants that carried the selective antibiotic and basta genes as indicated in the L2 plasmid maps. These plants when trans-potted to soil were further treated by topical application of the basta herbicide on their leaves and only the transgenic plants showed to have tolerated the discolouration effect of this selective maker and did not turn brown and/or died (Figures 4.8B to 4.8C).

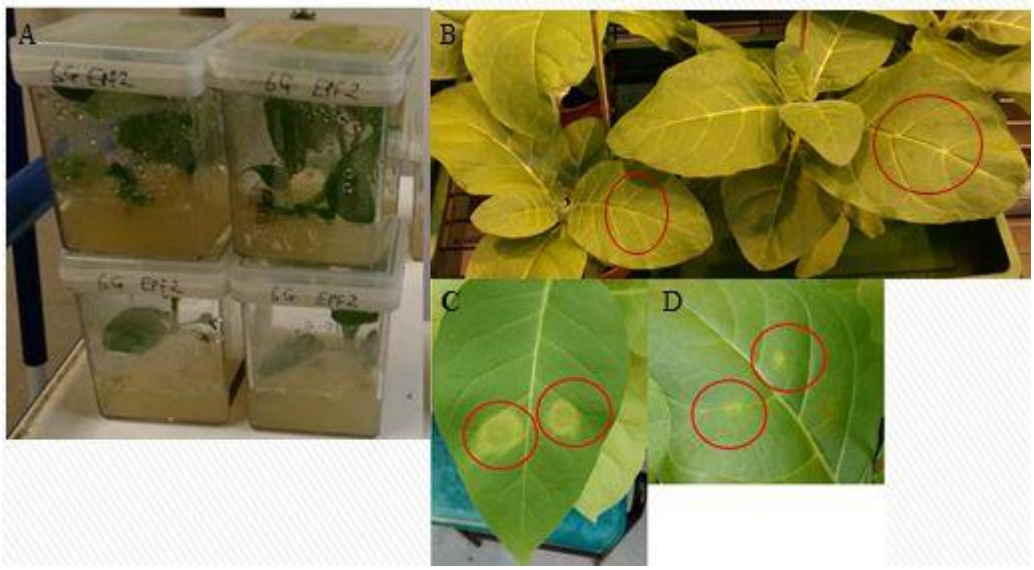

Figure 4. 8**:** Images of transgenic tobacco plants during different stages of growth and screening. (**A**) six weeks old plants grown in MS media. (**B**) Mature plants transferred to soil for herbicide screening. (**C**) treatment of WT and (**D**) ictB/EPF tobacco leaves with the basta herbicide to select transformants. After one week, WT leaf continues to turn yellowish while the transgenic line neutralised the effects of the herbicide. The red circles represent points of application of the herbicide. Only the plants carrying the resistant gene for the basta herbicide are able to resist the herbicide in growth media and leaf treatment. All trans-potted 19 independent transgenic tobacco plants including ictB/Fd (Table 2.4) were maintained in soils placed under controlled growth conditions for the collection of T1 generation seeds for further analysis.

4. 2. 3 Stomata Density analysis

Stomata density analysis of the T0 transgenic EPF plants was done as described in the material and methods section and this was used to trim down the plants to be selected for use in the next phase of screening (Figures 4.9A to 4.9J). The variation in stomatal numbers and patterns was easily observable from the resultant images

from the different fields of views under a light microscope. This initial finding showed and supported evidence that the EPFs are key regulators of the stomata lineage (Hara *et al.,* 2007; Hunt and Gray, 2009; Doheny-Adams *et al.,* 2012; Graham *et al*., 2017; Caine *et al.,* 2018). There was observable significant difference among all transgenic lines (Figure 4.9K), error bars were an indication of the standard error of mean.

Four independent T0 lines were selected using stomata density analysis technique and same number was used for the T1 segregating generations of these plants (Figure 4.10). The data from the T1 plants, showed lesser divergence from the T0 across the groups and this is possibly an indication of the segregating population in these sets of plants (Figure 4.11). Amongst the T1 generation there was a significant difference between the EPFL9 plants as compared to all other transgenic lines. These EPFL9 plants showed more stomata, that are evenly distributed over the leaves' surfaces. The stomata on these plants seemed to be of similar sizes. On the other hand, at least two of the T1 EPF1 and EPF2 population was significantly different across the two groups and when compared to WT. These plants were shown to have a lower number of stomata of different sizes and developmental stages. Some of these observable stomata on these plants were so small, underdeveloped and undifferentiated (error bars represent the standard error of means across the groups).

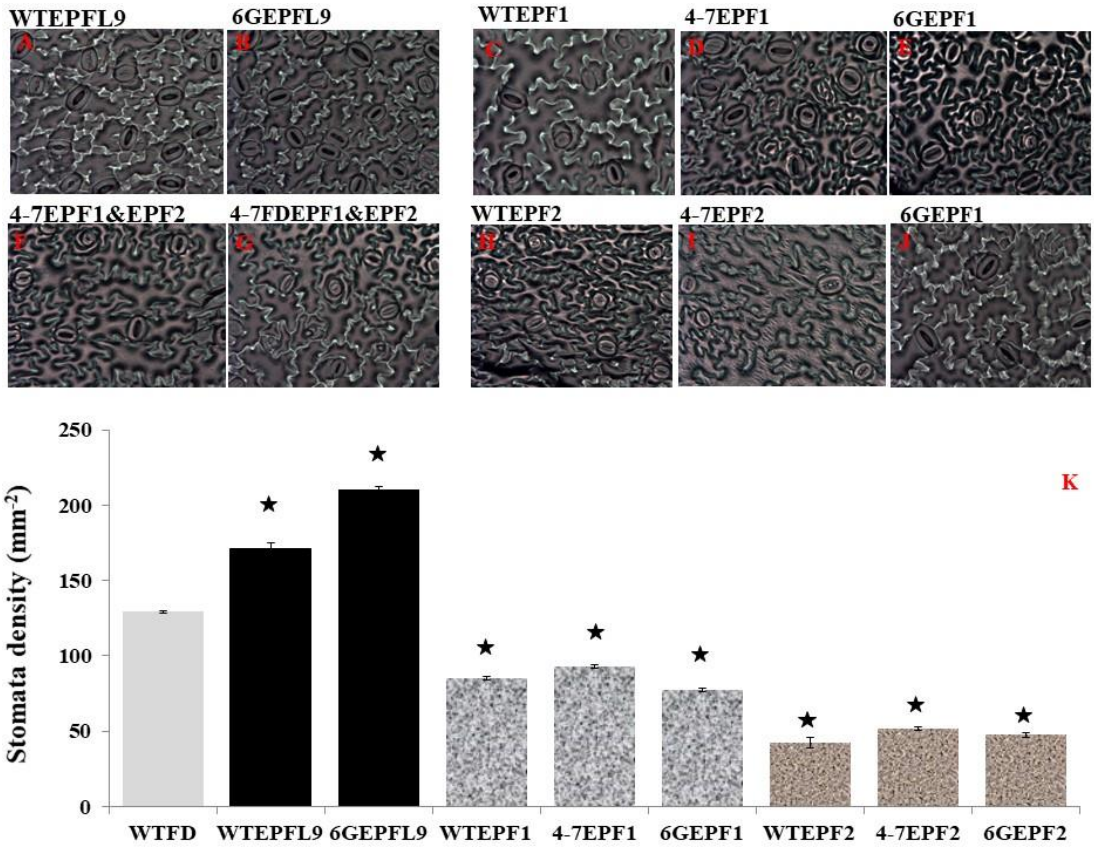

Figure 4. 9**:** Images of adaxial leaf stomatal impressions of some of the T0 tobacco EPF mutants revealing four classes of transformants. (**A-B**) EPFL9 tobacco leaves that overexpresses stomata, (**C-J**) single and double transformants of EPF1 and EPF2 with reduced stomata development and expression. All images of the epidermis are at the same magnification (x20). The genotype of each image is defined by the values at the top of each image (n=3 for all EPF mutants). (**K)**There are significant differences between the stomata densities of the EPFs and WT ($p<0.05$).

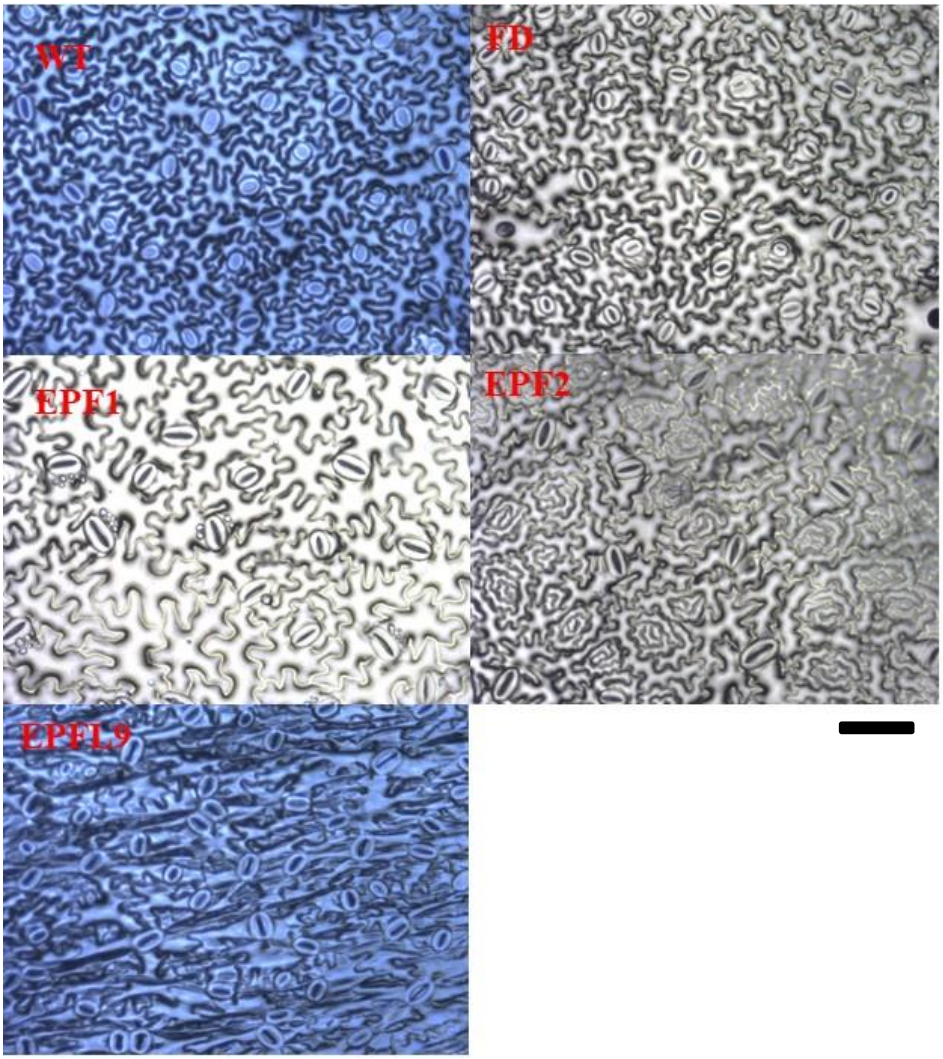

Figure 4. 10**:** Images of adaxial leaf stomatal impressions of some of the T1 transgenic tobacco and WT. The EPF1 and EPF2 tobacco leaves exhibited the lowest stomata density when compared to WT and FD plants whose stomata density have not been manipulated. The EPFL9 leaf could be seen to have the most stomata density because they are positive regulators of stomata development. All images of the epidermis are at the same magnification (x20). The genotype of each image is defined by the value at the top left corner of each image. There is no sinificant difference between the stomata densities of the WT and FD plants but when both are compares to the EPF1 and EPF2, there are clear significant differences in stomata densities. The EPFL9 mutants also showed more stomata density when compared to every other group including WT. Scale represents 50 µm.

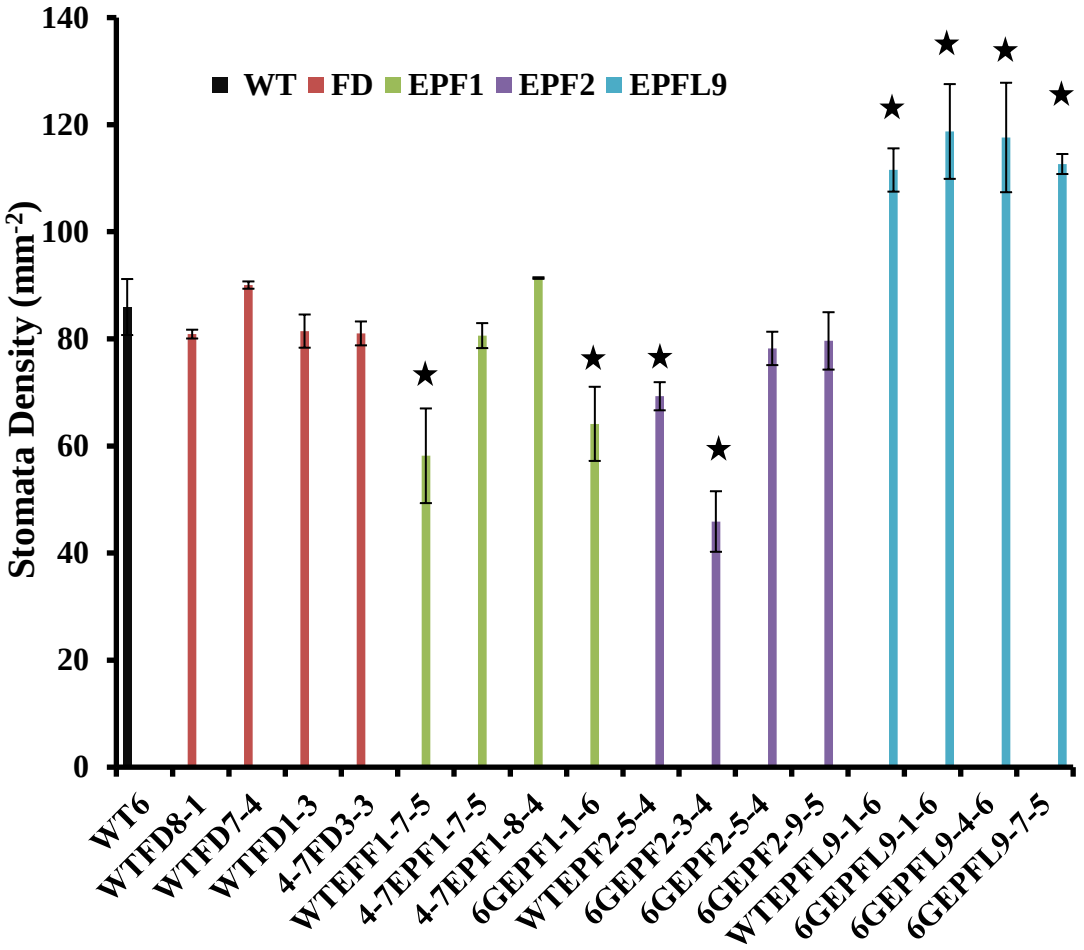

Figure 4. 11**:** From the chart and statistical analysis, there is a significant different between the EPFL9 lines and WT. Two independent lines each of EPF1 and EPF2 also displayed significant difference from WT. All lines from the transgenic FD displayed no significant difference from the WT. filled five-point star represent significant differences ($p < 0.05$).

4. 2. 4 Infra-red gas exchange

All plants were grown under the same condition as in chapter 3. The gas exchange data analysis of the T1 generation was done using Licor 6800 portable photosynthesis

system developed by the same manufacturer as the Licor 6400 indicated in the material and method. The resultant A/C_i curve (Figure 4.12) represents 3 plants from 4 independent lines across the EPFs. From this data, it can be deduced that almost one plant from each independent line across the groups had a significantly different electron transport rate within the group. This observable variation across the groups was suspected to be influenced by the high temperature during the month of July, 2018 and the segregating population of the T1 transgenic plants.

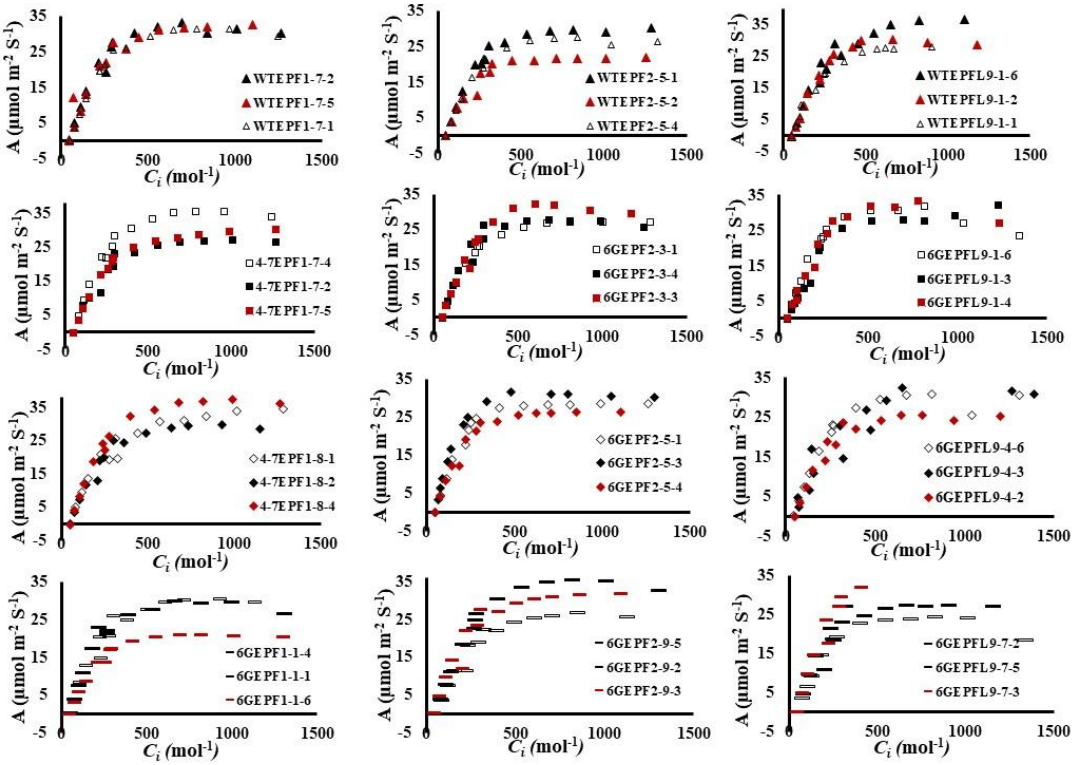

Figure 4. 12**:** A/C_i curves indicating photosynthetic responses of all transgenic tobacco plants from each T1 EPF groups as a function of internal CO_2 concentration. Rates of photosynthetic CO_2 fixation were recorded when rates were stable at different CO_2 concentrations and saturating light levels in fully expanded leaf from all EPF plants. Temperature was very high and unstable during growth period, averaging 45^{o}C for most of the month. All plants were grown in natural light conditions in the

greenhouse, light levels were between 600 and 1400 μmol m^{-2} s^{-1} (supplemental light maintain a minimum of 600 μmol m^{-2} s^{-1}) (Lefebvre *et al.,* 2005).

4. 2. 5 qPCR reaction analysis

The tissues integrity was maintained as described in the material and method chapter. After the qPCR thermocycling, it could be seen that not all the plants in the different groups were expressing the *At*EPF genes (Figure 4.13A to C). All the transgenic tobacco plants expressing the transgenes were indicated with (filled 5-point star). The gene expression analysis of the T1 generation did not always correlate with the stomata density analysis and/or other physiological analysis. For example a plant showing a high expression level of *At*EPF2 with a visible trait of bigger sizes of stomata that are sparsely distributed across the surface of the leaf did not always have the highest rate of electron transport chain as indicative of these sets of plants (Doheny-Adams *et al.*, 2012).

4. 3 Discussion

Out of all transformed plants (Table 2.3), four independent T0 lines from the EPFs and Fd were analysed and cultivated for T1 seeds. WT plants were also grown under similar conditions to serve as control. Stomata density analysis at the T0 stage showed an overview of the variation of stomata patterning of the EPF leaves. It is expected that these transformed ictB plants with EPF constructs would display varied ratios of stomatal density to sizes (Caine *et al*., 2018).

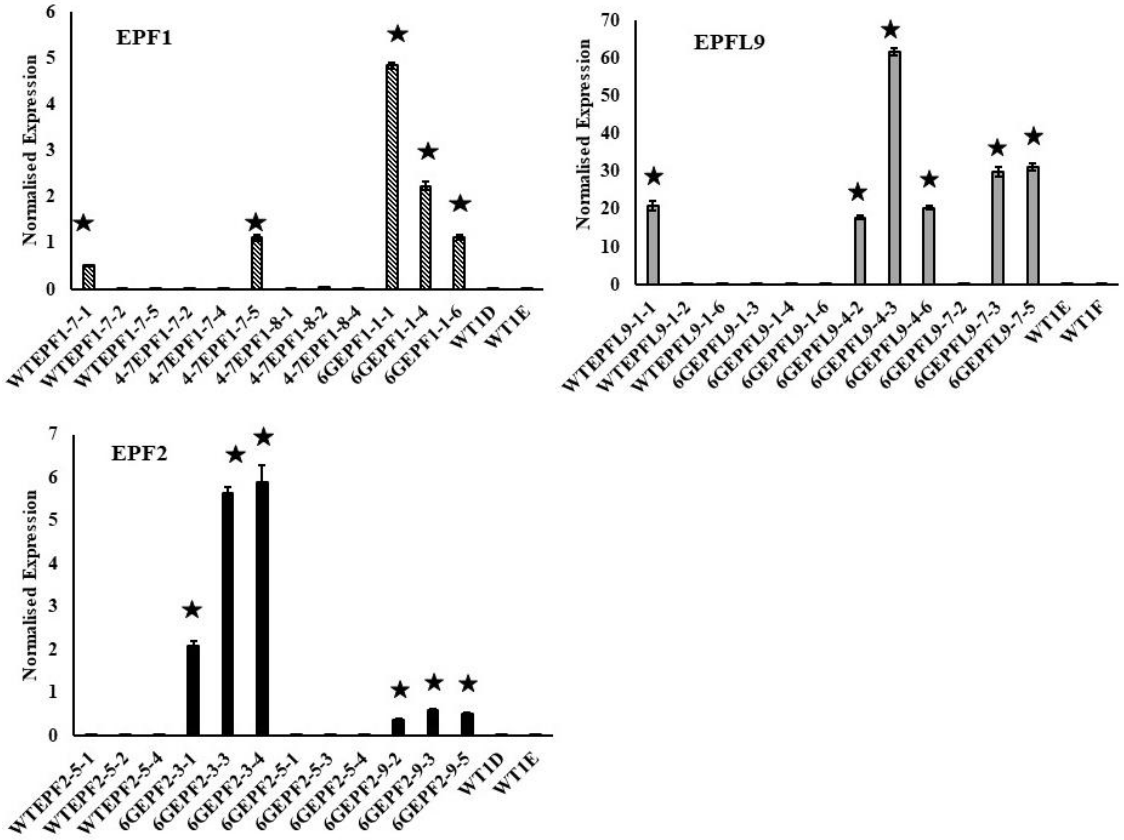

Figure 4. 13**:** The qPCR validation experiments of T1 EPF generations shown: the three bar charts are the relative expression of EPF genes against actin. Four independent lines of each EPF gene as normalised to WT (Each gene; n=12). The error bars represent the standard error of the mean. Five plants from the EPF1 showed significant expression level of the gene, six plants each from the EPF2 and EPFL9 showed significant levels of expressions of these genes. Filled 5-point star represent plants with high expression levels of the foreign genes ($p < 0.05$).

These sets of transgenic plants served as excellent tools for the assessment of the impact of altered stomata density and function. Previous studies have shown that plants expressing the different EPF genes would exhibit a great variation in stomatal size and density as well as stomatal response time to internal and external stimuli

(Doheny-Adams *et al.,* 2012). Some of the Arabidopsis plants manipulated to have lower stomatal density by Doheny-Adams *et al,*.(2012) appeared to have larger sizes of stomata, reduced transpiration, large biomass and increased growth tolerance to limited water availability. Therefore, overexpressing these EPFs traits in crop plants could be used in future for economic agronomy.

During the later stages of vegetative germination of these plants in July, summer 2018, the temperature and natural lighting was so intense that most of the photosynthetic gas exchange analysis was repeated more than two times due to the inability of these plants to adapt to high light intensity and temperature increase (Athanasiou *et al.,* 2010). Low light adapted plants develop larger antennae and more chlorophyll per reaction centre so that the rate of light energy will be faster and more efficient in low light. Higher light tends to oversaturate PSII centres and renders the electron transport chain less effective in these plants. PSII was also observed to be prone to photoinhibition that ultimately result to a decrease in CO_2 fixation (Athanasiou, 2008).

Kulheim *et al.*, (2002), showed that plants rapidly switch to NPQ within a matter of seconds after the light exposure. This among the previous paragraph explains why the chlorophyll fluorescence image and gas exchange did not change so much in all transgenic plants. Offspring from the same line did not always display consistency in their response to blue light and gas exchange analysis.

Although, the ictB plants have shown high photosynthetic capacity (Simkin *et al.*, 2015), manipulation of stomatal density on these plants was important as it

introduced another dimension to further enhance CO_2 assimilation (*A*'), $g_{s'}$ and WUE. It is not yet ascertained if the expected positive effect on photosynthesis would be as a result or a combination of the varying stomata number, size of aperture, improved GC electron transport and RubisCO enzymes' activities.

This work has most importantly enabled further analysis of ictB plants by overexpressing the multiple EPF genes in direct comparative studies with the WT. Although, multigene manipulation of crop plant in the field is still premature, there is the urgent need to provide solid evidence for the multigene manipulation of Calvin cycle enzymes and structural CO_2 pathways such as stomata to increase the yield of food crops for the ever-growing global population.

5. 0 Chapter 5

5. 1 Characterising the physiology of transgenic ictB/Fd tobacco plants to determine effect on guard cell photosynthesis.

The signals and energy sources for GC functions during photosynthesis come from various sources but a look at altering the GC metabolism will give an insight on the function of GC and water use regulation in plant during photosynthesis. GC metabolism is a crucial energy source for the functioning of the stomata and possibly involves both electron transport and Calvin cycle activity (Lawson *et al*., 2008). One important molecule in this process is the Ferredoxin (Fd) protein with key roles in photosynthetic electron transport as well light activation of Calvin cycle enzymes, making it a prime target for manipulation (Raines and Lloyd, 2001; Guy and Paula, 2013). The data provided here focused on the analysis of transgenic plants overexpressing guards cell specific *At*Fd in order to study the impact of stomata response and metabolism on the plant's photosynthetic capacity.

It has been demonstrated that activities of the GCs require energy in form of ATP which can be provided by the GC electron transport chain (ETC) (Guy and Paula, 2013). This process can take place in the chloroplasts and mitochondria during photophosphorylation and oxidative phosphorylation respectively (Figure 5.1). Fds present at photosystem I (PS1) are actively involved in linear electron transfer (LET) to generate NADPH required for the reduction of CO_2 in the Calvin cycle. In addition to the LET, Fds also function in cyclic electron transfer (CET) of photosynthetic electrons for increased ATP synthesis without concomitant accumulation of NADPH (Guy and Paula, 2013). GC chloroplasts have been shown

to have all biochemistry machinery necessary to synthesize sucrose and degrade starch evidence indicates that guard cells can also fix HCO3 via phosphoenolpyruvate carboxylase (PEPc) (Daloso et al., 2015)

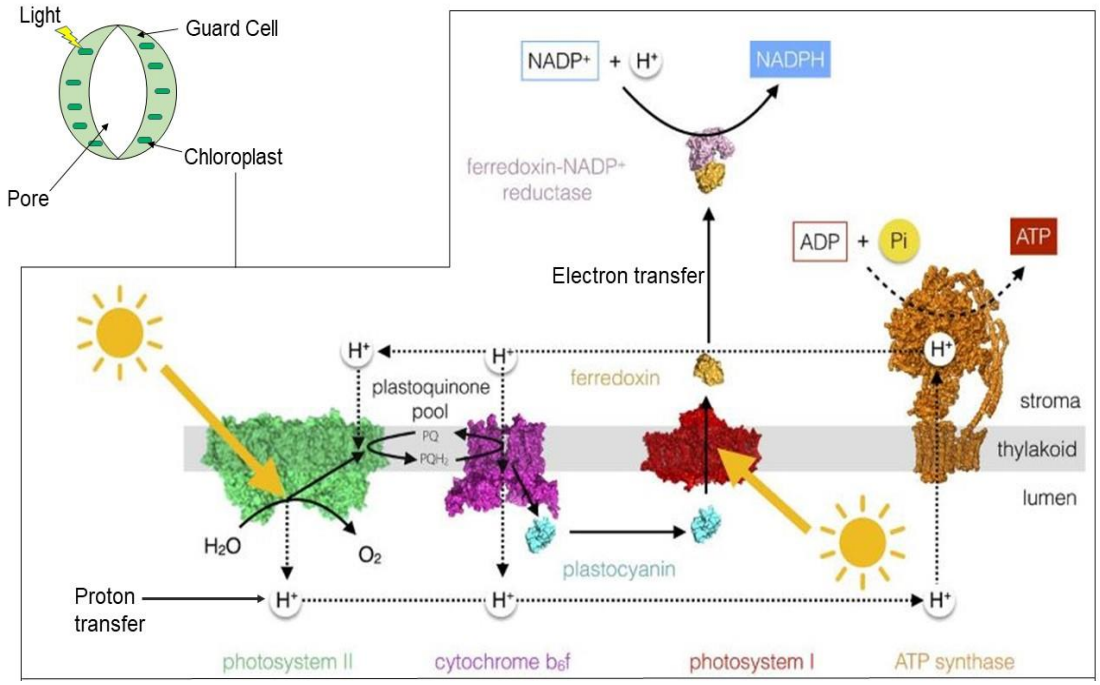

Figure 5. 1: Generation of high energy molecules in the guard cells during photosynthesis. The light induced electron transfer begins with the splitting of H_20 by Photosystem II (PSII) to produce oxygen and reduction of the electron acceptor plastoquinone (PQ) to plastoquinol (PQH_2). PQH_2 in turn carries the electrons to a thylakoid-embedded protein complex called cytochrome b6f (cytb6f) and becomes oxidized to plastoquinone by cytb6f which releases the electron to a small water-soluble electron carrier protein plastocyanin in the lumen. In the Photosystem I (PSI), the light-driven reaction propagates the transfer of the electron from plastocyanin and reduces another electron carrier ferredoxin that is located in the stroma. Ferredoxin can then be used by the ferredoxin–NADP+ reductase (FNR) enzyme to reduce NADP+ to NADPH (Adapted from Matthew 2016).

5. 1. 1 PCR and Fd DNA sequence

Colony PCR reactions were carried out using the specific primers for the L1 plasmids (PL1Forward and pL1Reverse as shown on Table of primers) for the genes of interest and following the protocol description in the material and methods. The PCR screening showed the expected bands for the selected constructs during gel electrophoresis. The expected band size for L1*At*Fd cds was 2,112bp (Figure 5.2) after amplification of the target DNA sequence and this was visible in colony 2 (lane 2). All PCR results were validated by virtual primer analysis using the physical map (Figures 2.9 and 2.10) in the geneious molecular genetics software and also by sequencing of the products.

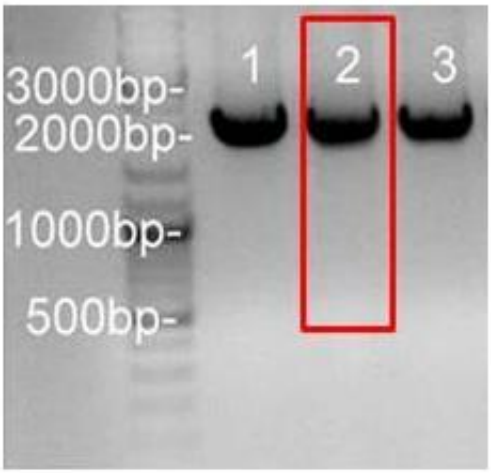

Figure 5. 2**:** Colony PCR with primers (pL1MForward and pL1MReverse) gave the expected band size on agarose gel image (2,112bp). Sequencing data confirmed the colony in lane 2 on the gel image to be L1AtFd and DNA from this *E.coli* colony was used for making L2s. DNA sequencing was used to confirm plasmid DNA from colony 2 before using this sample to generate level 2 plasmid.

Following that, the L2 Fd single and multiple constructs were made and colony PCR done according to the same protocol and primers specific for the bar gene (Bar4F and Bar1R) were used in the EPFs L2 sequence analysis. The L2*At*FD and L2 *At*FdYFP gave band sizes 552bp (Figures 5.3 and 5.4A) respectively upon gel electrophoresis. The PCR results were compared to the virtual PCR analysis using geneious software and all reactions yielded the same result as shown on the physical maps (chapter 2). EcoR1 restrictions digest of this plasmid yielded three different bands of 1,120bp, 1,941bp and 7,065bp (Figure 5.4B). These bands were verified by a virtual EcoRI digest using the geneious bioinformatics software. When overexpressing the Fd and the yellow fluorescence protein (YFP) genes together in a given plant, a double ligation of these two gene were made. It is expected that plants over-expressing the FdYFP genes combination would emit the YFP signal in the epidermal layers of the leaves to give an indication of the localization of Fd gene as targeted in the GC.

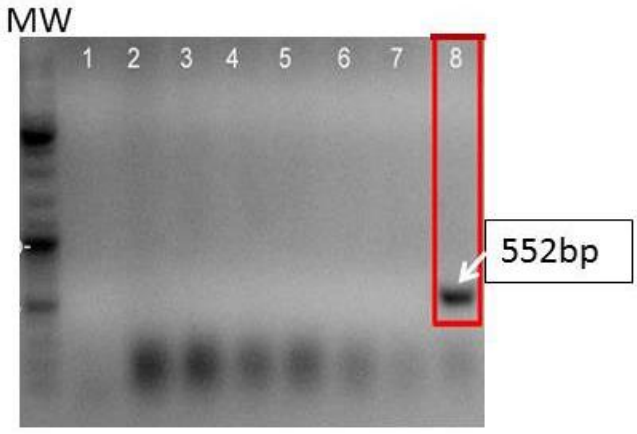

Figure 5. 3**:** PCR fragment of L2AtFd using primers (Bar4F and Bar1R) to check the presence of the bar gene was positive. Expected band size on agarose gel image was

(552bp). The highlighted column (colony 8) was sequenced and plasmid DNA was used for agrobacterium transformation.

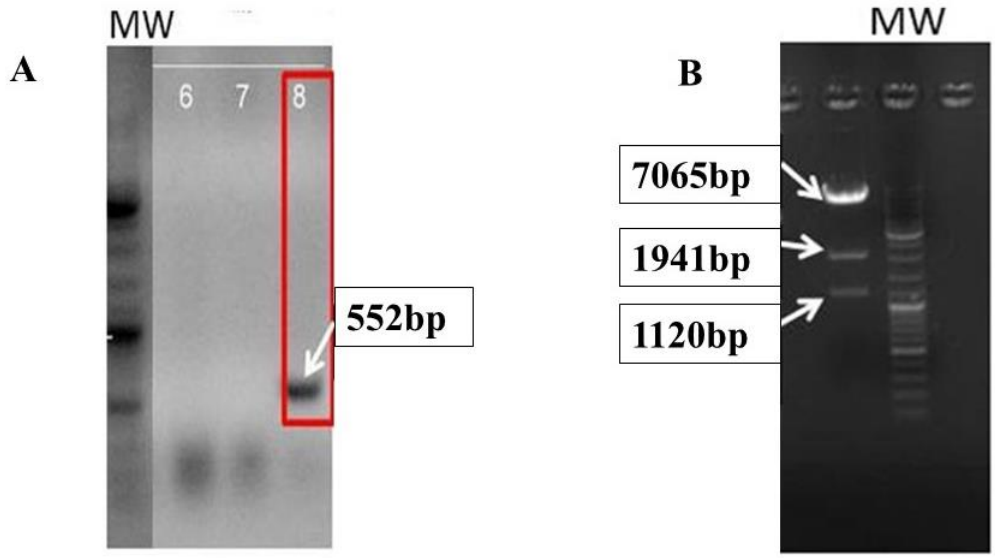

Figure 5. 4**: (A)** Colony PCR fragment using primer (Bar4F and Bar1R) to check the presence of the bar gene on the L2AtFdYFP plasmid yielded the expected band size on agarose gel image is (552 bp). (**B**) EcoRI digestion of the L2AtFdYFP construct gave the distinctive bands (1,120bp, 1,941bp and 7,065bp) and these bands were verified by a virtual EcoRI digest using the geneious bioinformatics software.

Another L2 Fd multiple construct developed was the L2*At*FdEPF1&EPF2 plasmids; the PCR analysis of this construct using these primers (Bar4F and Bar1R) also confirmed the presence of the basta gene in the physical map of the plasmid. Further EcoR1 restriction digest yielded four different sizes (1120bp, 1203bp, 1941bp and 6117bp) that were verified by a virtual EcoRI digest using the geneious bioinformatics software (Figure 5.5). Result of sequence analysis can be found in the appendix. Although, further results from these plants were not reported here because these plants possessed unique features of the CAM plants such as thick, smaller

leaves and lower stomata conductance when compared to other transgenic plants. Plants with these triple genes construct are expected to have very few developed stomata as a result of the combined negative effects of the AtEPF1 and AtEPF2 genes and lower g_s (Figure 5.12). These plants also took longer time to flower so there were not carried forward.

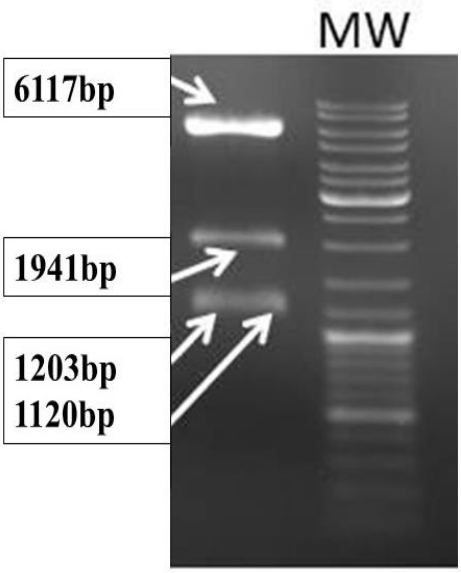

Figure 5. 5**:** EcoRI restriction digestion of the L2AtFdNtEPF1&NtEPF2 construct yielded four bands with two inseparable bands fused together due to the little difference in their molecular weights (1120bp, 1203bp, 1941bp and 6117bp). These bands were verified by a virtual EcoRI digest using the geneious bioinformatics software.

5. 1. 2 High resolution imaging

High resolution confocal microscopy has been used to show the localisation of Fd expression in the leaves of the ferredoxin transformants (Figure 5.6). YFP signal localized in GC, no signal detected in mesophyll. Therefore, it could be suggested

that the active form of Fd protein would be readily available for GC photoinduction during photosynthesis. At subcellular level, YFP show the typical cytosolic/nuclear localization. Clearly, YFP signal is not in chloroplasts and because the Fd gene was fused to the YFP gene on the L2 construct, it is expected that the Fd is expressed in the guard cells of these plants. Although, further q-PCR was not done with guard cell enrichment fragments to validate the localization of the Fd in GC.

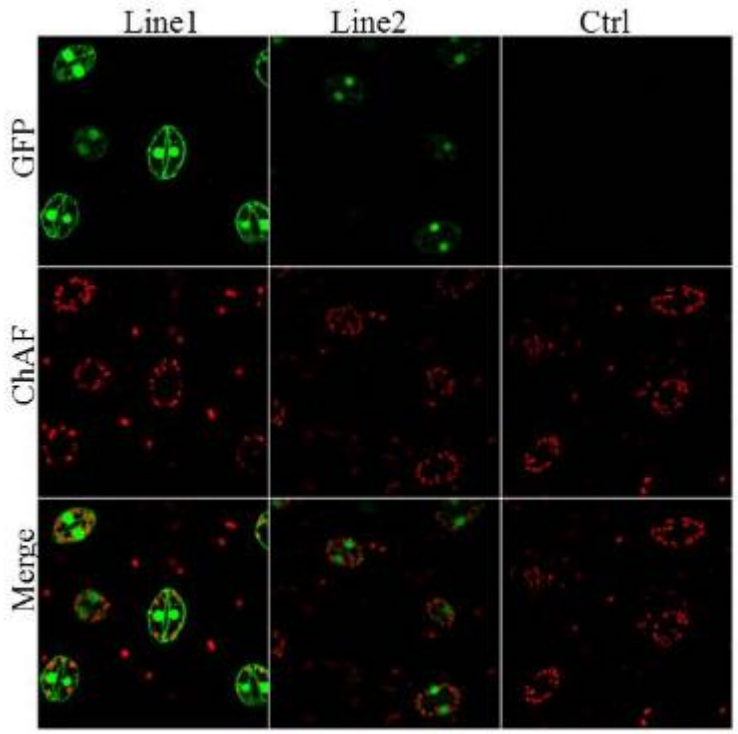

Figure 5. 6: A high resolution confocal images of a T1 FdYFP leaf. YFP signal localised in epidermal cells (Lines 1 and 2) and no signal detected in the mesophyll. At subcellular level, YFP shows the typical cytosolic/nuclear localization. The control plant (WT) did not show any signal of YFP at all.

5. 1. 3 qPCR reaction analysis

This was done as described in the material and method chapter to maintain the integrity of the RNA. It can be seen that not all the Fd plants were expressing the *At*Fd gene (Figure 5.7). Out of all four independent Fd tobacco lines, WTFD1 and WTFD7 were the ones that showed slightly relative expression levels of the *At*Fd gene but there was no significant difference among these plants.

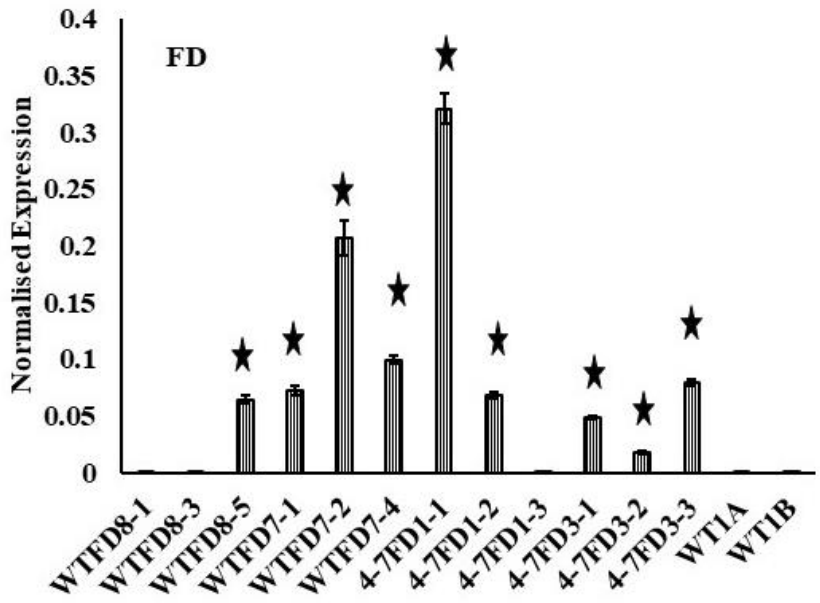

Figure 5. 7**:** Bar chart validating the qPCR experiments. Chart are the relative expression of Fd against actin. Four independent T1 lines of *At*Fd plants and two WT plants were tested (n=14). The error bars represent the standard error of the mean. There was significant difference in the relative expression of the Fd gene as indicated by filled 5-point star ($p < 0.05$).

5. 1. 4 Chlorophyll a Fluorescence (CF) Imaging of T1 seedlings

The CF imaging was done in order to detect potential changes in photosynthesis between all experimental plants. It is also a measure of how plants adapt photosynthetic activities at different light intensities. Altogether, 3 individual plants from 4 independent transgenic lines were analysed alongside 3 WT plants. The chlorophyll a fluorescence imaging system was used to examine the quantum photosynthetic efficiency (*Fq*'/*Fm*') of PS11 reaction centre. *Fq*'/*Fm*' was similar between all transgenic lines (Figure 5.8). However, there was no significant difference between values for transgenic plants and WT. This result indicated non-conformity with the expected outcome. The transgenic lines were supposed to show some major difference, but this is not the case and could be due to the fact that these plants are still undergoing segregating and\or due to the harsh summer weather condition in the greenhouse.

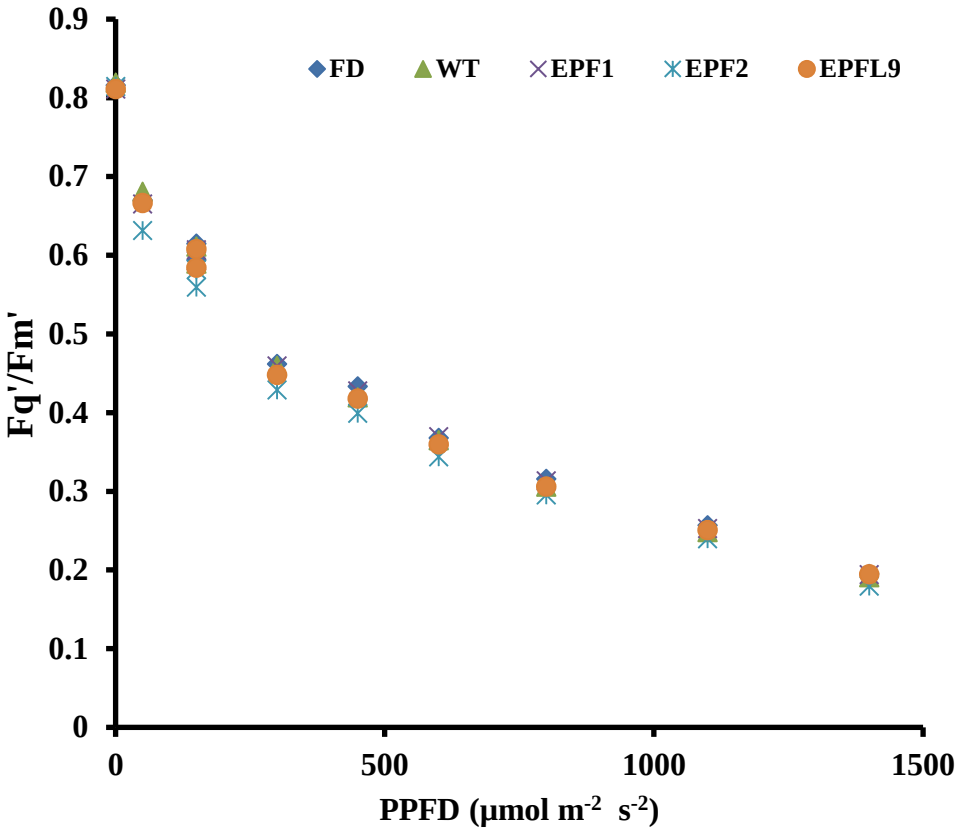

Figure 5. 8**:** Chlorophyll fluorescence imaging of 3 weeks old T1 generation transgenic lines as compared to WT. Chlorophyll fluorescence was used to determine *F*q'/*F*m' (maximum PSII operating efficiency) at nine light intensities: 0, 300, 150, 50, 150, 450, 600, 800, 1100, and 1400 µmol m^{-2} s^{-1} respectively. The data were obtained using 3 individual plants from 4 independent transgenic lines alongside 3 WT (n=52). There were no significant differences across all transgenic lines as compared to WT (P>0.05). Error bars represent standard errors of mean.

5. 1. 5 Infra-red gas exchange

This followed the same protocol used to germinate the T1 generations of all EPFs in chapter 4. Three plants each from 4 independent lines were measure and the group A/C_i curve is shown in Figure 5.9. Plant from Fd lines also showed higher rates of assimilation but only at the higher C_i concentration. The maximum rate of RubisCO

carboxylation (Vc_{max}) determined from the initial part of the curves was not significantly different between transgenic and WT plants. However, the maximum electron transport rate (J_{max}) taken from the saturating part of the curves was significantly higher in two of the lines (4-7Fd1 and WTFd8) when compared with the other groups and WT controls. High J_{max} corresponds to higher maximum rate of photosynthesis and therefore greater photosynthetic capacity (Sharkey *et al.*, 2007). The average *A/Ci* response curve of all T1 Fd and EPFs generations can be seen in Figure 5.10.A. From this, Vc_{max} remained fairly similar across the groups. Only the Fd lines reflected a significant difference in J_{max} when compared to other groups and WT (Figure 5.10B to C).

In order to study the stomata behaviour across the transformant, a different protocol was developed to observe the impact of stepwise increment of light on stomatal conductance g_s, and CO_2 assimilation *A* (Figures 5.11 A to F). This is important as it gives an indication of how fast the stomata respond, which determines plant productivity and water use efficiency WUE. Understanding and manipulating the speed of guard cells could be beneficial for developing novel crops that are able to synchronise stomata efficiency in gas exchange and improved photosynthetic productivity.

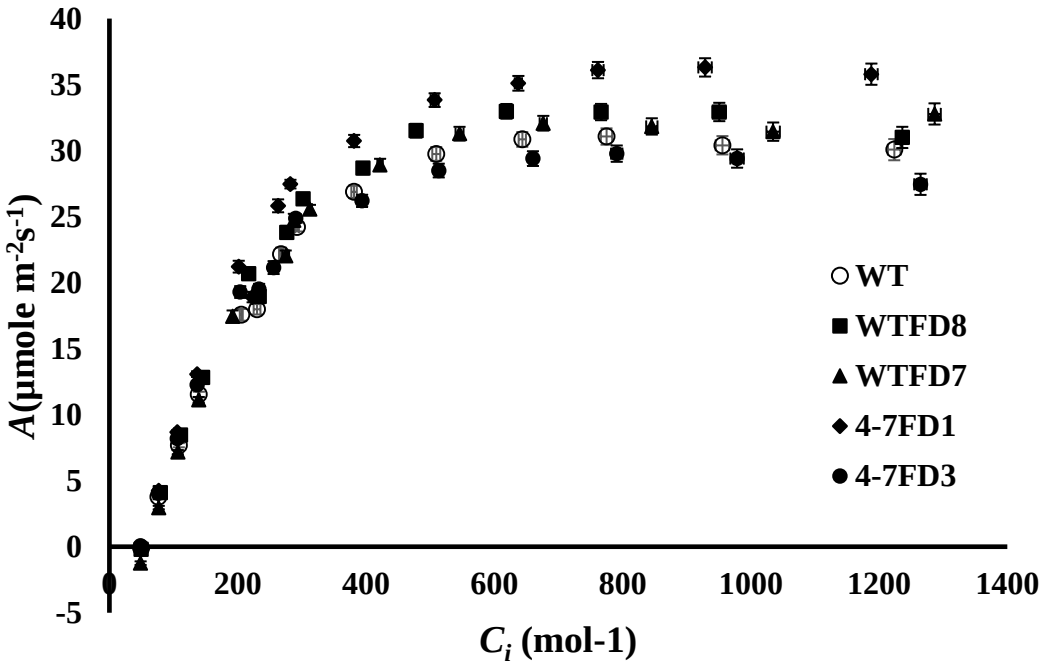

Figure 5. 9**:** *A*/C_i curves indicating photosynthetic responses of four independent Fd transgenic tobacco plants. The same protocol used in chapter 4 was followed in growing all T1 plant and also for this assessment of CO_2 response curve. 4-7Fd1 plants (filled diamond sign) showed a significant difference in J_{max} from all other tested lines in the chart. WTFd8 (filled square sign) also showed a higher J_{max} when compared to the WT (open circle sign) and 4-7Fd3 (filled circle sign). Vc_{max} was almost the same for all Fd plants and there was no significant difference. Error bar represents standard error of the mean across the groups (n=15) ($p < 0.05$).

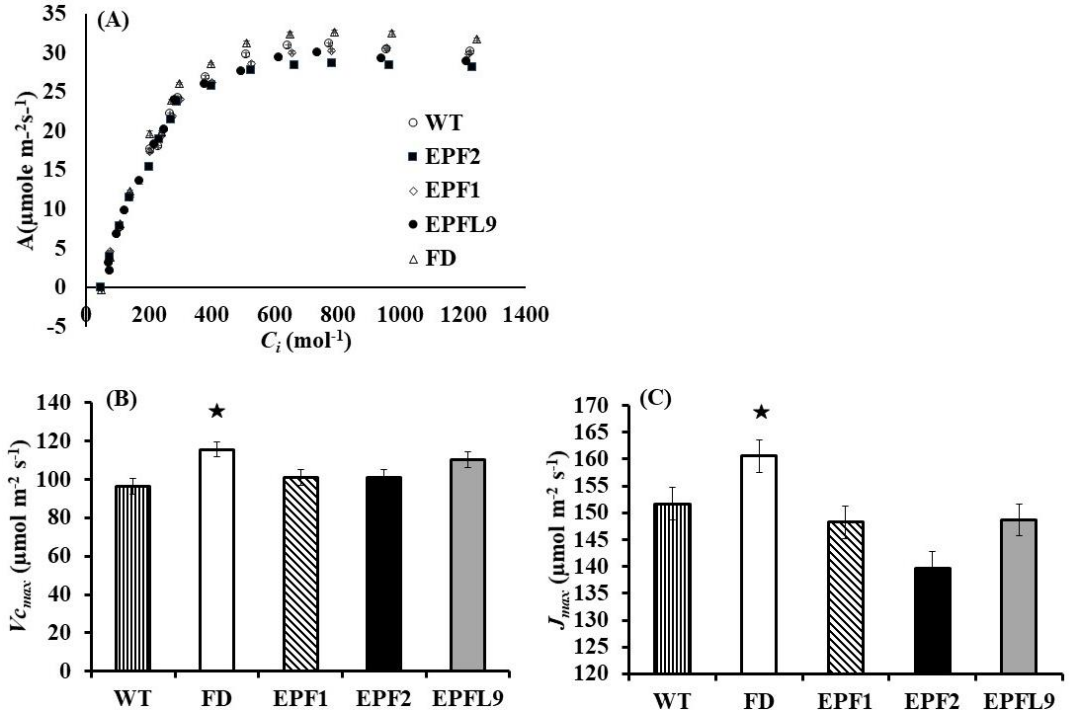

Figure 5. 10: Average A/*Ci* curves of all transgenic T1 plants as compared to WT (**A**). All the plants seem to have similar Vc_{mac} to the WT (open circle). (**C**) There was a significant difference on the J_{max} of the FD and all EPFs (filled square, open diamond and filled circle). (**B**) The WT showed to also have a similar range of V_{Cmax} as compared to EPF1 and EPF2 plants while J_{max} showed a significance difference between the Fd and all other observed plants (Analysis of the gas exchange parameters was done according to Sharkey *et al.*, 2007).

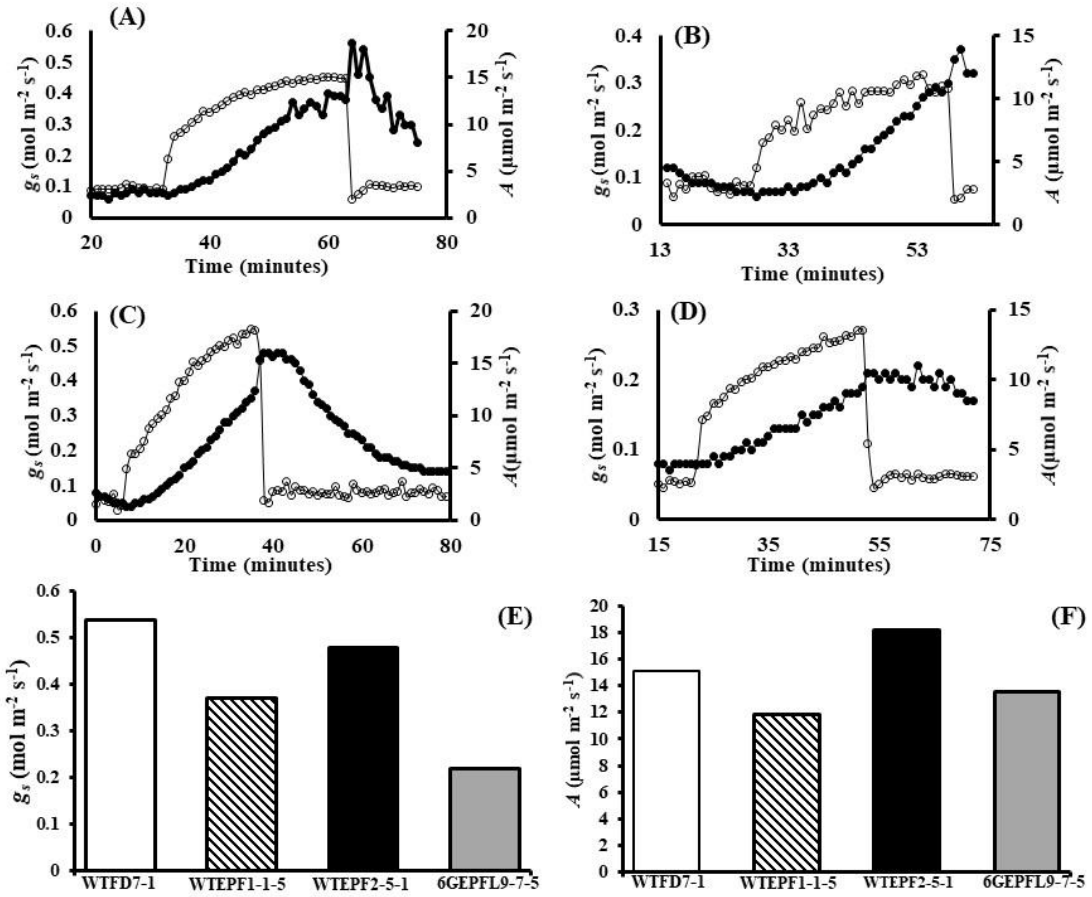

Figure 5. 11**:** Effects of two-steps PPFD changes from low light (100 µmol m^{-2} s^{-1} for 5 minutes) to high light (1000 µmol m^{-2} s^{-1} for 30 minutes). Measurements of *A* (white circles) and g_s (black circles) were made every 1 minute with cuvette CO_2 concentration maintained at 400 µmol mol^{-1}, temperature at 25°C, and ambient VPD. The different lines (**A**) Fd, (**B**) EPF1, (**C**) EPF2 and (**D**) EPFL9 of tobacco plants responded differently to the increase in light intensity. **(E)** Chart showing the variation in stomatal conductance g_s across the four transgenics, while **(F)** is a representation of the CO_2 assimilation across the group.

5. 2 Discussion

Although, the ictB plants have shown high photosynthetic capacity in line with Simkin *et al*. (2015), manipulation of stomatal density on these plants introduced another dimension to further enhance CO_2 assimilation (*A*), g_s, and WUE. It is not ascertained if the expected positive effect on photosynthesis was as a result or a combination of the varying stomata number, size of aperture, improved GC electron transport and changes in Calvin cycle enzymes.

Guard cell chloroplast has been implicated in several energy generation steps during photosynthesis (Lawson et al., 2008). As a potential source of ATP, several other enzymes that are induced by Fd such as NAD+-MDH, PEPc have been shown to be very active in the guard cells as compared to the mesophyll layers (Daloso *et al*., 2017).

Some important factors to consider for engineering water use efficiency in plants are the size, number and speed of stomata response to open and close. From Figure 5.9, the difference in g_s was clearly significant between Fd and other experimental plants. The effect of Fd on guard could not be estimated from the gas exchange step change measurement because the experiment did not run long enough and the plants were undergoing during the summer. Although, the q-PCR result showed the presence of the foreign Fd some of the segregating T1 population (Figure 5.7), the expression level of AtFd in the guard cell was not checked. A more concise protocol would be used to access the guard cell levels of Fd gene in the T2 generation after identifying the homozygous lines.

On a normal growth environment, it will be possible to evaluate the estimated time it took the stomata to close in all the plants. It can also be seen in the step change reaction that g_s peaked and dipped faster in the Fd plant when the light intensity was increased to 1000 µmol m^{-2} s^{-1} which gives an indicated of the rapid stomata behaviour. The speed and magnitude of g_s response to light was specific to each transgenic line but may be dependent of differences in stomatal sensitivity or signalling mechanism across these transformants (Lawson et al., 2010; Lawson and Blatt, 2014). The prospect of engineering GC Fd is to aid and improve the speed of stomata responses thereby increasing stomatal CO_2 conductance from the air space into the chloroplast stroma for the plant's photosynthetic gains. Other factors associated with the speed of stomatal response include water status, history of stress, leaf age, and the magnitude and duration of change in irradiance (Lawson and Blatt, 2014).

This work has most importantly enabled further analysis of multiple gene transgenic plants by overexpressing the Fd genes in direct comparative studies with the WT. Although, multigene manipulation of crop plant in the field is still premature, there is the urgent need to provide solid evidence for the multigene manipulation of Calvin cycle enzymes and structural CO_2 pathways such as stomata to increase the yield of food crops for the teeming global population. *The* A/C_i curve in Figure 5.8A shows that Fd plants have a higher electron transport rate due to their high J_{max}. Thus, the need for further experiments directed at characterising the magnitude of CO_2 fixation during guard cell photosynthesis.

6. 0 Chapter 6

6. 1 General Discussion

The research work determines the effect of manipulating stomatal density and function in tobacco plants which have increased levels of photosynthetic carbon assimilation driven by the over expression of the cyanobacterial putative inorganic carbon transporter gene ictB (Simkin *et al*., 2015). These ictB tobacco plants were transformed with plasmid constructs driving increased expression of Arabidopsis genes from the EPF family; EPF1, EPF2 and EPFL9. Stomatal function was altered in some of the ictB plants that were transformed with plasmid constructs driving increased guard cell expression of ferredoxin (Fd) gene from Arabidopsis thaliana. Fd is an important electron carrier and redox signal regulator during photosynthesis (Hedrich et al., 1985; Guo et al., 2006; Michelet et al., 2013; Daloso et al., 2015). The role of Fd in these plants was to enhance guard cell response time to opening and closing as well as increase guard cell starch biosynthesis. Azoulay-Shemer *et al*., (2016) in an excellent study showed that starch biosynthesis in guard cell (GC) is involved in CO_2-induced stomatal closing.

The EPF1 and EPF2 genes are negative regulators of stomata density which mean that plants expressing these genes will have reduced stomata density whereas the EPFL9 gene is a positive regulator of stomata development (Jie *et al*., 2014). EPF1 and EPF2 act through overlapping extracellular pathway within the aerial epidermal cell layer to supress stomata development (Hunt and Gray 2009; Hunt et al., 2010; Wang et al., 2007). Reducing stomata in plants have been shown to enhance water-use efficiency and draught tolerance (Caine *et al*., 2018; Hughes et al., 2019).

The Fd gene was specifically targeted to the guard cells of the stomata on the corresponding plants so as to assess the effect on stomata behaviour. Overall these plants present an opportunity to determine how ictB tobacco plants which already have high photosynthetic productivity can be further enhanced to meet the needs of agriculture in the future. These plants with speedy reduced stomata density and enhanced photosynthetic capacity will have better water-use efficiency and more adapted more adapted to draught (Lawson, T. and Vialet-Chabrand, 2018).

Although, extensive work has been done in multiple gene cloning and development of *Nicotiana tobacco* crop with improved photosynthetic capacities, the *cyanobacteria* ictB has shown promises in promoting photosynthesis and biomass yield in greenhouse conditions (Simkin *et al*., 2015). Lieman-Hurwitz et al., (2005), also showed that introduction of ictB in transgenic *Arabidopsis thaliana* and *Nicotiana tabacum* plants enhanced photosynthetic rates significantly than the wild types under limiting intercellular CO_2 concentrations. In the greenhouse and in field trials, Hay *et al*., (2017) demonstrated that ictB as a single-gene contributed to enhancement in various yield parameters in soybean making this *cyanobacteria* gene as a key player in helping to meet increased global food demands.

The ictB plants for transformation were selected to manipulate stomatal density and function due to the large increases in assimilation rate and plant growth observed by Simkin et al. (2015) with the aim of maintaining assimilation rate that is driven by ictB but with a reduction in stomatal conductance driven by the reduced stomata density. Stomata are the gate keeper to CO_2 uptake for photosynthesis and water lost via transpiration (Lawson *et al*., 2010) and therefore very important in manipulating

water-use efficiency (Lawson & Blatt, 2014). Recently several studies have demonstrated that by altering stomatal density that it is possible to improve drought tolerance and WUE in several species (Hepworth *et al*., 2015; Caine *et al.*, 2018; Hughes *et al*., 2019).

All the transgenic tobacco plants developed from the precursor ictB tobacco and WT plants are listed in Table 2.4. These plants are all the T1 generations of the transformed plant. The transgenic plants with altered stomatal numbers as a result of expressing the EPF1 and EPF2 genes had fewer stomata compared to the EPFL9 (which resulted in increased stomatal density) and WT plants. These characteristics were visible in both the T0 and T1 generation of EPFs. Although, at this stage these plants were still segregating, these findings support the existing evidence that the EPF genes are major player in stomata development and distribution (Kondo *et al*., 2010; Caine *et al*., 2018). I have been able to show that manipulating EPF1 and EPF2 genes lead to the development of reduced stomata density in transgenic tobacco plants in greenhouse conditions while manipulating EPFL9 gene lead to increase stomata density.

Stomata density analysis of EPF1 and EPF2 leaves showed varying restrictive development and distribution of stomata across the abaxial and adaxial leaves' surfaces. Plants expressing these two negative regulators of stomata development did not only showed reduced stomata densities but bigger stomata sizes. The EPF2 particularly showed a lot more of partially developed stomata of varying sizes. There was no way to find out if all or some of these smaller and partially developed stomata are functional (Figures 4.9 and 4.10). My result supported the suggestion by

Hunt and Gray (2009), that EPF2 peptides may affect neighbouring epidermal cells by inhibiting meristemoids fate and promoting pavement cell fate through a pathway that is independent of EPF1. Apart from those observations, my results are in agreement with the existing knowledge about these two negative regulators of the stomata. Therefore, EPF1 and EPF2 plants have reduced stomatal density that should enhance efficient water use and drought tolerance suitable for future predicted climate conditions (Caine *et al*., 2018).

As shown in chapter 4, different publication have supported that the EPF1 and EPF2 plants are able to conserve more water due to their fewer numbers of stomata, making plants with fewer stomata density to be more adaptable for agricultural practices (Hughes et al., 2017; Caine *et al*., 2018). It has also been suggested in previous work by (Lawson and Blatt, 2014), that the bigger sizes of these stomata on the EPF1 and EPF2 plants could be a compensation for their reduced stomata density and in turn means that bigger sizes in stomata could counterbalance stomata conductance g_s.

The EPFL9 plants that were developed on the other hand have more developed and well distributed stomata that will make these plants to lose more water to the environment due to their high stomatal density. Stomata pairing was also visible on the image of the leave impressions that were made from the EPFL9 plants (Figure 4.10) and this supports the existing knowledge on the positive role of this gene on stomata development (Kondo *et al*., 2010). The formation of clusters containing numerous stomata in pairs as supported by (Kondo *et al*., 2010; Sugano *et al*.,2010) supports the evidence that EPFL9 is secreted from internal tissues and interact with

that underlying cells in optimizing the stomatal formation and patterning (Abrash and Bergmann, 2010; Kondo *et al*., 2010; Sugano *et al*.,2010).

Ishihara and Saito, (1987) and Hirasawa *et al*., (1988) showed that in rice (*Oryza sativa* L.), stomatal aperture as well as conductance was strongly correlated with leaf photosynthesis. Whereas photosynthesis in rice leaves was also influenced by other factors, such as leaf nitrogen content and content of the enzyme ribulose-1,5-bisphosphate carboxylase/oxygenase (Rubisco) (Makino *et al*., 1987; Makino *et al*., 1988). Therefore, stomatal conductance is co-dominantly correlated with the rate of leaf photosynthesis for high yielding rice variety such as an *indica* rice variety Takanari and another variety Habataki that are known to have higher grain yields and dry matter production when compared with common rice varieties even at the same rate of nitrogen application (Xu *et al*., 1997; Adachi *et al*., 2011).

Other factors, such as cuticular and leaf boundary layer conductance, were reported to contribute to whole leaf conductance. These studies show a high correlation between leaf conductance and stomatal conductance as commonly observed in EPFL9 plants exhibiting higher stomata density. (Lawson *et al.,* 2008; von Caemmerer *et al.,* 2004; Kusumi *et al*., 2012). Tanaka et al., (2013) also showed that increased stomatal density in EPFL9-overexpressing plants enhanced the photosynthetic rate by 30% compared to wild-type plants but reduced water-use efficiency due to increased stomatal conductance under ambient CO_2 conditions. These morphological diversity of stomata on the transgenic EPF plants can be attributed to spatial heterogeneity in the stomatal behaviour observed in different

species and lead to a considerable mechanical and functional diversity (Lawson *et al*., 1998; von Caemmerer *et al*., 2004).

The single Fd transgenic plants that did not contain the *At*EPF genes on the other hand showed to have similar stomata density as the WT plants (Fig. 4.10). This indicates that stomatal density in the *At*Fd tobacco plants had not been altered in the process of the genetic transformation. The location of the foreign Fd in the guard cells was accessed using confocal microscopy to visualise the Fd plants that was co-expressing the yellow fluorescent protein (YFP). The plants with the FdYFP double construct showed visible fluorescence signals which indicated the localization of the FdYFP gene combination on the guard cell and absence on the mesophyll layers (Figure 5.6). Although there was no molecular work done on guard cell enrichment sample to support the result of the confocal microscopic image, further quantitative PCR needs to be conducted for comparative expression analysis of Fd on GC and mesophyll extracts.

In an excellent study, Busch (2014), suggested that the redox state of chloroplastic quinone A (Q_A) is the early signal for stomatal opening in response to light. As can be seen from Figure 1.8A, Q_A is a primary electron acceptor downstream of PSII and its oxidation state reflects the balance between excitation energy at photosystem II and the rate of Calvin cycle (Głowacka, *et al.,* 2018). Following this mechanism of linear electron transport, a decrease in the excitation pressure at photosystem II should directly affect stomatal opening in response to light by keeping Q_A more oxidized (Głowacka, *et al.,* 2018). Therefore, it was expected that plants expressing the single Fd construct in their guard cells would exhibit some altered stomata

behaviour because guard cell Fds play important redox roles in cyclic electron transport (CET), the generation of ATP, the activation of Calvin cycle enzymes activity and the production of osmotic pressure for guard cell responses among other known activities of the Fd. The role of Fd on the downstream component of the CET is supported by the gas exchange measurements which demonstrated that *At*Fd plants tend to have speedy stomata and higher J_{max} compared to the *At*EPFs and WT plants (Figure 5.10).

Plants expressing the triple constructs of the EPF1/EPF2/Fd should be able to conserve more water during photosynthesis due to the cumulative effects of these triple constructs but unfortunately this was not validated during this research work due to the limited time. It is already known that plants engineered to have reduced stomata density and speedy stomata can conserve water more than those with more stomata (Caine *et al.*, 2018; Lawson and Vialet-Chabrand, 2018), multiple gene-expressing plants with EPF1/EPF2/Fd should exhibit low g_s, high electron transport rate and *A*. So far, there is no evidence to show that the products of guard cell chloroplast's electron transport chain are not relevant to the operations of the stomata but there is evidence that GCs have a higher anaplerotic CO_2 fixation catalysed by phosphoenolpyruvate carboxylase (PEPc) in accordance with the higher relative contents found in the GCs compared to mesophyll cells (Daloso *et al.*, 2015; 2017).

Chlorophyll fluorescence imaging of photosynthetic efficiency in the transgenic T0 and T1 plants showed no significant differences compared with WT, suggesting that the altered expression of Fd and EPFs targeted at manipulating stomatal behavior and density did not impacted on photosynthetic potential. Gas exchange

measurements yielded varying CO_2 response curves across the different groups of transgenics. This did not correlate to the expected *A/Ci* response curves because throughout the summer weeks of July, 2018 there was a heatwave across the UK prior, during and after measurement periods and the temperature caused some heat associated wilting stress to the plants. The evidence from the T1 generation *A/Ci* curve and Chlorophyll fluorescence measurements did not correspond to the work of Simkin *et al*., (2015) and Lieman-Hurwitz *et al*., (2003), which supported the earlier finding in T0 generation that ictB is results in increased photosynthetic carbon assimilation. The stimulation of photosynthesis was not seen in all generations which suggest impact of the variation in environmental conditions on the transgenic plants during physiology measurements in the summer.

The calculated average of Vc_{max}, the maximum rate of RubisCO carboxylase activity was similar and there was no significant difference among all plants. The major difference was seen in J_{max}, the determined maximum rate of photosynthetic electron transport, where the WT and Fd showed significant higher values as compared to all EPFs (Figure 4.5). The products of photosynthesis are the primary determinants of plant productivity and increasing J_{max} correlates to improved photosynthesis capacity (Simkin *et al*., 2015). Therefore, the Fd transgenic plants have shown to be more photosynthetically efficient.

Q-PCR analysis of the T0 generation was used to further select plants that were cultivated for T1 seeds. Data from the T1 q-PCR showed that not all the seedling were expressing the associated genes (Figures 4.13 and 5.7). The observed variation in the expression levels of these foreign genes was as a result of the nature of the

chromosomal insertions of these constructs and the fact that these plants are still segregating. This quantitative molecular analysis helped to select plants for T2 seeds and iDNA analysis to determine homozygosity on the T2. The non-segregating second generation would serve the best purpose for analysing the impact of these foreign genes on ictB tobacco plants.

Apart from the adverse weather condition that affected most physiology analysis, the major limitation of this work was not being able to generate the homozygous second generation (T2) from all EPF and Fd transgenic plants. Therefore, the experiments that needs to be finished up if given time or in the future will be to carryout GC and mesophyll tissue specific q-PCR and western blot to determine expression and presence of the Fd protein on these tissues. A repeat of all physiology analysis as will be done with the T2 generation when the result of the iDNA homozygosity testing arrives. The seeds from the homozygous T2 generation would have to be cultivated during the winter or spring to avoid the heat stress problems experienced during the summer. I would also like to carryout growth and drought analysis on these plants to determine water-use efficiency and biomass yield.

Stomata density manipulation through altering the EPF genes and guard cell Fd provided an ideal unexploited target for manipulation for improving crop performance because stomatal conductance controls the amount of CO_2 taken up for photosynthesis and water lost (Hunt and Gray, 2009; Doheny-Adams *et al*., 2012; Lawson and Blatt, 2014; Caine *et al*., 2018; Hughes *et al*., 2019). Stomatal conductance or the maximum capacity for CO_2 diffusion is determined by both the number of stomata and pore aperture, this research therefore took a two-pronged

approach in order to try and manipulate stomatal conductance so as to improve assimilation rate and/or water use efficiency.

Success of modern crop production to sustain the world growing population depends on our ability to develop novel crops that would adapt to the predicted changes in current climate conditions (Long *et al*., 2006; Zhu *et al*., 2007; 2010; Braun *et al*., 2010; Fita *et al*., 2015). Climate variations such as increase in CO_2, temperature, drought and intense weather warming have been associated with low yield in agricultural production but plants that have been engineered to overcome these negative effects of climate change are able to benefit from these adverse conditions (Solomon *et al*., 2009; Vikram *et al*., 2015; Korres *et al*., 2017). Therefore, for plants to adapt to climate change special genetic and physiological modifications of photosynthetic apparatus like stomata are needed to increase yield and performance (Caine *et al*., 2018; Hughes *et al*., 2019). This work was done in the hope of better understanding and manipulating stomata regulation to develop novel plants that would cope with global warming. So far, a few of the transgenic plants that were developed demonstrated improved photosynthesis. These plants are model for important future works that would ensure enough crop and food protection for the world population.

References

Abrash, E. B., and Bergmann, D. C. (2010). Regional specification of stomatal production by the putative ligand CHALLAH. *Development* 137, 447–455.

Adachi, S., Tsuru, Y., Nito, N., Murata, K., Yamamoto, T., Ebitani, T., Ookawa, T. and Hirasawa, T. (2011). Identification and characterization of genomic regions on chromosomes 4 and 8 that control the rate of photosynthesis in rice leaves. Journal of Experimental Botany. 62: 1927–1938.

Antunes, W., Provart, N., Williams, T. and Loureiro, M. (2011). Changes in stomatal function and water use efficiency in potato plants with altered sucrolytic activity. *Plant, Cell & Environment*, 35(4), pp.747-759.

Asada, K. (1999). The water-water cycle in chloroplasts: scavenging of active oxygens and dissipation of excess photons. *Annual Review of Plant Physiology and Plant Molecular Biology* 50, 601–639.

Athanasiou, K. (2008). Acclimation to Light in Arabidopsis thaliana. Faculty of Life Sciences, University of Manchester. PhD: 179.

Athanasiou, K., Dyson, B., Webster, R. E. and Johnson G. N (2010). "Dynamic Acclimation of Photosynthesis Increases Plant Fitness in Changing Environments." Plant Physiology 152(1): 366-373.

Azoulay-Shemer, T., Bagheri, A., Wang, C., Palomares, A., Stephan, A. B., Kunz, H. and Schroeder, J. I. (2016). Starch Biosynthesis in Guard Cells But Not in Mesophyll Cells Is Involved in CO2-Induced Stomatal Closing. *Plant Physiology* 171, 788-798.

Baker, N. R. and Rosenqvist, E. (2004). Applications of chlorophyll fluorescence can improve crop production strategies: an examination of future possibilities. *Journal of Experimental Botany* 55, 1607–1621.

Baker, N. R., Oxborough, K., Lawson, T. and Morison, J. I. (2001). High resolution imaging of photosynthetic activities of tissues, cells and chloroplasts in leaves. Journal of Experimental Botany 52, 615-621.

Bechtold, U., Penfold, C. A., Jenkins, D. J., Legaie, R., Moore, J. D., Lawson, T., Matthews, J. S. A., Vialet-Chabrand, S. R. M., Baxter, L., Subramaniam, S., Hickman, R., Florance, H., Sambles, C., Salmon, D. L., Feil, R., Bowden, L., Hill, C., Baker, N. R., Lunn, J. E., Finkenstädt, B., Mead, A., Buchanan-Wollaston, V., Beynon, J., Rand, D. A., Wild, D. L., Denby, K. J., Ott, S., Smirnoff, N., and Mullineaux, P. M. (2016). Time-Series Transcriptomics Reveals That AGAMOUS-LIKE22 Affects Primary Metabolism and Developmental Processes in Drought-Stressed Arabidopsis. *The Plant Cell* 28, 345-366.

Berg, J. M, Tymoczko, J. L. and Stryer, L. (2002). Biochemistry. 5th edition. New York: W H Freeman. Section 5.6, Most Eukaryotic Genes Are Mosaics of Introns and Exons. Available from: https://www.ncbi.nlm.nih.gov/books/NBK22348/

Berger, S. L., Manrow, R. E., Lee, H. Y. (1993). Phoenix mutagenesis: one-step reassembly of multiply cleaved plasmids with mixtures of mutant and wild-type fragments. Anatytical Biochemistry 214: 571–579.

Bertini, I., Luchinat, C., Provenzani, A., Rosato, A. and Vasos, P. R. (2002). Browsing gene banks for Fe2S2 ferredoxins and structural modelling of 88 plant-type sequences: an analysis of fold and fuction. Proteins 46, 110-127.

Bowsher, C. G., Dunbar, B. and Emes, M. J. (1993). The purification and properties of ferredoxin-$NADP^+$ oxidoreductase from the roots of *Pisum sativum* L. *Protein Expression and Purification* 4, 512-518.

Boxall, S. F., Dever, L. V. and Hartwell, J. (2016). Emerging model systems for functional genomics analysis of Crassulacean acid metabolism. *Current Opinion in Plant Biology*, 31:100–108.

Braun, H. J., Atlin, G. and Payne, T. (2010). Multi-location testing as a tool to identify plant response to global climate change. In: Reynolds MP, ed. Climate change and crop production. Surrey, UK: CABI Climate Change Series, 115–138.

Buick, R. (1992). The antiquity of oxygenic photosynthesis: evidence from stromatolites in sulphate-deficient Archaean lakes. Science, 255: 74–77.

Busch, F. A. (2014). Opinion: the red-light response of stomatal movement is sensed by the redox state of the photosynthetic electron transport chain. Photosynth. Res. 119, 131–140.

Caine, R. S., Yin, X., Sloan, J., Harrison, E. L., Mohammed, U., Fulton, T., Biswal, A. K., Dionora, J., Chater, C. C., Coe, R. A., Bandyopadhyay, A., Murchie, E. H., Swarup, R., Quick, W. P. and Grey, J. E. (2018). Rice with reduced stomatal density conserves water and has improved drought tolerance under future climate conditions. New Phytologist, Volume 221, Issue 1.

Campbell, N. A. (1990). Biology, 2nd ed. Benjamin/Cummings Publishing Company, Redwood City, Calif.

Casson, S. A. and Hetherington, A. M. (2014). Phytochrome B Is Required for Light-Mediated Systemic Control of Stomatal Development. *Current Biology* 24, 1216–1221.

Cotelle, V. and Leonhardt, N. (2016). 14-3-3 Proteins in Guard Cell Signaling. Front. Plant Sci. 6 (1210): 1-10.

Cui, H., Kong, D., Wei, P., Hao, Y., Torii, K. U., Lee, J. S. and Li, J. (2014). SPINDLY, ERECTA, and Its Ligand STOMAGEN Have a Role in Redox-Mediated Cortex Proliferation in the Arabidopsis Root. Mol. Plant. 7, 1727–1739.

Dammeyer, T. and Frankenberg-Dinkel, N. (2008). Function and distribution of bilin biosynthesis enzymes in photosynthetic organisms. *Photochemical & Photobiological Sciences* **7,** 1121–1131.

Daloso, D. M., Antunes, W. C., Pinheiro, D. P., Waquim, J. P., Araujo, W. L., Loureiro, M. E., Fernie, A. R. and Williams, T. C. R. (2015). Tobacco guard cells fix CO_2 by both RubisCO and PEPcase while sucrose acts as a substrate during light-induced stomatal opening. Plant, Cell & Environment 38: 2353–2371.

Daloso, D. M., Medeiros, D. B., Anjos, L. D., Yoshida, T., Araujo, W. L. and Fernie, A. R. (2017). Metabolism within the specialized guard cells of plants. New Phytol. 216:1018–1033.

David, L. N. and Michael, M. C. (2005). Lehninger PRINCIPLES OF BIOCHEMISTRY, 4th ed. W. H. Freeman and Company, New York.

Daszkowska-Golec, A. and Szarejko, I. (2013). Open or close the gate – stomata action under the control of phytohormones in drought stress conditions. *Front. Plant Sci*. 4, 138; 1-16.

Dammeyer, T. and Frankenberg-Dinkel, N. (2008). Function and distribution of bilin biosynthesis enzymes in photosynthetic organisms. Photochemical and Photobiological Sciences 7: 1121–1130.

Doheny-Adams, T., Hunt, L., Franks, P. J., Beerling, D. J. and Gray, J. E. (2012). Genetic manipulation of stomatal density influences stomatal size, plant growth and restricted water supply across a growth carbon dioxide gradient. Philos Trans R Soc Lond B Biol Sci 367: 549-555.

Eckardt, N. A. (2005). Photorespiration Revisited, The Plant Cell. 17, 2139–2141.

Engler, C., Kandzia, R. and Marillonne, S. (2008). A One Pot, One Step, Precision Cloning Method with High Throughput Capability. PLoS ONE, 2: 1-7.

Fita, A., Rodríguez-Burruezo, A., Boscaiu, M., Prohens, J. and Vicente, O. (2015). Breeding and domesticating crops adapted to drought and salinity: a new paradigm for increasing food production. Front Plant Sci 6: 978.

Fukuzawa, H., Kaplan, A. and Ogawa, T. (2012). The uptake of CO_2 by cyanobacteria and microalgae. In: Eaton-Rye, J. J., Tripathy, B. C. and Sharkey, T. D., eds. Photosynthesis: Plastid Biology, Energy Conversion and Carbon Assimilation, Advances in Photosynthesis and Respiration. Dordrecht: Springer Netherlands; 34: 625–650.

Głowacka, K., Kromdijk, J., Kucera, K., Xie, J., Cavanagh, A. P., Leonelli, L., Leakey, A. D. B., Ort, D. R., Niyogi, K. K. and Long, S. P. (2018). Photosystem II Subunit S overexpression increases the efficiency of water use in a field-grown crop. Nature communications, 9(1).

Guy, A. and Paula, M. (2013). Plant type ferredoxins and ferredoxin-dependent metabolism. Plant, Cell and Environment 36, 1071-1084.

Gou, P., Hanke, G. T., Kimata-Ariga, Y., Standley, D. M., Kubo, A., Taniguchi, I., Nakamura, H. and Hase, T. (2006). Higher order structure contributes to specific differences in redox potential and electron transfer efficiency of root and leaf ferredoxins. Biochemistry, 45, 14389-14396.

Hanke, G. and Mulo, P. (2013). Plant type ferredoxins and ferredoxin-dependent metabolism. Plant, Cell and Environment 36, 1071–1084.

Hanke, G. T., Kimata-Ariga, Y., Taniguchi, I., and Hase, T. (2004) A post genomic characterization of Arabidopsis ferredoxins, Plant Physiol. 134, 255-64.

Hara, K., Kajita, R., Torii, K. U., Bergmann, D. C., and Kakimoto, T. (2007). The secretory peptide gene EPF1 enforces the stomatal one-cell-spacing rule. Genes Dev. 21, 1720–1725.

Hara, K., Yokoo, T., Kajita, R., Onishi, T., Yahata, S., Peterson, K. M., Torii, K. U. and Kakimoto, T. (2009). Epidermal cell density is autoregulated via a secretory peptide, EPIDERMAL PATTERNING FACTOR 2 in Arabidopsis Leaves. Plant Cell Physiol. 50, 1019–1031.

Hay, W. T., Bihmidine, S., Mutlu, N., Hoang, K. L., Awada, T., Weeks, D. P., Clemente, T. and Long, S.P. (2017). "Enhancing soybean photosynthetic CO_2 assimilation using a cyanobacterial membrane protein,ictB". *Journal of plant physiology*, 212: 58-68.

Hedrich, R., Raschke, K. and Stitt, M. (1985). A role for fructose 2,6-bisphosphate in regulating carbohydrate metabolism in guard cells. Plant Physiology 79: 977–982.

Hepworth, C., Caine, R. S., Harrison, E. L., Sloan, J. and Gray, J. E. (2018). Stomatal development: focusing on the grasses. Current Opinion in Plant Biology 41:1–7.

Hirasawa, T., Iida, Y. and Ishihara, K. (1988). Effect of leaf water potential and air humidity on photosynthetic rate and diffusive conductance in rice plants. Japanese Journal of Crop Science. 57: 112–118.

Hoagland, D. R. and Arnon, D. I. (1950). The water culture method for growing plants without soil. California Agricultural Experiment Station Circular 347, 1–32.

http://imagej.nih.gov/ij/index.html

Hudson, G. S., Evans, J. R., von-Caemmerer, S., Arvidsson, Y. B. and Andrews, T. J. (1992). Reduction of ribulose-1,5-bisphosphate carboxylase/oxygenase content by antisense RNA reduces photosynthesis in transgenic tobacco plants. *Plant Physiology* 98, 294–302.

Hughes, J., Hepworth, C., Dutton, C., Dunn, J. A., Hunt, L., Stephens, J., Waugh, R., Cameron, D. D. and Gray, J. E. (2017). Reducing Stomatal Density in Barley Improves Drought Tolerance without Impacting on Yield. Plant Physiology, Vol. 174, pp. 776–787.

Huner, N. P. A., Bode, R., Dahal, K., Hollis, L., Rosso, D., Krol, M. and Ivanov, A. G. (2012). Chloroplast redox imbalance governs phenotypic plastidity; the "grand design of photosynthesis" revisited. *Front. Plant Sci*. 3, 149-160

Hunt, L., Bailey, K. J., and Gray, J. E. (2010). The signalling peptide EPFL9 is a positive regulator of stomatal development. *New Phytol.* 186, 609–614.

Hunt, L. and Gray, J. E. (2009). The signaling peptide EPF2 controls asymmetric cell divisions during stomatal development. *Curr. Biol*. 19, 864–869.

Ishihara, K. and Saito, K. (1987). Diurnal courses of photosynthesis, transpiration, and diffusive conductance in the single-leaf of the rice plants grown in the paddy field under submerged condition. Japanese Journal of Crop Science. 56: 8–17.

http://www.idnagenetics.com/pdf/IDna_ServiceFlier_g-Count.pdf

Jie, L., Junjie, Z., Kezhen, Y. and Ming, W. (2014). Signaling to stomatal initiation and cell division. Front. Plant Sci. 5 (292): 1-6.

Karplus, P. A. and Bruns, C. M. (1994). Structure-function relations for ferredoxin reductase. J Bioenerg Biomembr, 26: 89–99.

Karplus, P. A., Daniels, M. J. and Herriott, J. R. (1991). Atomic structure of ferredoxin-NADP+ reductase: prototype for a structurally novel flavoenzyme family. Science 251: 60–66.

Kebeish, R., Niessen, M., Thiruveedhi, K., Bari, R., Hirsch, H., Rosenkranz, R., Stabler, N., Schonfeld, B., Kreuzaler, F. and Peterhansel, C. (2007). Chloroplastic photorespiratory bypass increases photosynthesis and biomass production in Arabidopsis thaliana. Nature Biotechnology; 25(5):593-9.

Kaplan, A. and Reinhold, L. (1999). CO_2 concentrating mechanisms in photosynthetic microorganisms. Annu Rev Plant Physiol Plant Mol Biol., 50: 539–570.

Katsir, R., Davies, K. A., Berminique, C. B. and Laux, T. (2011). Peptide signalling in Plant Development. *Current Biology* 21, 356-364.

Kondo, T., Kajita, R., Miyazaki, A., Hokoyama, M., Nakamura-Miura, T., Mizuno, S., Masuda, Y., Irie, K., Tanaka, Y., Takada, S., Kakimoto, T. and Sakagami, Y. (2010). Stomatal density is controlled by a mesophyll-derived signaling molecule. *Plant Cell Physiol.* 51, 1–8.

Korres, N. E., Norsworthy, J. K., Burgos, N. R. and Oosterhuis, D. M. (2017). Temperature and drought impacts on rice production: an agronomic perspective regarding short- and long-term adaptation measures. Water Resources and Rural Development. 9:12–27.

Kulheim, C., Agren, J. and Jansson, S. (2002). "Rapid regulation of light harvesting and plant fitness in the field." Science 297(5578): 91-93.

Kusumi, K., Hirotsuka, S., Kumamaru, T. and Iba, K. (2012). Increased leaf photosynthesis caused by elevated stomatal conductance in a rice mutant deficient in SLAC1, a guard cell anion channel protein. Journal of Experimental Botany. 63(15): 5635-5644.

Lawson, T., Weyers, J. D. B. and A'Brook, R. (1998). The nature of heterogeneity in the stomatal behaviour of *Phaseolus vulgaris* L. primary leaves. J. Exp Bot 49: 1387-1395.

Lawson, T., Lefebvre, S., Baker, N. R., Morison, J. I. L. and Raines, C. A. (2008). Reductions in mesophyll and guard cell photosynthesis impact on the control of

stomatal responses to light and CO_2. *Journal of Experimental Botany 59(13), 3609-3619.*

Lawson, T., Kramer, D. M. and Raines, C. A. (2012). Improving yield by exploiting mechanisms underlying natural variation of photosynthesis. *Curr Opin Biotechnol* 23: 215-220.

Lawson, T. and Murchie, E. H. (2013). Chlorophyll fluorescence analysis: a guide to good practice and understanding some new applications. Journal of Experimental Botany. 64: 3983-3998.

Lawson, T. and Blatt, M. R. (2014). Size, speed and responsiveness of stomata impact on photosynthesis and water use efficiency. Plant Physiol in press: 164: 1556-1570.

Lawson, T., Oxborough, K., Morison, J. I. L. and Baker, N. R. (2002). Responses of photosynthetic electron transport in stomatal guard cells and mesophyll cells in intact leaves to light, CO_2, and humidity. *Plant Physiology* 128: 52–62.

Lawson, T., Oxborough, K., Morison, J. I. L. and Baker, N. R. (2003). The response of guard cell photosynthesis to CO_2, O_2, light and water stress in a range of species are similar. *Journal of Experimental Botany* 54: 1734–1752.

Lawson, T. (2009). Guard cell photosynthesis and stomatal function. *New Phytologist* 54: 1734–1752.

Lawson, T. and Vialet-Chabrand, S. (2018). 'Speedy stomata, photosynthesis and plant water use efficiency.' New Phytologist. 221: 93-98.

Lee, J. S., Hnilova, M., Maes, M., Lin, Y. L., Putarjunan, A., Han, S., Avila, J. and Torii, K. U. (2015). Competitive binding of antagonistic peptides fine-tunes stomatal patterning. Nature, 522: 439-443.

Lefebvre S., Lawson T., Zakhlenivk O.V., Fryer M., Lloyd J.C. & Raines C.A. (2005) Increased SBPase activity in transgenic tobacco plants stimulates photosynthesis and growth during early development. *Plant Physiology* 138: 451-460.

Lehtimäki, N., Lintala, M., Allahverdiyeva, Y., Aro, E. and Mulo, P. (2010). Drought stress-induced upregulation of components involved in ferredoxin-dependent cyclic electron transfer. Journal of plant physiology. 167: 1018-22.

Lehti-Shiu, M. D., Zou, C., Hanada, K. and Shiu, S. H. (2009). Evolutionary history and stress regulation of plant receptor-like kinase/pelle genes. Plant Physiol. 150, 12–26.

Lichter, A. and Haberlein, I. (1998). A light dependent redox signal participates in the regulation of ammonia fixation in chloro-plasts of higher plants. J Plant Physiol 153: 83-90.

Lieman-Hurwitz, J., Rachmilevitch, S., Mittler, R., Marcus, Y. and Kaplan A. (2003). Enhanced photosynthesis and growth of transgenic plants that express ictB, a gene involved in HCO3- accumulation in cyanobacteria. Plant Biotechnol. J., 1: 43-50.

Lieman-Hurwitz, J., Asipov, L., Rachmilevitch S., Marcus Y. and Kaplan A. (2005). Expression of cyanobacterial *ictB* in higher plants enhanced photosynthesis and growth. In: Omasa K, Nouchi I, De Kok LJ, eds. *Plant responses to air pollution and global change*. Tokyo: Springer-Verlag, 133–139.

Li, J., Li, L. and Sheen, J. (2010). Protocol: a rapid and economical procedure for purification of plasmid or plant DNA with diverse applications in plant biology. *Plant Methods*, 6(1), p.1.

Long, S. P., Zhu, X. G., Naidu, S. L. and Ort, D. R. (2006). Can improvement in photosynthesis increase crop yields? *Plant, Cell and Environment* 29, 315–330.

MacAlister, C. A., Ohashi-Ito, K. and Bergmann, D. C. (2007). Transcription factor control of asymmetric cell divisions that establish the stomatal lineage. Nature 445, 537–540.

Makino, A., Mae, T. and Ohira, K.(1987). Variation in the contents and kinetic properties of ribulose-1,5-bisphosphate carboxylases among rice species. Plant and Cell Physiology. 28: 799–804.

Makino, A., Mae, T. and Ohira, K.(1988). Differences between wheat and rice in the enzymic properties of ribulose-1,5-bisphosphate carboxylase/oxygenase and the relationship to photosynthetic gas exchange. *Planta*. 174: 30–38.

Makino, A., Miyake, C. and Yokota, A. (2002). Physiological functions of the water-water cycle (Mehler reaction) and the cyclic electron flow around PSI in rice leaves. Plant Cell Physiol. 43: 1017–1026.

Masle, J., Gilmore, S. R. and Farquhar, G. D. (2005). The ERECTA gene regulates plant transpiration efficiency in Arabidopsis. Nature 436: 866–870.

Matile, P., Hörtensteiner, S. and Thomas, H. (1999). Annu. Rev. Plant Physiol. Plant Mol. Biol. 50, 67-95.

McAusland, L., Davey, P. A., Kanwal, N., Baker, N. R., and Lawson, T. (2013). A novel system for spatial and temporal imaging of intrinsic plant water use. Journal of Experimental Botany. 64: 4993-5007.

McCormick, S., Niedermeyer, J., Fry, J., Barnason, A., Horsch, R. and Fraley, R. (1986). Leaf disc transformation of cultivated tomato (L. esculentum) using Agrobacterium tumefaciens. Plant Cell Rep. 5:81-84.

Marchand, C., Johnson, A. A., Karki, R. G., Pais, G. C. G., Zhang, X., Cowansage, K., Patel, T. A., Nicklaus, M. C., Burke, T. R. and Pommier, Y. (2003).

Metaldependent inhibition of HIV-1 integrase by -diketo acids and resistance of the soluble double-mutant (F185K/C280S). Molecular pharmacology. 64(3), 600.

Matile, P., Hörtensteiner, S. and Thomas, H. (1999). Chlorophyll degradation. Annu. Rev. Plant Physiol. Plant Mol. Biol. 50: 67–95.

Matsumura, T., Sakakibara, H., Nakano, R., Kimata, Y., Sugiyama, T. and Hase, T. (1997). A nitrate-inducible ferredoxin in maize roots: genomic organization and differential expression of two non-photosynthetic ferredoxin isoproteins. Plant Physiol 114:563–660.

Matthew P. J. (2016). Photosynthesis. Essays In Biochemistry, 60(3) 255-273.

McKeon, T. A. and Stumpf, P. K. (1982). Purification and characterization of the stearoyl-acyl carrier protein desaturase and the acyl-acyl carrier protein thioesterase from maturing seeds of safflower, J. Biol. Chem. 257,12141-12147.

Meguro, M., Ito, H., Takabayashi, A., Tanaka, R. and Tanaka, A. (2011). Identification of the 7-hydroxymethyl chlorophyll a reductase of the chlorophyll cycle in Arabidopsis, Plant Cell, 23, 3442-3453.

Michelet, L., Zaffagnini, M., Morisse, S., Sparla, F., Pérez-Pérez, M. E., Francia, F., Danon, A., Marchand, C. H., Fermani, S., Trost, P. and Lemaire, S. D. (2013). Redox regulation of the Calvin–Benson cycle: something old, something new. Frotiers in plant science, 4 (470); 1-21.

Ming, R. and Wai, C. M. (2016). Pineapple Genome: A Reference for Monocots and CAM Photosynthesis. *Trends in Genetics*, Vol. 32, No. 11.

Minguet-Parramona, C., Wang, Y., Hills, A., Vialet-Chabrand, S., Griffiths, H., Rogers, S., Lawson, T., Lew, V. L. and Blatt, M. R. (2016). An optimal frequency in Ca2+ oscillations for stomatal closure is an emergent property of ion transport in guard cells. Plant Physiol 170: 33–42.

Miyake, C. and Asada, K. (1992). Thylakoid-bound ascorbate peroxidase in spinach chloroplasts and photoreduction of its primary oxidation product monodehydroascorbate radicals in thylakoids. Plant Cell Physiol. 33: 541–553.

Murchie, E. H. and Lawson, T. (2013). Chlorophyll fluorescence analysis: a guide to good practice and understanding some new applications. J Exp Bot 64: 3983–3998.

Nadeau, J. A., and Sack, F. D. (2002). Control of stomatal distribution on the Arabidopsis leaf surface. *Science* 296, 1697–1700.

Neil, R. B. (2008). Chlorophyll Fluorescence: A Probe of Photosynthesis In Vivo. The *Annual Review of Plant Biology* 59: 89-113.

New England Biolabs. Golden Gate Assembly. 2016. <https://www.neb.com/applications/cloning-and-synthetic-biology/dna-assembly-and-cloning/golden-gate-assembly>.

Onda, Y., Matsumura, T., Kimata-Ariga, Y., Sakakibara, H., Sugiyama, T. and Hase, T. (2000). Differential interaction of maize root ferredoxin:NADP+ oxidoreductase with photosynthetic and nonphotosynthetic ferredoxin isoenzymes. Plant Physiol 123: 1037–1045.

Park, Y. I., Choi, S. B. and Liu, J. R. (2009). Transgenic plants with cyanobacterial genes. Plant Biotechnol Rep. 3: 267–275.

Parry, A. J., Andralojc, P. J.,Scales, J. C., Salvucci, M. E., Carmo-Silva, A. E. Alonso, H. and Whitney, S. M. (2012). Rubisco activity and regulation as targets for crop improvement. J Exp Bot 64 (3): 717-730.

Peterson, K. M., Rychel, A. L. and Torii, K. U. (2010). Out of the mouths of plants: the molecular basis of the evolution and diversity of stomatal development. Plant Cell 22, 296–306.

Potters, G., Pasternak, T. P., Guisez, Y. and Jansen, M. A. (2009). Different stresses, similar morphogenic responses: integrating a plethora of pathways. Plant Cell Environ. 32, 158–169.

Price, G. D., Klughammer, B., Ludwig, M. and Badger, M. R. (1998). The functioning of the CO_2 concentrating mechanism in several cyanobacterial strains: a review of general physiological characteristics, genes, proteins, and recent advances. Can J Bot., 76 (6): 973–1002.

Price, G. D., Badger, M. R. and von Caemmerer, S. (2011). The prospect of using cyanobacterial bicarbonate transporters to improve leaf photosynthesis in C3 crop plants. Plant Physiol., 155: 20-26.

Qi, Y., Sun, Y., Xu, L., Xu, Y. and Huang, H. (2004). ERECTA is required for protection against heat-stress in the AS1/AS2 pathway to regulate adaxial–abaxial leaf polarity in Arabidopsis. Planta 219: 270–276.

Quick, W. P., Schurr, U., Fichtner, K., Schulze, E-D., Rodermel, S. R., Bogorad, L. and Stitt, M. (1991). The impact of decreased Rubisco on photosynthesis, growth, allocation and storage in tobacco plants which have been transformed with antisense *rbcs*. *The Plant Journal* 1, 51–58.

Raines, C. A. (2011). Increasing photosynthetic carbon assimilation in C3 plants to improve crop yield: current and future strategies. *Plant Physiology:* 155, 36–42.

Redei, G. P. (1965). Non-mendelian megagametogenesis in Arabidopsis. Genetics 51:857–872.

Reinbothe, C., Buhr, F., Bartsch, S., Desvignes, C., Quigley, F., Pesey, H. and Reinbothe, S. (2006). In vitro-mutagenesis of NADPH:protochlorophyllide oxidoreductase B: two distinctive protochlorophyllide binding sites participate in enzyme catalysis and assembly, Mol. Gen. Genomics , 275, 540-552.

Rodoni, S., Mühlecker, W., Anderl, M., Kräutler, B., Moser, D., Thomas, H., Matile, P. and Hörtensteiner, S. (1997). Chlorophyll breakdown in senescent chloroplasts. Cleavage of pheophorbide a in two enzymic steps. Plant Physiol. 115: 669–676.

Rosenthal, D. M., Locke, A. M., Khozaei, M., Raines, C. A., Long, S. P. and Ort, D. R. (2011). Over-expressing the C3 photosynthesis cycle enzyme sedoheptulose-1-7 bisphosphatase improves photosynthetic carbon gain and yield under fully open-air CO_2 fumigation (FACE). BMC Plant Biology 11, 123.

Sage, F. R. and Stata, M. (2015). Photosynthetic diversity meets biodiversity: The C4 plant example. *Journal of Plant Physiology* 172; 104–119.

Schürmann, P. and Buchanan, B. B. (2001). The structure and function of the ferredoxin/thioredoxin system in photosynthesis. Advances in Photosynthesis and Respiration 11: 331-361.

Schürmann, P. and Buchanan, B. B. (2008). The Ferredoxin/Thioredoxin System of Oxygenic Photosynthesis. Antioxid Redox Signal 10: 1235-1274.

Sharkey, T. D., Bernacchi, C. J., Farquhar, G. D. and Singsaas, E. L. (2007). Fitting photosynthetic carbon dioxide response curves for C3 leaves. Plant, Cell &Environment 30: 1035–1040.

Simkin, A. J., MCausland, L., Headland, L. R., Lawson, T. and Raines, C. A. (2015). 'Multigene Manipulation of Photosynthetic Carbon Assimilation Increases CO_2

Fixation and Biomass Yield In Tobacco'. *Journal of Experimental Botany* 66.13 (2015): 4075-4090.

Sokal, R. R. and Rohlf, F. J.(1981). Biometry. 2nd ed. Freeman, New York.

Shpak, E. D., Berthiaume, C. T., Hill, E. J. and Torii, K. U. (2004). Synergistic interaction of three ERECTA-family receptor-like kinases controls Arabidopsis organ growth and flower development by promoting cell proliferation. *Development* 131, 1491–1501.

Shpak, E. D., McAbee, J. M., Pillitteri, L. J. and Torii, K. U. (2005). Stomatal patterning and differentiation by synergistic interactions of receptor kinases. Science 309: 290 – 293 .

SINGH. (2007). Molecular Analysis of the Arabidopsis CP12 Gene Family PhD, University of Essex.

Solomon, S., Plattner, G-K., Knutti, R. and Friedlingstein, P. (2009). Irreversible climate change due to carbon dioxide emissions. Proceedings of the National Academy of Sciences. 106: 1704–1709.

Sugano, S. S., Shimada, T., Imai, Y., Okawa, K., Tamai, A., Mori, M. and Hara-Nishimura, I. (2010). Stomagen positively regulates stomatal density in Arabidopsis. *Nature* 463, 241-244.

Tanaka, Y., Sugano, S. S., Shimada, T. and Hara-Nishimura, I. (2013). Enhancement of leaf photosynthetic capacity through increased stomatal density in Arabidopsis. New Phytologist. Volume 198, 3:

Takata, N., Yokota, K., Ohki, S., Mori, M., Taniguchi, T. and Kurita, M. (2013). Evolutionary Relationship and Structural Characterization of the EPF/EPFL Gene Family. PLoS ONE 8(6): e65183.

Tanaka, A. and Tanaka, R. (2006). Chlorophyll metabolism. Curr. Opin. Plant Biol. 9: 248–255.

Tanaka, R. and Tanaka, A. (2007). Tetrapyrrole biosynthesis in higher plants. Annu. Rev. Plant Biol. 58: 321–346.

Terauchi, A. M., Petroutsos, D., Busch, A., Hirschmann, I., Merchant, S. S., Finazzi, G. and Hippler, M. (2009). PGRL1 Participates in Iron-induced Remodeling of the Photosynthetic Apparatus and in Energy Metabolism in Chlamydomonas reinhardtii. Journal of Biological Chemistry, 284(47): 32770-81.

https://www.thermofisher.com/us/en/home/life-science/cloning/gene-synthesis/geneart-gene-synthesis.html?gclid=EAIaIQobChMIxvH6rY6h3wIVGud3Ch3iRQXgEAAYAiAAEgLD0fD_BwE&s_kwcid=AL!3652!3!316510616618!p!!s!!geneart&ef_id=EAIaIQob

ChMIxvH6rY6h3wIVGud3Ch3iRQXgEAAYAiAAEgLD0fD_BwE:G:s&s_kwcid=AL!3652!3!316510616618!p!!s!!geneart

Thomsen-Zieger, N., Pandini, V., Caprini, G., Aliverti, A., Cramer, J., Selzer, P. M., Zanetti, G. and Seeber, F. (2004). A single in vivo-selected point mutation in the active center of Toxoplasma gondii ferredoxin-NADPþ reductase leads to an inactive enzyme with greatly enhanced affinity for ferredoxin. FEBS Letters 576, 375–380.

Uchida, N., Lee, J. S., Horst, R. J., Lai, H-H., Kajita, R., Kakimoto, T., Tasaka, M. and Torii, K. U. (2012). Regulation of inflorescence architecture by intertissue layer ligand–receptor communication between endodermis and phloem. Proceedings of the National Academy of Sciences, USA 109, 6337–6342.

Urban, J., Ingwers, M., McGuire, M. A. and Teskey, R. O. (2017). Stomatal conductance increases with rising temperature. Plant Signaling & Behavior, 12 (8): e1356534.

Vikram, P., Swamy, B. P. M., Dixit, S., Singh, R., Singh, B. P., Miro, B., Kohli, A., Henry, A., Singh, N. K. and Kumar, A. (2015). Drought susceptibility of modern rice varieties: an effect of linkage of drought tolerance with undesirable traits. Scientific Reports 5: e18.

Voss, I., Goss, T., Murozuka, E., Altmann, B., Mclean, K. J., Rigby, S. E., Munro, A. W., Scheibe, R., Hase, T. and Hanke, G. T. (2011). FdC1, a novel ferredoxin protein

capable of alternative electron partitioning, increases in conditions of acceptor limitation at photosystem I. J. Biol. Chem. 286, 50–59.

Wada, M., Grolig, F. and Haupt, W. (1993). Light-oriented chloroplast positioning. Contribution to progress in photobiology. J Photochem Photobiol B Biol 17: 3 – 25.

Wang, H., Ngwenyama, N., Liu, Y., Walker, J. C. and Zhang S. (2007). Stomatal development and patterning are regulated by environmentally responsive mitogen-activated protein kinases in *Arabidopsis*. *Plant Cell* 19 63–73.

Williams-Smith, D. L. and Cammack, R. (1977). Oxidation-reduction potentials of cytochromes P-450 and ferredoxin in the bovine adrenal.Their modification by substrates and inhibitors. Biochimica Et Biophysica Acta 499, 432–442.

https://www.ipcc.ch/pdf/assessment-report/ar4/wg2/ar4_wg2_full_report.pdf

Xu, Y-F., Ookawa, T. and Ishihara, K. (1997). Analysis of the photosynthetic characteristics of the high-yielding rice cultivar Takanari. Japanese Journal of Crop Science. 66: 616–623.

Xuan, M., Zhao, J., Shao, J., Li, Q. and Li, J. (2017). Perspective of energy transfer from light energy into biological energy. Green Energy & Environment 1-5.

Yang, M. and Sack, F. D. (1995). The too many mouths and four lips Mutations Affect Stomatal Pnoduction in Arabidopsis. The Plant Gell, 7, 2227-2239.

Yamamoto, H. and Shikanai, T. (2017). Contribution of Cyclic and Pseudo-cyclic Electron Transport to the Formation of ProtonMotive Force in Chloroplasts. Molecular Plant 10, 20–29.

Yingjun, W., Dan, J. S. and Martin H. S. (2015). The CO_2 concentrating mechanism and photosynthetic carbon assimilation in limiting CO_2: how Chlamydomonas works against the gradient.Development, The Plant Journal, 82; 429–448.

Zhang, X., Henriques, R., Lin S. S., Niu, Q.W. and Chua, N. H. (2006). *Agrobacterium*-mediated transformation of *Arabidopsis thaliana* using the floral dip method. *Nat Protocol* 1: 1–6.

Zhu, X. G., de Sturler, E. and Long, S. P. (2007). Optimizing the distribution of resources between enzymes of carbon metabolism can dramatically increase photosynthetic rate: a numerical simulation using an evolutionary algorithm. *Plant Physiology* 145, 513–526.

Zhu, X. G., Long. S. P. and Ort, D. R. (2010). Improving photosynthetic efficiency for greater yield. *Annual Review of Plant Biology* 61, 235–226.

Appendix

Table of Primer Sequences for PCR

EPF1 forward	CACCCATGAGCAATGAAGGACAAGG
EPF1 reverse	ATGAACCCAACCAGTAATCTAAGGA
EPF2 forward	CACCAGGGATCAGTTAGGAATGGCT
EPF2 reverse	GGTACGAGATGGATCAATTGG
NOS terminator reverse	TGCCAAATGTTTGAACGATC
ictB forward:	ACTGTCTGGCAAACTCTGACTTTTGC
EPF9 forward	CACCGAATTCAAGAAGGTTGATGATAGGA
scr-BAR-3'-FP (pNos)	CTGAGTGGCTCCTTCAACGT
scr-BAR-3'-FP2	ACGGAAGTTGACCGTGCTTG
scr-BAR-5'-RP	TTCTGGCAGCTGGACTTCAG
EPF9 reverse	CTGACAAAGCAGAATTAGCGG
scr-pL2M-FPrimer	CACGCCCTCCTACATCGAAG
scr-pL2M-RPrimer	CGGTCACATGTGCATCCTC
seq-BAR1	ATGAGCCCAGAACGACG
seq-BAR4	TCAAATCTCGGTGACGGG
pL1M Forward	CGGATAAACCTTTTCACGCCC
pL1M Reverse	TACTGGGGTGGATGCAGTG

Table of Primer Sequences for qPCR

Primer qEPF1F	GTACGAATCCACCGGAAAAC
Primer qEPF1R	AACAACTGCCATCCTTGCAT
Primer qEPF2F	TCACAATGACCACAAGAACGA
Primer qEPF2R	TCGAATTCACCAAGAGTGGA
Primer qEPF9F	GTTGGTGCTGTCGACCCTAT
Primer qEPF9R	CAAGCCTCAAGACCTCGTTC
Primer qFdF	AGCGTCGAGGACGTAGACAT
Primer qFdR	ACAATCTCTCTTCGGCCTCA
Primer qE.factorF	CCAACATTGTCACCAGGAA
Primer qE.factorR	TGAGATGCACCACGAAGCT

Multiple sequence alignment of physical maps and sequence data

*At*EPFL1 reverse alignment

```
L1AtEPF1
ATACAAATGGACGAACGGATAAACCTTTTCACGCCCTTTTAAATATCCGATTATTCTAAT
pL1MReverse     ------------------------------------------------------------

L1AtEPF1
AAACGCTCTTTTCTCTTAGGTTTACCCGCCAATATATCCTGTCAAACACTGATAGTTTAA
pL1MReverse     ------------------------------------------------------------

L1AtEPF1
ACCACTTCGTGCAGAAGACAATAGTGGAGGTCAACATGGTGGAGCACGACACTCTGGTCT
pL1MReverse     ------------------------------------------------------------

L1AtEPF1
ACTCCAAAAATGTCAAAGATACAGTCTCAGAAGATCAAAGGGCTATTGAGACTTTTCAAC
pL1MReverse     ------------------------------------------------------------

L1AtEPF1
AAAGGATAATTTCGGGAAACCTCCTCGGATTCCATTGCCCAGCTATCTGTCACTTCATCG
pL1MReverse     ------------------------------------------------------------

L1AtEPF1
AAAGGACAGTAGAAAAGGAAGGTGGCTCCTACAAATGCCATCATTGCGATAAAGGAAAGG
pL1MReverse     ------------------------------------------------------------

L1AtEPF1
CTATCATTCAAGATCTCTCTGCCGACAGTGGTCCCAAAGATGGACCCCCACCCACGAGGA
pL1MReverse     ------------------------------------------------------------

L1AtEPF1
GCATCGTGGAAAAAGAAGAGGTTCCAACCACGTCTACAAAGCAAGTGGATTGATGTGATA
pL1MReverse     ------------------------------------------------------------

L1AtEPF1
ACATGGTGGAGCACGACACTCTGGTCTACTCCAAAAATGTCAAAGATACAGTCTCAGAAG
pL1MReverse     ------------------------------------------------------------

L1AtEPF1
ATCAAAGGGCTATTGAGACTTTTCAACAAAGGATAATTTCGGGAAACCTCCTCGGATTCC
pL1MReverse     ----------CTATGAGACTTTTCAACAAAGGATAATTTCGGGAAACCTNCTCGGATTCC
************************************ **********

L1AtEPF1
ATTGCCCAGCTATCTGTCACTTCATCGAAAGGACAGTAGAAAAGGAAGGTGGCTCCTACA
pL1MReverse
ATTGCCCAGCTATCTGTCACTTCATCGAAAGGACAGTAGAAAAGGAAGGTGGCTCCTACA
************************************************************

L1AtEPF1
AATGCCATCATTGCGATAAAGGAAAGGCTATCATTCAAGATCTCTCTGCCGACAGTGGTC
pL1MReverse
AATGCCATCATTGCGATAAAGGAAAGGCTATCATTCAAGATCTNTCTGCCGACAGTGGTC
******************************************* ****************
```

L1AtEPF1
CCAAAGATGGACCCCCACCCACGAGGAGCATCGTGGAAAAAGAAGAGGTTCCAACCACGT
pL1MReverse
CCAAAGATGGACCCCCACCCACGAGGAGCATCGTGGAAAAAGAAGAGGTTCCAACCACGT
****

L1AtEPF1
CTACAAAGCAAGTGGATTGATGTGACATCTCCACTGACGTAAGGGATGACGCACAATCCC
pL1MReverse
CTACAAAGCAAGTGGATTGATGTGACATCTCCACTGACGTAAGGGATGACGCACAATCCC
****

L1AtEPF1
ACTATCCTTCGCAAGACCCTTCCTCTATATAAGGAAGTTCATTTCATTTGGAGAGGACAC
pL1MReverse
ACTATCCTTCGCAAGACCCTTCCTCTATATAAGGAAGTTCATTTCATTTGGAGAGGACAC
****

L1AtEPF1
GCAATGTTTGCTATATACAAATCAACCCTTCTTCTTCTTCCTCTCATTCTCATTCTTCTC
pL1MReverse
GCAATGTTTGCTATATACAAATCAACCCTTCTTCTTCTTCCTCTCATTCTCATTCTTCTC
****

L1AtEPF1
ATCACTCCACAAGTCTCATCCTTTCTTCAACCTATCCAACCTCCTATTTCTCCTCAAGTC
pL1MReverse
ATCACTCCACAAGTCTCATCCTTTCTTCAACCTATCCAACCTCCTATTTCTCCTCAAGTC
****

L1AtEPF1
GCTTTGATTGAAGATAAAGCAAGATTAGGTTCAACACCACCAAGCTGCCACAACAGATGC
pL1MReverse
GCTTTGATTGAAGATAAAGCAAGATTAGGTTCAACACCACCAAGCTGCCACAACAGATGC
****

L1AtEPF1
AACAACTGCCATCCTTGCATGGCTATTCAAGTACCAACTCTCCCGACTCGCTCCCGCTTC
pL1MReverse
AACAACTGCCATCCTTGCATGGCTATTCAAGTACCAACTCTCCCGACTCGCTCCCGCTTC
****

L1AtEPF1
ACACGAGTTAACCCGTTTTCCGGTGGATTCGTACGACCTCCTTCTTCTCTAACCACCGTT
pL1MReverse
ACACGAGTTAACCCGTTTTCCGGTGGATTCGTACGACCTCCTTCTTCTCTAACCACCGTT
****

L1AtEPF1
CTTGATCAGTACTCTAATTACAAACCTATGGGATGGAAATGTCATTGCAATGGCCACTTT
pL1MReverse
CTTGATCAGTACTCTAATTACAAACCTATGGGATGGAAATGTCATTGCAATGGCCACTTT
****

L1AtEPF1
TATAATCCTTAAGCTTATATGAAGATGAAGATGAAATATTTGGTGTGTCAAATAAAAAGC
pL1MReverse
TATAATCCTTAAGCTTATATGAAGATGAAGATGAAATATTTGGTGTGTCAAATAAAAAGC
****

L1AtEPF1
TTGTGTGCTTAAGTTTGTGTTTTTTTCTTGGCTTGTTGTGTTATGAATTTGTGGCTTTTT
pL1MReverse
TTGTGTGCTTAAGTTTGTGTTTTTTTCTTGGCTTGTTGTGTTATGAATTTGTGGCTTTTT
****

```
L1AtEPF1
CTAATATTAAATGAATGTAAGATCTCATTATAATGAATAAACAAATGTTTCTATAATCCA
pL1MReverse
CTAATATTAAATGAATGTAAGATCTCATTATAATGAATAAACAAATGTTTCTATAATCCA
************************************************************

L1AtEPF1
TTGTGAATGTTTTGTTGGATCTCTTCTGCAGCATATAACTACTGTATGTGCTATGGTATG
pL1MReverse
TTGTGAATGTTTTGTTGGATCTCTTCTGCAGCATATAACTACTGTATGTGCTATGGTATG
************************************************************

L1AtEPF1
GACTATGGAATATGATTAAAGATAAGCGCTAAGCTTGAATTCTTGCTTGTCTTCACAGAG
pL1MReverse     GACTATGGAATATGATTAAAGATAAGCGCTAAGCTGA----------------------
***********************************
```

*At*EPFL1 forward alignment

```
L1AtEPF1
ATACAAATGGACGAACGGATAAACCTTTTCACGCCCTTTTAAATATCCGATTATTCTAAT
pL1MForward     ------------------------------------------------------------


L1AtEPF1
AAACGCTCTTTTCTCTTAGGTTTACCCGCCAATATATCCTGTCAAACACTGATAGTTTAA
pL1MForward     ----
GCTCTTTTCTCTTAGGTTTACCCGCCAATATATCCTGTCAAACACTGATAGTTTAA
************************************************************

L1AtEPF1
ACCACTTCGTGCAGAAGACAATAGTGGAGGTCAACATGGTGGAGCACGACACTCTGGTCT
pL1MForward
ACCACTTCGTGCAGAAGACAATAGTGGAGGTCAACATGGTGGAGCACGACACTCTGGTCT
************************************************************

L1AtEPF1
ACTCCAAAAATGTCAAAGATACAGTCTCAGAAGATCAAAGGGCTATTGAGACTTTTCAAC
pL1MForward
ACTCCAAAAATGTCAAAGATACAGTCTCAGAAGATCAAAGGGCTATTGAGACTTTTCAAC
************************************************************

L1AtEPF1
AAAGGATAATTTCGGGAAACCTCCTCGGATTCCATTGCCCAGCTATCTGTCACTTCATCG
pL1MForward
AAAGGATAATTTCGGGAAACCTCCTCGGATTCCATTGCCCAGCTATCTGTCACTTCATCG
************************************************************

L1AtEPF1
AAAGGACAGTAGAAAAGGAAGGTGGCTCCTACAAATGCCATCATTGCGATAAAGGAAAGG
pL1MForward
AAAGGACAGTAGAAAAGGAAGGTGGCTCCTACAAATGCCATCATTGCGATAAAGGAAAGG
************************************************************

L1AtEPF1
CTATCATTCAAGATCTCTCTGCCGACAGTGGTCCCAAAGATGGACCCCCACCCACGAGGA
pL1MForward
CTATCATTCAAGATCTCTCTGCCGACAGTGGTCCCAAAGATGGACCCCCACCCACGAGGA
************************************************************

L1AtEPF1
GCATCGTGGAAAAAGAAGAGGTTCCAACCACGTCTACAAAGCAAGTGGATTGATGTGATA
pL1MForward
GCATCGTGGAAAAAGAAGAGGTTCCAACCACGTCTACAAAGCAAGTGGATTGATGTGATA
```

```
************************************************************

L1AtEPF1
ACATGGTGGAGCACGACACTCTGGTCTACTCCAAAAATGTCAAAGATACAGTCTCAGAAG
pL1MForward
ACATGGTGGAGCACGACACTCTGGTCTACTCCAAAAATGTCAAAGATACAGTCTCAGAAG
************************************************************

L1AtEPF1
ATCAAAGGGCTATTGAGACTTTTCAACAAAGGATAATTTCGGGAAACCTCCTCGGATTCC
pL1MForward
ATCAAAGGGCTATTGAGACTTTTCAACAAAGGATAATTTCGGGAAACCTCCTCGGATTCC
************************************************************

L1AtEPF1
ATTGCCCAGCTATCTGTCACTTCATCGAAAGGACAGTAGAAAAGGAAGGTGGCTCCTACA
pL1MForward
ATTGCCCAGCTATCTGTCACTTCATCGAAAGGACAGTAGAAAAGGAAGGTGGCTCCTACA
************************************************************

L1AtEPF1
AATGCCATCATTGCGATAAAGGAAAGGCTATCATTCAAGATCTCTCTGCCGACAGTGGTC
pL1MForward
AATGCCATCATTGCGATAAAGGAAAGGCTATCATTCAAGATCTCTCTGCCGACAGTGGTC
************************************************************

L1AtEPF1
CCAAAGATGGACCCCCACCCACGAGGAGCATCGTGGAAAAAGAAGAGGTTCCAACCACGT
pL1MForward
CCAAAGATGGACCCCCACCCACGAGGAGCATCGTGGAAAAAGAAGAGGTTCCAACCACGT
************************************************************

L1AtEPF1
CTACAAAGCAAGTGGATTGATGTGACATCTCCACTGACGTAAGGGATGACGCACAATCCC
pL1MForward
CTACAAAGCAAGTGGATTGATGTGACATCTCCACTGACGTAAGGGATGACGCACAATCCC
************************************************************

L1AtEPF1
ACTATCCTTCGCAAGACCCTTCCTCTATATAAGGAAGTTCATTTCATTTGGAGAGGACAC
pL1MForward
ACTATCCTTCGCAAGANCCTTCCTCTATATAAGGAAGTTCATTTCATTTGGAGAGGACAC
**************** ********************************************

L1AtEPF1
GCAATGTTTGCTATATACAAATCAACCCTTCTTCTTCTTCCTCTCATTCTCATTCTTCTC
pL1MForward
GCAATGTTTGCTATATACAAATCAACCCTTCTTCTTCTTCCTCTCATTCTCATTCTTCTC
************************************************************

L1AtEPF1
ATCACTCCACAAGTCTCATCCTTTCTTCAACCTATCCAACCTCCTATTTCTCCTCAAGTC
pL1MForward
ATCACTCCACAAGTCTCATCCTTTCTTCAACCTATCCAACCTNCNATTTCTCCTCAAGTC
****************************************** * ****************

L1AtEPF1
GCTTTGATTGAAGATAAAGCAAGATTAGGTTCAACACCACCAAGCTGCCACAACAGATGC
pL1MForward     GCTTTGATTGAAGANAA----------------------------------------
************** **

L1AtEPF1
AACAACTGCCATCCTTGCATGGCTATTCAAGTACCAACTCTCCCGACTCGCTCCCGCTTC
pL1MForward     ------------------------------------------------------
```

L1AtEPF1
ACACGAGTTAACCCGTTTTCCGGTGGATTCGTACGACCTCCTTCTTCTCTAACCACCGTT
pL1MForward ----------

L1AtEPF1
CTTGATCAGTACTCTAATTACAAACCTATGGGATGGAAATGTCATTGCAATGGCCACTTT
pL1MForward ----------

L1AtEPF1
TATAATCCTTAAGCTTATATGAAGATGAAGATGAAATATTTGGTGTGTCAAATAAAAAGC
pL1MForward ----------

L1AtEPF1
TTGTGTGCTTAAGTTTGTGTTTTTTTCTTGGCTTGTTGTGTTATGAATTTGTGGCTTTTT
pL1MForward ----------

L1AtEPF1
CTAATATTAAATGAATGTAAGATCTCATTATAATGAATAAACAAATGTTTCTATAATCCA
pL1MForward ----------

L1AtEPF1
TTGTGAATGTTTTGTTGGATCTCTTCTGCAGCATATAACTACTGTATGTGCTATGGTATG
pL1MForward ----------

L1AtEPF1
GACTATGGAATATGATTAAAGATAAGCGCTAAGCTTGAATTCTTGCTTGTCTTCACAGAG
pL1MForward ----------

*At*EPFL2 reverse alignment

L1AtEPF2
CCTGATCTGGGGAACCCTGTGGTTGGCATGCACATACAAATGGACGAACGGATAAACCTT
pL1MReverse ----------

L1AtEPF2
TTCACGCCCTTTTAAATATCCGATTATTCTAATAAACGCTCTTTTCTCTTAGGTTTACCC
pL1MReverse ----------

L1AtEPF2
GCCAATATATCCTGTCAAACACTGATAGTTTAAACCACTTCGTGCAGAAGACAATAGTGG
pL1MReverse ----------

L1AtEPF2
AGGTCAACATGGTGGAGCACGACACTCTGGTCTACTCCAAAAATGTCAAAGATACAGTCT
pL1MReverse ----------

L1AtEPF2
CAGAAGATCAAAGGGCTATTGAGACTTTTCAACAAAGGATAATTTCGGGAAACCTCCTCG
pL1MReverse ----------

L1AtEPF2
GATTCCATTGCCCAGCTATCTGTCACTTCATCGAAAGGACAGTAGAAAAGGAAGGTGGCT

```
pL1MReverse     ------------------------------------------------------------


L1AtEPF2
CCTACAAATGCCATCATTGCGATAAAGGAAAGGCTATCATTCAAGATCTCTCTGCCGACA
pL1MReverse     ------------------------------------------------------------


L1AtEPF2
GTGGTCCCAAAGATGGACCCCCACCCACGAGGAGCATCGTGGAAAAAGAAGAGGTTCCAA
pL1MReverse     ------------------------------------------------------------


L1AtEPF2
CCACGTCTACAAAGCAAGTGGATTGATGTGATAACATGGTGGAGCACGACACTCTGGTCT
pL1MReverse     ------------------------------------------------------------


L1AtEPF2
ACTCCAAAAATGTCAAAGATACAGTCTCAGAAGATCAAAGGGCTATTGAGACTTTTCAAC
pL1MReverse     --------------------------------AGATCAAAGGGCTATGAGACTTTTCAAC
** **    ***************

L1AtEPF2
AAAGGATAATTTCGGGAAACCTCCTCGGATTCCATTGCCCAGCTATCTGTCACTTCATCG
pL1MReverse
AAAGGATAATTTCGGGAAACCTNCTCGGATTCCATTGCCCAGCTATCTGTCACTTCATCG
********************** ****************************************

L1AtEPF2
AAAGGACAGTAGAAAAGGAAGGTGGCTCCTACAAATGCCATCATTGCGATAAAGGAAAGG
pL1MReverse
AAAGGACAGTAGAAAAGGAAGGTGGCTCCTACAAATGCCATCATTGCGATAAAGGAAAGG
************************************************************

L1AtEPF2
CTATCATTCAAGATCTCTCTGCCGACAGTGGTCCCAAAGATGGACCCCCACCCACGAGGA
pL1MReverse
CTATCATTCAAGATCTNTCTGCCGACAGTGGTCCCAAAGATGGACCCCCACCCACGAGGA
***************** **********************************************

L1AtEPF2
GCATCGTGGAAAAAGAAGAGGTTCCAACCACGTCTACAAAGCAAGTGGATTGATGTGACA
pL1MReverse
GCATCGTGGAAAAAGAAGAGGTTCCAACCACGTCTACAAAGCAAGTGGATTGATGTGACA
************************************************************

L1AtEPF2
TCTCCACTGACGTAAGGGATGACGCACAATCCCACTATCCTTCGCAAGACCCTTCCTCTA
pL1MReverse
TCTCCACTGACGTAAGGGATGACGCACAATCCCACTATCCTTCGCAAGACCCTTCCTCTA
************************************************************

L1AtEPF2
TATAAGGAAGTTCATTTCATTTGGAGAGGACACGCAATGGTGTGGAGCAGCAACATGTCA
pL1MReverse
TATAAGGAAGTTCATTTCATTTGGAGAGGACACGCAATGTTTGCTATATACAAATCAACC
****************************************** *   *   ***    *

L1AtEPF2        AGCTTTCTACTGATTTTGCTCATTCTTAATTCGACCCATTTC--AGTCTAAT----GGCT
pL1MReverse
CTTCTTCTTCTTCCTCTCATTCTCATTCTTCTCATCACTCCACAAGTCTCATCCTTTCTT
**** **  * * * * ** *  * * *    ***** **      *

L1AtEPF2
AATGGTAGACCAGAGCCTGACTCTGTCGAATTCACCAAGAGTGGAGATCAAGATGTGAAG
pL1MReverse     CAACCTATCCAACCTCCTATTTCTCCTCAAGTCGCTTTGATTGAAG----------
```

```
*  **  * *  ***  ***  ** ** *  ** ** **

L1AtEPF2
ATGATGATGAGAGGTCTAATAGGATCAAGACCACCAAGATGTGAGAGAGTAAGATGTCGT
pL1MReverse     -------ATAAAGCAAGATTAGGTTCAACACCACCAAGCTGCCACAACA---
GATGCAAC
* **   * **** **** ********* **  * *     ****

L1AtEPF2
TCTTGTGGTCATTGTGAAGCAATTCAAGTTCCTACAAATCCTCAAACAAAGCTTCACTCT
pL1MReverse
AACTGCCATCCTTGCATGGCTATTCAAGTACCAACTCTCCCGACTCGCTCCCGCTTCACA
**  ** ***   ** ******** ** **   **       *   * *

L1AtEPF2
CCTTTAACTACTTCTTCTTCTTCCTCTGAGACTATTCATCTTGACTACACCAGAGGA
pL1MReverse
CGAGTTAACCCGTTTTCCGGTGGATTCGTACGACCTCCTTCTTCTCTAACCACCGTTCTT
*  * *  * * ***  *  * *     ** * * *    ****

L1AtEPF2
GATGATAGTACTAATTACAAACCCATGAGCTGGAAATGCAAATGTGGTAACTCTATCTAC
pL1MReverse
GATCAGTACTCTAATTACAAACCTATGGGATGGAAATGTCATTGCAATGGCCACTTTTAT
*** *    ************** *** * ********  * **  *  *   * **

L1AtEPF2
AACCCTTGAGCTTATATGAAGATGAAGATGAAATATTTGGTGTGTCAAATAAAAAGCTTG
pL1MReverse
AATCCTTAAGCTTATATGAAGATGAAGATGAAATATTTGGTGTGTCAAATAAAAAGCTTG
** **** **********************************************************

L1AtEPF2
TGTGCTTAAGTTTGTGTTTTTTTCTTGGCTTGTTGTGTTATGAATTTGTGGCTTTTTCTA
pL1MReverse
TGTGCTTAAGTTTGTGTTTTTTTCTTGGCTTGTTGTGTTATGAATTTGTGGCTTTTTCTA
************************************************************

L1AtEPF2
ATATTAAATGAATGTAAGATCTCATTATAATGAATAAACAAATGTTTCTATAATCCATTG
pL1MReverse
ATATTAAATGAATGTAAGATCTCATTATAATGAATAAACAAATGTTTCTATAATCCATTG
************************************************************

L1AtEPF2
TGAATGTTTTGTTGGATCTCTTCTGCAGCATATAACTACTGTATGTGCTATGGTATGGAC
pL1MReverse
TGAATGTTTTGTTGGATCTCTTCTGCAGCATATAACTACTGTATGTGCTATGGTATGGAC
************************************************************

L1AtEPF2
TATGGAATATGATTAAAGATAAGCGCTAAGCTTGAATTCTTGCTTGTCTTCACAGAGTGG
pL1MReverse     TATGGAATATGATTAAAGATAAGCGCTAAGCTGA-------------------------
*********************************
```

AtEPFL2 forward alignment

```
L1AtEPF2
CCTGATCTGGGGAACCCTGTGGTTGGCATGCACATACAAATGGACGAACGGATAAACCTT
pL1MForward     ------------------------------------------------------------
```

```
L1AtEPF2
TTCACGCCCTTTTAAATATCCGATTATTCTAATAAACGCTCTTTTCTCTTAGGTTTACCC
pL1MForward     ----------------------------------GCTCTTTTCTCTTAGGTTTACCC
**********************

L1AtEPF2
GCCAATATATCCTGTCAAACACTGATAGTTTAAACCACTTCGTGCAGAAGACAATAGTGG
pL1MForward
GCCAATATATCCTGTCAAACACTGATAGTTTAAACCACTTCGTGCAGAAGACAATCTGGG
**************************************************** **

L1AtEPF2
AGGTCAACATGGTGGAGCACGACACTCTGGTCTACTCCAAAAATGTCAAAGATACAGTCT
pL1MForward
AGGTCAACATGGTGGAGCACGACACTCTGGTCTACTCCAAAAATGTCAAAGATACAGTCT
************************************************************

L1AtEPF2
CAGAAGATCAAAGGGCTATTGAGACTTTTCAACAAAGGATAATTTCGGGAAACCTCCTCG
pL1MForward
CAGAAGATCAAAGGGCTATTGAGACTTTTCAACAAAGGATAATTTCGGGAAACCTCCTCG
************************************************************

L1AtEPF2
GATTCCATTGCCCAGCTATCTGTCACTTCATCGAAAGGACAGTAGAAAAGGAAGGTGGCT
pL1MForward
GATTCCATTGCCCAGCTATCTGTCACTTCATCGAAAGGACAGTAGAAAAGGAAGGTGGCT
************************************************************

L1AtEPF2
CCTACAAATGCCATCATTGCGATAAAGGAAAGGCTATCATTCAAGATCTCTCTGCCGACA
pL1MForward
CCTACAAATGCCATCATTGCGATAAAGGAAAGGCTATCATTCAAGATCTCTCTGCCGACA
************************************************************

L1AtEPF2
GTGGTCCCAAAGATGGACCCCCACCCACGAGGAGCATCGTGGAAAAAGAAGAGGTTCCAA
pL1MForward
GTGGTCCCAAAGATGGACCCCCACCCACGAGGAGCATCGTGGAAAAAGAAGAGGTTCCAA
************************************************************

L1AtEPF2
CCACGTCTACAAAGCAAGTGGATTGATGTGATAACATGGTGGAGCACGACACTCTGGTCT
pL1MForward
CCACGTCTACAAAGCAAGTGGATTGATGTGATAACATGGTGGAGCACGACACTCTGGTCT
************************************************************

L1AtEPF2
ACTCCAAAAATGTCAAAGATACAGTCTCAGAAGATCAAAGGGCTATTGAGACTTTTCAAC
pL1MForward
ACTCCAAAAATGTCAAAGATACAGTCTCAGAAGATCAAAGGGCTATTGAGACTTTTCAAC
************************************************************

L1AtEPF2
AAAGGATAATTTCGGGAAACCTCCTCGGATTCCATTGCCCAGCTATCTGTCACTTCATCG
pL1MForward
AAAGGATAATTTCGGGAAACCTCCTCGGATTCCATTGCCCAGCTATCTGTCACTTCATCG
************************************************************

L1AtEPF2
AAAGGACAGTAGAAAAGGAAGGTGGCTCCTACAAATGCCATCATTGCGATAAAGGAAAGG
pL1MForward
AAAGGACAGTAGAAAAGGAAGGTGGCTCCTACAAATGCCATCATTGCGATAAAGGAAAGG
************************************************************

L1AtEPF2
CTATCATTCAAGATCTCTCTGCCGACAGTGGTCCCAAAGATGGACCCCCACCCACGAGGA
```

```
pL1MForward
CTATCATTCAAGATCTCTCTGCCGACAGTGGTCCCAAAGATGGACCCCCACCCACGAGGA
************************************************************

L1AtEPF2
GCATCGTGGAAAAAGAAGAGGTTCCAACCACGTCTACAAAGCAAGTGGATTGATGTGACA
pL1MForward
GCATCGTGGAAAAAGAAGAGGTTCCAACCACGTCTACAAAGCAAGTGGATTGATGTGACA
************************************************************

L1AtEPF2
TCTCCACTGACGTAAGGGATGACGCACAATCCCACTATCCTTCGCAAGACCCTTCCTCTA
pL1MForward
TCTCCACTGACGTAAGGGATGACGCACAATCCCACTATCCTTCGCAAGACCCTTCCTCTA
************************************************************

L1AtEPF2
TATAAGGAAGTTCATTTCATTTGGAGAGGACACGCAATGGTGTGGAGCAGCAACATGTCA
pL1MForward
TATAAGGAAGTTCATTTCATTTGGAGAGGACACGCAATGGTGTGGAGCAGCAACATGTCA
************************************************************

L1AtEPF2
AGCTTTCTACTGATTTTGCTCATTCTTAATTCGACCCATTTCAGTCTAATGGCTAATGGT
pL1MForward
AGCTTTCTACTGATTTTGCTCATTCTTAATTCGACCCATTTCAGTCTAATGGCTAATGGN
************************************************************

L1AtEPF2
AGACCAGAGCCTGACTCTGTCGAATTCACCAAGAGTGGAGATCAAGATGTGAAGATGATG
pL1MForward
AGACCAGANCCTGACTCTGTCGAATTCACCAAGAGTGGNNATCAAGATGTGAAGATGATG
******** ******************************  ********************

L1AtEPF2
ATGAGAGGTCTAATAGGATCAAGACCACCAAGATGTGAGAGAGTAAGATGTCGTTCTTGT
pL1MForward     ATGANAGGTCTAATAGGATCAGACCACCAAGATGTGA----------------------
**** *****************   *  * *

L1AtEPF2
GGTCATTGTGAAGCAATTCAAGTTCCTACAAATCCTCAAACAAAGCTTCACTCTCCTTTA
pL1MForward     ------------------------------------------------------------


L1AtEPF2
ACTACTTCTTCTTCTTCTTCCTCTGAGACTATTCATCTTGACTACACCAGAGGAGATGAT
pL1MForward     ------------------------------------------------------------


L1AtEPF2
AGTACTAATTACAAACCCATGAGCTGGAAATGCAAATGTGGTAACTCTATCTACAACCCT
pL1MForward     ------------------------------------------------------------


L1AtEPF2
TGAGCTTATATGAAGATGAAGATGAAATATTTGGTGTGTCAAATAAAAAGCTTGTGTGCT
pL1MForward     ------------------------------------------------------------


L1AtEPF2
TAAGTTTGTGTTTTTTTCTTGGCTTGTTGTGTTATGAATTTGTGGCTTTTTCTAATATTA
pL1MForward     ------------------------------------------------------------


L1AtEPF2
AATGAATGTAAGATCTCATTATAATGAATAAACAAATGTTTCTATAATCCATTGTGAATG
pL1MForward     ------------------------------------------------------------
```

L1AtEPF2
TTTTGTTGGATCTCTTCTGCAGCATATAACTACTGTATGTGCTATGGTATGGACTATGGA
pL1MForward ----------

L1AtEPF2
ATATGATTAAAGATAAGCGCTAAGCTTGAATTCTTGCTTGTCTTCACAGAGTGGGGCCCA
pL1MForward ----------

*At*EPFL9 reverse alignment

L1AtEPF9
GCATGCACATACAAATGGACGAACGGATAAACCTTTTCACGCCCTTTTAAATATCCGATT
pL1MReverse ----------

L1AtEPF9
ATTCTAATAAACGCTCTTTTCTCTTAGGTTTACCCGCCAATATATCCTGTCAAACACTGA
pL1MReverse ----------

L1AtEPF9
TAGTTTAAACCACTTCGTGCAGAAGACAATAGTGGAGGTCAACATGGTGGAGCACGACAC
pL1MReverse ----------

L1AtEPF9
TCTGGTCTACTCCAAAAATGTCAAAGATACAGTCTCAGAAGATCAAAGGGCTATTGAGAC
pL1MReverse ----------

L1AtEPF9
TTTTCAACAAAGGATAATTTCGGGAAACCTCCTCGGATTCCATTGCCCAGCTATCTGTCA
pL1MReverse ----------

L1AtEPF9
CTTCATCGAAAGGACAGTAGAAAAGGAAGGTGGCTCCTACAAATGCCATCATTGCGATAA
pL1MReverse ----------

L1AtEPF9
AGGAAAGGCTATCATTCAAGATCTCTCTGCCGACAGTGGTCCCAAAGATGGACCCCCACC
pL1MReverse ----------

L1AtEPF9
CACGAGGAGCATCGTGGAAAAAGAAGAGGTTCCAACCACGTCTACAAAGCAAGTGGATTG
pL1MReverse ----------

L1AtEPF9
ATGTGATAACATGGTGGAGCACGACACTCTGGTCTACTCCAAAAATGTCAAAGATACAGT
pL1MReverse ----------

L1AtEPF9
CTCAGAAGATCAAAGGGCTATTGAGACTTTTCAACAAAGGATAATTTCGGGAAACCTCCT
pL1MReverse ----------

L1AtEPF9
CGGATTCCATTGCCCAGCTATCTGTCACTTCATCGAAAGGACAGTAGAAAAGGAAGGTGG

```
pL1MReverse      ------------------------------------------------------------


L1AtEPF9
CTCCTACAAATGCCATCATTGCGATAAAGGAAAGGCTATCATTCAAGATCTCTCTGCCGA
pL1MReverse      --
CTTACAAATGCCATCATTGCGATAAAGGAAAGGCTNTCATTCAAGATCTCTCTGCCGA
* ********************************* **********************

L1AtEPF9
CAGTGGTCCCAAAGATGGACCCCCACCCACGAGGAGCATCGTGGAAAAAGAAGAGGTTCC
pL1MReverse
CAGTGGTCCCAAAGATGGACCCCCACCCACGAGGAGCATCGTGGAAAAAGAAGAGGTTCC
************************************************************

L1AtEPF9
AACCACGTCTACAAAGCAAGTGGATTGATGTGACATCTCCACTGACGTAAGGGATGACGC
pL1MReverse
AACCACGTCTACAAAGCAAGTGGATTGATGTGACATCTCCACTGACGTAAGGGATGACGC
************************************************************

L1AtEPF9
ACAATCCCACTATCCTTCGCAAGACCCTTCCTCTATATAAGGAAGTTCATTTCATTTGGA
pL1MReverse
ACAATCCCACTATCCTTCGCAAGACCCTTCCTCTATATAAGGAAGTTCATTTCATTTGGA
************************************************************

L1AtEPF9
GAGGACACGCAATGAAGCATGAAATGATGAACATCAAGCCAAGATGCATAACCATCTTCT
pL1MReverse
GAGGACACGCAATGAAGCATGAAATGATGAACATCAAGCCAAGATGCATAACCATCTTCT
************************************************************

L1AtEPF9
TTCTTCTTTTTGCTTTGCTTCTTGGAAATTATGTAGTTCAAGCCTCAAGACCTCGTTCTA
pL1MReverse
TTCTTCTTTTTGCTTTGCTTCTTGGAAATTATGTAGTTCAAGCCTCAAGACCTCGTTCTA
************************************************************

L1AtEPF9
TCGAAAATACAGTGTCCCTTCTCCCACAAGTACATCTCCTGAATTCAAGGAGGAGGCATA
pL1MReverse
TCGAAAATACAGTGTCCCTTCTCCCACAAGTACATCTCCTGAATTCAAGGAGGAGGCATA
************************************************************

L1AtEPF9
TGATAGGGTCGACAGCACCAACTTGTACGTACAACGAGTGCAGAGGATGCAGATACAAGT
pL1MReverse
TGATAGGGTCGACAGCACCAACTTGTACGTACAACGAGTGCAGAGGATGCAGATACAAGT
************************************************************

L1AtEPF9
GCAGAGCAGAGCAAGTTCCAGTCGAAGGAAATGACCCTATCAACAGTGCTTATCATTATA
pL1MReverse
GCAGAGCAGAGCAAGTTCCAGTCGAAGGAAATGACCCTATCAACAGTGCTTATCATTATA
************************************************************

L1AtEPF9
GATGTGTTTGTCATAGATAAGCTTATATGAAGATGAAGATGAAATATTTGGTGTGTCAAA
pL1MReverse
GATGTGTTTGTCATAGATAAGCTTATATGAAGATGAAGATGAAATATTTGGTGTGTCAAA
************************************************************

L1AtEPF9
TAAAAAGCTTGTGTGCTTAAGTTTGTGTTTTTTTCTTGGCTTGTTGTGTTATGAATTTGT
pL1MReverse
TAAAAAGCTTGTGTGCTTAAGTTTGTGTTTTTTTCTTGGCTTGTTGTGTTATGAATTTGT
```

```
************************************************************

L1AtEPF9
GGCTTTTTCTAATATTAAATGAATGTAAGATCTCATTATAATGAATAAACAAATGTTTCT
pL1MReverse
GGCTTTTTCTAATATTAAATGAATGTAAGATCTCATTATAATGAATAAACAAATGTTTCT
************************************************************

L1AtEPF9
ATAATCCATTGTGAATGTTTTGTTGGATCTCTTCTGCAGCATATAACTACTGTATGTGCT
pL1MReverse
ATAATCCATTGTGAATGTTTTGTTGGATCTCTTCTGCAGCATATAACTACTGTATGTGCT
************************************************************

L1AtEPF9
ATGGTATGGACTATGGAATATGATTAAAGATAAGCGCTAAGCTTGAATTCTTGCTTGTCT
pL1MReverse     ATGGTATGGACTATGGAATATGATTAAAGATAAGCGCTCCATGGGA----------
```

*At*EPFL9 reverse alignment

```
L1AtEPF9
GCATGCACATACAAATGGACGAACGGATAAACCTTTTCACGCCCTTTTAAATATCCGATT
pL1MForward     ------------------------------------------------------------


L1AtEPF9
ATTCTAATAAACGCTCTTTTCTCTTAGGTTTACCCGCCAATATATCCTGTCAAACACTGA
pL1MForward     ---------AACGCTCTTTTCTCTTAGGTTTACCCGCCAATATATCCTGTCAAACACTGA
************************************************

L1AtEPF9
TAGTTTAAACCACTTCGTGCAGAAGACAATAGTGGAGGTCAACATGGTGGAGCACGACAC
pL1MForward
TAGTTTAAACCACTTCGTGCAGAAGACAATCTGGGAGGTCAACATGGTGGAGCACGACAC
******************************  ****************************

L1AtEPF9
TCTGGTCTACTCCAAAAATGTCAAAGATACAGTCTCAGAAGATCAAAGGGCTATTGAGAC
pL1MForward
TCTGGTCTACTCCAAAAATGTCAAAGATACAGTCTCAGAAGATCAAAGGGCTATTGAGAC
************************************************************

L1AtEPF9
TTTTCAACAAAGGATAATTTCGGGAAACCTCCTCGGATTCCATTGCCCAGCTATCTGTCA
pL1MForward
TTTTCAACAAAGGATAATTTCGGGAAACCTCCTCGGATTCCATTGCCCAGCTATCTGTCA
************************************************************

L1AtEPF9
CTTCATCGAAAGGACAGTAGAAAAGGAAGGTGGCTCCTACAAATGCCATCATTGCGATAA
pL1MForward
CTTCATCGAAAGGACAGTAGAAAAGGAAGGTGGCTCCTACAAATGCCATCATTGCGATAA
************************************************************

L1AtEPF9
AGGAAAGGCTATCATTCAAGATCTCTCTGCCGACAGTGGTCCCAAAGATGGACCCCCACC
pL1MForward
AGGAAAGGCTATCATTCAAGATCTCTCTGCCGACAGTGGTCCCAAAGATGGACCCCCACC
************************************************************

L1AtEPF9
CACGAGGAGCATCGTGGAAAAAGAAGAGGTTCCAACCACGTCTACAAAGCAAGTGGATTG
pL1MForward
CACGAGGAGCATCGTGGAAAAAGAAGAGGTTCCAACCACGTCTACAAAGCAAGTGGATTG
```

```
************************************************************

L1AtEPF9
ATGTGATAACATGGTGGAGCACGACACTCTGGTCTACTCCAAAAATGTCAAAGATACAGT
pL1MForward
ATGTGATAACATGGTGGAGCACGACACTCTGGTCTACTCCAAAAATGTCAAAGATACAGT
************************************************************

L1AtEPF9
CTCAGAAGATCAAAGGGCTATTGAGACTTTTCAACAAAGGATAATTTCGGGAAACCTCCT
pL1MForward
CTCAGAAGATCAAAGGGCTATTGAGACTTTTCAACAAAGGATAATTTCGGGAAACCTCCT
************************************************************

L1AtEPF9
CGGATTCCATTGCCCAGCTATCTGTCACTTCATCGAAAGGACAGTAGAAAAGGAAGGTGG
pL1MForward
CGGATTCCATTGCCCAGCTATCTGTCACTTCATCGAAAGGACAGTAGAAAAGGAAGGTGG
************************************************************

L1AtEPF9
CTCCTACAAATGCCATCATTGCGATAAAGGAAAGGCTATCATTCAAGATCTCTCTGCCGA
pL1MForward
CTCCTACAAATGCCATCATTGCGATAAAGGAAAGGCTATCATTCAAGATCTCTCTGCCGA
************************************************************

L1AtEPF9
CAGTGGTCCCAAAGATGGACCCCCACCCACGAGGAGCATCGTGGAAAAAGAAGAGGTTCC
pL1MForward
CAGTGGTCCCAAAGATGGACCCCCACCCACGAGGAGCATCGTGGAAAAAGAAGAGGTTCC
************************************************************

L1AtEPF9
AACCACGTCTACAAAGCAAGTGGATTGATGTGACATCTCCACTGACGTAAGGGATGACGC
pL1MForward
AACCACGTCTACAAAGCAAGTGGATTGATGTGACATCTCCACTGACGTAAGGGATGACGC
************************************************************

L1AtEPF9
ACAATCCCACTATCCTTCGCAAGACCCTTCCTCTATATAAGGAAGTTCATTTCATTTGGA
pL1MForward
ACAATCCCACTATCCTTCGCAAGACCCTTCCTCTATATAAGGAAGTTCATTTCATTTGGA
************************************************************

L1AtEPF9
GAGGACACGCAATGAAGCATGAAATGATGAACATCAAGCCAAGATGCATAACCATCTTCT
pL1MForward
GAGGACACGCAATGAAGCATGAAATGATGAACATCAAGCCAAGATGCATAACCATCTTCT
************************************************************

L1AtEPF9
TTCTTCTTTTTGCTTTGCTTCTTGGAAATTATGTAGTTCAAGCCTCAAGACCTCGTTCTA
pL1MForward
TTCTTCTTTTTGCTTTGCTTCTTGGAAATTATGTAGTTCAAGCCTCAAGACCTCGTTCTA
************************************************************

L1AtEPF9
TCGAAAATACAGTGTCCCTTCTCCCACAAGTACATCTCCTGAATTCAAGGAGGAGGCATA
pL1MForward
TCGAAAATACAGTGTCCCTTCTCCCACAAGTACATCTCCTGAATTCANGGAGGANGCATA
********************************************** ****** *****

L1AtEPF9
TGATAGGGTCGACAGCACCAACTTGTACGTACAACGAGTGCAGAGGATGCAGATACAAGT
pL1MForward     TGATAGGGTCGA--------------------------------------------
************
```

L1AtEPF9
GCAGAGCAGAGCAAGTTCCAGTCGAAGGAAATGACCCTATCAACAGTGCTTATCATTATA
pL1MForward ----------

L1AtEPF9
GATGTGTTTGTCATAGATAAGCTTATATGAAGATGAAGATGAAATATTTGGTGTGTCAAA
pL1MForward ----------

L1AtEPF9
TAAAAAGCTTGTGTGCTTAAGTTTGTGTTTTTTTCTTGGCTTGTTGTGTTATGAATTTGT
pL1MForward ----------

L1AtEPF9
GGCTTTTTCTAATATTAAATGAATGTAAGATCTCATTATAATGAATAAACAAATGTTTCT
pL1MForward ----------

L1AtEPF9
ATAATCCATTGTGAATGTTTTGTTGGATCTCTTCTGCAGCATATAACTACTGTATGTGCT
pL1MForward ----------

L1AtEPF9
ATGGTATGGACTATGGAATATGATTAAAGATAAGCGCTAAGCTTGAATTCTTGCTTGTCT
pL1MForward ----------

*At*Fd reverse alignment

L1AtFd
CATGCACATACAAATGGACGAACGGATAAACCTTTTCACGCCCTTTTAAATATCCGATTA
pL1MReverse ----------

L1AtFd
TTCTAATAAACGCTCTTTTCTCTTAGGTTTACCCGCCAATATATCCTGTCAAACACTGAT
pL1MReverse ----------

L1AtFd
AGTTTAAACCACTTCGTGCAGAAGACAATAGTGGAGAAGCTTTTAAACATCGATAATTCA
pL1MReverse ----------

L1AtFd TCACTTTTATTTTTTGTACTCTTCTTCTTCTTCCTTCCTTTCTTTTTTTTTTTTTTGTGTG
pL1MReverse ----------

L1AtFd
AAATTTGATATTTTTTGTCTTAAATGATTAATCTATTGTGTAGAAAATAGATTTTCTTGT
pL1MReverse ----------

L1AtFd
TAGTGTATAAATTTTATAAAATAAATTTAAAGACCTCTTAATATAATTTTCGCTTAGGCC
pL1MReverse ----------

L1AtFd
ACGAGATTTGTTGAGCCGCCCTGATTATCATAAATTATTTGAAGATTTTGGTCTGCAATT
pL1MReverse ----------

```
L1AtFd
GTCAGCTAATCTCCAACTAAATAATGTCCAACATAATTTGGACCCTACCAAATATTTAAC
pL1MReverse     ------------------------------------------------------------

L1AtFd
GGGCAAAGATTAATATAACACTATAGTATATAAAATGACATTCATGAGTGTGAAATTGTA
pL1MReverse     ------------------------------------------------------------

L1AtFd
TATAGTGTTCATGTGCATATTTTACTATTTTCTTGCAAATCATATGGTTCATATACAATA
pL1MReverse     ------------------------------------------------------------

L1AtFd
ATAACAATGGAAAAGACAGGTGTTTGGCCTGTAATGGGTCTATATTGTCCAGATCTTGGT
pL1MReverse     ------------------------------------------------------------

L1AtFd
GGACCCTACACACTATGACGTCTGTCAAATAATCTTGGAAAAATAACTTGTTGCACGACT
pL1MReverse     ------------------------------------------------------------

L1AtFd
CTTCGAGTCTAATTTTCAGTGATTTATTTAATAATGACTAAGTTTTATCGCTTTTATAAT
pL1MReverse     ------------------------------------------------------------

L1AtFd
GACAAAAAGGATTTCTTATTATTACTATCTCTGTTCTATATTAATTGAATCGATGAGCCA
pL1MReverse     ------------------------------------------------------------

L1AtFd
ATTATATGAAATTTTATCAAATATTCATTTTAAATTTTGAACGATAAAAAAAGCCTCATG
pL1MReverse     ------------------------------------------------------------

L1AtFd
AGAATTTTATCAAAGTAAAATATGAAAAAAATGATTATCAAGTAAAAATGAACAAAGAGA
pL1MReverse     ------------------------------------------------------------

L1AtFd
ATAATATGAAGGTTTTATCAAACATTCATCTTAAATTTTGAACGATAAAAAAAGCTTCGT
pL1MReverse     ----------------------------------AATTTGAACGATAAAAAAAGNTCGT
**  *    ******   ****

L1AtFd
AAAGAATATTTTATCATAGTAAAACATGATTATCAAGTAAAAGTGAACAAAGGGAGTAAT
pL1MReverse
AAAGAATATTTNNTCATAGTAAAACATGATTATCAAGTAAAAGTGAACAAAGGGAGTAAT
***********  **************************************************

L1AtFd
ATGAAGATTTATCATGTATTTAAAAGCTCAATAGTGATTATAATTTGAGGGACTAAATAA
pL1MReverse
ATGAAGATTTATCATGTATTTAAAAGCTCAATAGTGATTATAATTTGAGGGACTAAATAA
************************************************************

L1AtFd
ATTTAAGGAGTTGTTAATATATTCCGAGAAAATAAAATATTGTTTAAGTAGAAAAGTTAT
pL1MReverse
ATTTAAGGAGTTGTTAATATATTCCGAGAAAATAAAATATTGTTTAAGTAGAAAAGTTAT
************************************************************
```

L1AtFd
GGGGTGTATAAGTTAAATAATAATATTTTGTAAATAGGGATATGGAAATGAGTATAAATA
pL1MReverse
GGGGTGTATAAGTTAAATAATAATATTTTGTAAATAGGGATATGGAAATGAGTATAAATA
****

L1AtFd
GAAAGATAGCAAGGTTTCTCGTGAGAGTTCACAAGCCAATAAAGCTGATCACACTCCCCT
pL1MReverse
GAAAGATAGCAAGGTTTCTCGTGAGAGTTCACAAGCCAATAAAGCTGATCACACTCCCCT
****

L1AtFd
TTGTATGTCCACTCAACAACACAACTTCTTGTGATTCACTTTCAATTCTAGATCAATGGC
pL1MReverse
TTGTATGTCCACTCAACAACACAACTTCTTGTGATTCACTTTCAATTCTAGATCAATGGC
****

L1AtFd
TTCCACTGCTCTCTCCAGCGCAATCGTAAGCACCTCTTTCCTCCGCCGTCAACAGACACC
pL1MReverse
TTCCACTGCTCTCTCCAGCGCAATCGTAAGCACCTCTTTCCTCCGCCGTCAACAGACACC
****

L1AtFd
AATCAGCCTCAGATCCCTCCCGTTTGCCAACACACAATCTCTCTTCGGCCTCAAATCTTC
pL1MReverse
AATCAGCCTCAGATCCCTCCCGTTTGCCAACACACAATCTCTCTTCGGCCTCAAATCTTC
****

L1AtFd
CACCGCTCGCGGCGGCCGCGTCACGGCCATGGCTACCTACAAGGTCAAGTTCATCACACC
pL1MReverse
CACCGCTCGCGGCGGCCGCGTCACGGCCATGGCTACCTACAAGGTCAAGTTCATCACACC
****

L1AtFd
TGAGGGAGAACAAGAGGTCGAATGCGAAGAAGATGTCTACGTCCTCGACGCTGCTGAGGA
pL1MReverse
TGAGGGAGAACAAGAGGTCGAATGCGAAGAAGATGTCTACGTCCTCGACGCTGCTGAGGA
****

L1AtFd
AGCCGGACTCGACTTGCCCTACTCATGCCGTGCCGGTTCTTGCTCAAGTTGCGCCGGGAA
pL1MReverse
AGCCGGACTCGACTTGCCCTACTCATGCCGTGCCGGTTCTTGCTCAAGTTGCGCCGGGAA
****

L1AtFd
AGTCGTCTCTGGTTCTATTGACCAGTCGGACCAGAGCTTCTTAGACGATGAACAGATGAG
pL1MReverse
AGTCGTCTCTGGTTCTATTGACCAGTCGGACCAGAGCTTCTTAGACGATGAACAGATGAG
****

L1AtFd
TGAGGGCTATGTCTTGACCTGTGTGGCTTATCCGACTTCTGATGTCGTCATCGAAACCCA
pL1MReverse
TGAGGGCTATGTCTTGACCTGTGTGGCTTATCCGACTTCTGATGTCGTCATCGAAACCCA
****

L1AtFd
CAAAGAAGAAGCCATTATGGCTTATATGAAGATGAAGATGAAATATTTGGTGTGTCAAAT
pL1MReverse
CAAAGAAGAAGCCATTATGGCTTATATGAAGATGAAGATGAAATATTTGGTGTGTCAAAT
****

```
L1AtFd
AAAAAGCTTGTGTGCTTAAGTTTGTGTTTTTTTCTTGGCTTGTTGTGTTATGAATTTGTG
pL1MReverse
AAAAAGCTTGTGTGCTTAAGTTTGTGTTTTTTTCTTGGCTTGTTGTGTTATGAATTTGTG
************************************************************

L1AtFd
GCTTTTTCTAATATTAAATGAATGTAAGATCTCATTATAATGAATAAACAAATGTTTCTA
pL1MReverse
GCTTTTTCTAATATTAAATGAATGTAAGATCTCATTATAATGAATAAACAAATGTTTCTA
************************************************************

L1AtFd
TAATCCATTGTGAATGTTTTGTTGGATCTCTTCTGCAGCATATAACTACTGTATGTGCTA
pL1MReverse
TAATCCATTGTGAATGTTTTGTTGGATCTCTTCTGCAGCATATAACTACTGTATGTGCTA
************************************************************

L1AtFd
TGGTATGGACTATGGAATATGATTAAAGATAAGCGCTAAGCTTGAATTCTTGCTTGTCTT
pL1MReverse     TGGTATGGACTATGGAATATGATTAAAGATAAGCGCTAAG----------
****************************************
```

*At*Fd forward alignment

```
L1AtFd
CATGCACATACAAATGGACGAACGGATAAACCTTTTCACGCCCTTTTAAATATCCGATTA
pL1MForward     ------------------------------------------------------------


L1AtFd
TTCTAATAAACGCTCTTTTCTCTTAGGTTTACCCGCCAATATATCCTGTCAAACACTGAT
pL1MForward     ----------GCTCTTTTCTCTTAGGTTTACCCGCCAATATATCCTGTCAAACACTGAT
**************************************************

L1AtFd
AGTTTAAACCACTTCGTGCAGAAGACAATAGTGGAGAAGCTTTTAAACATCGATAATTCA
pL1MForward
AGTTTAAACCACTTCGTGCAGAAGACAATAGTGGAGAAGCTTTTAAACATCGATAATTCA
************************************************************

L1AtFd          TCACTTTTATTTTTTGTACTCTTCTTCTTCTTCCTTCCTTTCTTTTTTTTTTTTTTGTGTG
pL1MForward
TCACTTTTATTTTTTGTACTCTTCTTCTTCTTCCTTCCTTTCTTTTTTTTTTTTTTGTGTG
************************************************************

L1AtFd
AAATTTGATATTTTTTGTCTTAAATGATTAATCTATTGTGTAGAAAATAGATTTTCTTGT
pL1MForward
AAATTTGATATTTTTTGTCTTAAATGATTAATCTATTGTGTAGAAAATAGATTTTCTTGT
************************************************************

L1AtFd
TAGTGTATAAATTTTATAAAATAAATTTAAAGACCTCTTAATATAATTTTCGCTTAGGCC
pL1MForward
TAGTGTATAAATTTTATAAAATAAATTTAAAGACCTCTTAATATAATTTTCGCTTAGGCC
************************************************************

L1AtFd
ACGAGATTTGTTGAGCCGCCCTGATTATCATAAATTATTTGAAGATTTTGGTCTGCAATT
pL1MForward
ACGAGATTTGTTGAGCCGCCCTGATTATCATAAATTATTTGAAGATTTTGGTCTGCAATT
************************************************************
```

```
L1AtFd
GTCAGCTAATCTCCAACTAAATAATGTCCAACATAATTTGGACCCTACCAAATATTTAAC
pL1MForward
GTCAGCTAATCTCCAACTAAATAATGTCCAACATAATTTGGACCCTACCAAATATTTAAC
************************************************************

L1AtFd
GGGCAAAGATTAATATAACACTATAGTATATAAAATGACATTCATGAGTGTGAAATTGTA
pL1MForward
GGGCAAAGATTAATATAACACTATAGTATATAAAATGACATTCATGAGTGTGAAATTGTA
************************************************************

L1AtFd
TATAGTGTTCATGTGCATATTTTACTATTTTCTTGCAAATCATATGGTTCATATACAATA
pL1MForward
TATAGTGTTCATGTGCATATTTTACTATTTTCTTGCAAATCATATGGTTCATATACAATA
************************************************************

L1AtFd
ATAACAATGGAAAAGACAGGTGTTTGGCCTGTAATGGGTCTATATTGTCCAGATCTTGGT
pL1MForward
ATAACAATGGAAAAGACAGGTGTTTGGCCTGTAATGGGTCTATATTGTCCAGATCTTGGT
************************************************************

L1AtFd
GGACCCTACACACTATGACGTCTGTCAAATAATCTTGGAAAAATAACTTGTTGCACGACT
pL1MForward
GGACCCTACACACTATGACGTCTGTCAAATAATCTTGGAAAAATAACTTGTTGCACGACT
************************************************************

L1AtFd
CTTCGAGTCTAATTTTCAGTGATTTATTTAATAATGACTAAGTTTTATCGCTTTTATAAT
pL1MForward
CTTCGAGTCTAATTTTCAGTGATTTATTTAATAATGACTAAGTTTTATCGCTTTTATAAT
************************************************************

L1AtFd
GACAAAAAGGATTTCTTATTATTACTATCTCTGTTCTATATTAATTGAATCGATGAGCCA
pL1MForward
GACAAAAAGGATTTCTTATTATTACTATCTCTGTTCTATATTAATTGAATCGATGAGCCA
************************************************************

L1AtFd
ATTATATGAAATTTTATCAAATATTCATTTTAAATTTTGAACGATAAAAAAAGCCTCATG
pL1MForward
ATTATATGAAATTTTATCAAATATTCATTTTAAATTTTGAACGATAAAAAAAGCCTCATG
************************************************************

L1AtFd
AGAATTTTATCAAAGTAAAATATGAAAAAAATGATTATCAAGTAAAAATGAACAAAGAGA
pL1MForward
AGAATTTTATCAAAGTAAAATATGAAAAAAATGATTATCAAGTAAAAATGAACAAAGAGA
************************************************************

L1AtFd
ATAATATGAAGGTTTTATCAAACATTCATCTTAAATTTTGAACGATAAAAAAAGCTTCGT
pL1MForward
ATAATATGAAGGTTTTATCAAACATTCATCTTAAATTTTGAACGATAAAAAAAGCTTCGT
************************************************************

L1AtFd
AAAGAATATTTTATCATAGTAAAACATGATTATCAAGTAAAAGTGAACAAAGGGAGTAAT
pL1MForward
AAAGAATATTTTATCATAGTAAAACATGATTATCAAGTAAAAGTGAACAAAGGGAGTAAT
************************************************************
```

```
L1AtFd
ATGAAGATTTATCATGTATTTAAAAGCTCAATAGTGATTATAATTTGAGGGACTAAATAA
pL1MForward     ATGAAGATTTATCATG----------------------------------------
****************

L1AtFd
ATTTAAGGAGTTGTTAATATATTCCGAGAAAATAAAATATTGTTTAAGTAGAAAAGTTAT
pL1MForward     ------------------------------------------------------------

L1AtFd
GGGGTGTATAAGTTAAATAATAATATTTTGTAAATAGGGATATGGAAATGAGTATAAATA
pL1MForward     ------------------------------------------------------------

L1AtFd
GAAAGATAGCAAGGTTTCTCGTGAGAGTTCACAAGCCAATAAAGCTGATCACACTCCCCT
pL1MForward     ------------------------------------------------------------

L1AtFd
TTGTATGTCCACTCAACAACACAACTTCTTGTGATTCACTTTCAATTCTAGATCAATGGC
pL1MForward     ------------------------------------------------------------

L1AtFd
TTCCACTGCTCTCTCCAGCGCAATCGTAAGCACCTCTTTCCTCCGCCGTCAACAGACACC
pL1MForward     ------------------------------------------------------------

L1AtFd
AATCAGCCTCAGATCCCTCCCGTTTGCCAACACACAATCTCTCTTCGGCCTCAAATCTTC
pL1MForward     ------------------------------------------------------------

L1AtFd
CACCGCTCGCGGCGGCCGCGTCACGGCCATGGCTACCTACAAGGTCAAGTTCATCACACC
pL1MForward     ------------------------------------------------------------

L1AtFd
TGAGGGAGAACAAGAGGTCGAATGCGAAGAAGATGTCTACGTCCTCGACGCTGCTGAGGA
pL1MForward     ------------------------------------------------------------

L1AtFd
AGCCGGACTCGACTTGCCCTACTCATGCCGTGCCGGTTCTTGCTCAAGTTGCGCCGGGAA
pL1MForward     ------------------------------------------------------------

L1AtFd
AGTCGTCTCTGGTTCTATTGACCAGTCGGACCAGAGCTTCTTAGACGATGAACAGATGAG
pL1MForward     ------------------------------------------------------------

L1AtFd
TGAGGGCTATGTCTTGACCTGTGTGGCTTATCCGACTTCTGATGTCGTCATCGAAACCCA
pL1MForward     ------------------------------------------------------------

L1AtFd
CAAAGAAGAAGCCATTATGGCTTATATGAAGATGAAGATGAAATATTTGGTGTGTCAAAT
pL1MForward     ------------------------------------------------------------

L1AtFd
AAAAAGCTTGTGTGCTTAAGTTTGTGTTTTTTTCTTGGCTTGTTGTGTTATGAATTTGTG
```

pL1MForward ----------

L1AtFd
GCTTTTTCTAATATTAAATGAATGTAAGATCTCATTATAATGAATAAACAAATGTTTCTA
pL1MForward ----------

L1AtFd
TAATCCATTGTGAATGTTTTGTTGGATCTCTTCTGCAGCATATAACTACTGTATGTGCTA
pL1MForward ----------

L1AtFd
TGGTATGGACTATGGAATATGATTAAAGATAAGCGCTAAGCTTGAATTCTTGCTTGTCTT
pL1MForward ----------